Ganzevles, Irene (2024) ***Using foraminifera to reconstruct Holocene cyclone occurrences at Middle Island on the central Great Barrier Reef, Queensland, Australia.*** **Masters (Research) Thesis, James Cook University.**

https://doi.org/10.25903/ggsz%2Djk75

Using foraminifera to reconstruct Holocene cyclone occurrences at Middle Island on the central Great Barrier Reef, Queensland, Australia

Thesis submitted by:

Irene Ganzevles, B.Sc.

In June 2024

For the degree of Master of Philosophy

In the College of Earth and Environmental Sciences

James Cook University

Statement of the Contribution of Others

Financial support

- Graduate Research School, James Cook University (tuition fee waiver)
- College of Science and Engineering, James Cook University (HDR Competitive Research Grant)

Supervisors

- Prof. Scott Smithers, College of Science and Engineering, James Cook University
- Dr. Jack Koci, TropWater, James Cook University

Data collection

- Field work assistants and volunteers Scott, Tom, Emma, and Tess
- Laboratory assistants Lauren, Marika, and Emily

Statistical analyses

- Empro. Rhondda Jones, Australian Institute of Tropical Health and Medicine, James Cook University

Intellectual support

- Prof. Scott Smithers
- Dr. Jack Koci

Permits

- Research Permit P-PTUKI-100477780, Department of Environment and Science/Queensland Parks and Wildlife Services (granted to Prof. Scott Smithers)
- Research Permit G23/49080.1, Great Barrier Reef Marine Park Authority (granted to Prof. Scott Smithers)

Acknowledgements

To my amazing supervisors Scott and Jack, it was your enthusiasm and passion that inspired me to continue my studies after my bachelor's degree and to branch out from marine biology into the fascinating world of geomorphology. Thank you for all your time and support and the countless meetings and discussions. Thank you for always providing detailed feedback, even if that required working in the evenings or on weekends. Thank you for your continued belief in my capabilities and for the words of encouragement when I needed them most. I could not have wished for better supervisors, and I am incredibly grateful to you both for offering me this amazing opportunity.

To my wonderful volunteers Tom, Emma, Tess, Lauren, Marika, and Emily. You helped make the field trips and the laboratory analyses much more enjoyable and I could not have finished my work in time without you. Thanks to Greg and Glenn from the Boating and Diving Register at JCU for their help in organising the field trips and in making sure I had all the necessary equipment. Special thanks to Rhondda for her statistical advice and for making the statistical analyses a bit less daunting.

I am also grateful to Jamie, Debbie and Melissa at the College of Science and Engineering reception for their support, their words of encouragement and the numerous chats throughout my degree. Special thanks to Debbie for informing me about the possibility to obtain a tuition fee waiver, and for the subsequent help in submitting the required paperwork.

To my parents and brother, thank you for supporting me throughout my university career, even though I am living halfway across the world and I do not get to see you as often as we all would like. Thank you for your emotional, intellectual, and financial support and for always believing in me and for letting me follow my dreams.

Abstract

Tropical cyclones are natural disasters that can severely impact the lives and livelihoods of people living in coastal communities. Cyclone modelling is used to predict the frequency and intensity of cyclones in the present and future, but the models are based on instrumental cyclone records that are too short to capture long-term variation in cyclone frequency and intensity due to climatic variations. As a result, cyclone modelling is paired with a considerable amount of uncertainty. To extend instrumental cyclone records and to improve our cyclone models, paleotempestologists use a range of archives and proxies in the geological record to reconstruct paleocyclone occurrences. Commonly used paleotempestological archives are overwash deposits and beach ridges, since they consist of marine sediments that are deposited on land beyond the reach of fair-weather waves and therefore indicate the occurrence of extreme events such as cyclones. These overwash deposits and beach ridges provide a conservative, low-resolution estimate of the number of washover events and the intensity of the cyclones that deposited them. Foraminifera are a group of marine protists that have the potential to greatly improve the resolution of paleocyclone reconstructions, if their tests are preserved in overwash deposits in protected nearshore environments. Foraminifera exhibit species-specific habitat and depth preferences, which can be used for paleocyclone reconstructions by linking provenance depth of foraminifera in overwash deposits to wavelength, wave height and cyclone intensity through established wave theory. Despite their potential, foraminifera are underrepresented as a proxy in paleotempestological research and have rarely been used in Australia, and species-specific depth preferences have never been used for paleocyclone reconstructions in Queensland.

Based on these knowledge gaps, this study addressed the following objectives: 1) To describe and quantify the distribution, habitat and depth preferences of contemporary foraminifera from Middle Island on the central GBR; 2) To analyse sediment cores from the ephemeral lake on Middle Island for overwash deposits and foraminiferal presence; 3) To reconstruct Holocene cyclone occurrences at Middle Island based on the collected data; 4) To assess the strengths and limitations of a novel research method that uses species-specific depth preferences of foraminifera to reconstruct paleocyclone occurrences at Middle Island on the central Great Barrier Reef. Middle Island was selected as the study location due to its excellent potential for washover deposit preservation and due to previous studies at this location that provided an age limit for potential overwash deposits.

Foraminiferal assemblages and habitat types and cover from the reef flat and reef slopes around Middle Island were described and quantified. Statistical analyses were performed to determine if foraminifera exhibited species-specific habitat and depth preferences. Foraminifera species conformed to the current knowledge about habitat preferences, and the analyses revealed that 17 foraminifera species could be assigned to 5 m depth intervals: *Amphistegina lobifera* to 5-0 m above LAT, *Ammonia aoteana, Clavulina pacifica, Elphidium advenum, Elphidium excavatum, Elphidium hispidulum, Operculina ammonoides, Parasorites orbiculus, Quinqueloculina crassicarinata, Quinqueloculina parvaggluta, Quinqueloculina polygona, Sahulia conica, Sigmoihauerina involuta, Siphonaperta arenata, Spiroloculina communis* and *Textularia dupla* to 5-10 m below LAT and *Elphidium crispum* to 0-10 m below LAT.

Nine percussion cores were collected from the ephemeral lake behind the shingle ridge on Middle Island. Sediment samples were taken at 5 cm intervals from two of the cores, and stratigraphic and sedimentary analyses and foraminifera identification were used to distinguish overwash deposits from lacustrine sediments. Based on grain size distribution, sediment colour, and presence of marine material such as coral clasts and foraminifera, three overwash deposits were identified at ~45-50 cm downcore, ~65-90 cm downcore and ~115 cm downcore. These sediments were estimated to have been deposited ~3,980, ~2,600 and ~1,740 years ago, based on the age of the shingle ridge (~4,500 years), assumed sedimentation rates within the lake and respective depths of the overwash deposits downcore. All recognised overwash deposits contained depth-specific foraminifera belong to 5-10 m below LAT: *Clavulina pacifica, Elphidium excavatum*, *Elphidium hispidulum, Quinqueloculina crassicarinata, Sahulia conica, Spiroloculina communis and Textularia dupla.* Cyclone modelling was beyond the scope of this study, but the three overwash deposits were assigned to severe Category 5 cyclones based on the bathymetry around Middle Island, the height of the shingle ridge that fronts the lake, and total inundation levels and cyclone intensities that were calculated in previous studies for locations across Queensland. The average return periods for these cyclones (~750 years for all three cyclones and ~430 years for the two most recent cyclones) contradict the calculated return periods from previous studies at other locations across Queensland and emphasise the need for further paleotempestological research to resolve these differences.

This study provides the first description of foraminiferal assemblages and habitat types from the reef flat and reef slopes around Middle Island on the central Great Barrier Reef. Furthermore, this study has shown that foraminifera exhibit species-specific depth preferences at Middle Island on the central Great Barrier Reef and that foraminifera can be used to reconstruct paleocyclone occurrences at this location with greater precision than currently possible. Since the use of this novel research method has been validated, future studies can greatly improve the resolution of paleocyclone reconstructions by employing the same method. The improved resolution will result in more accurate cyclone modelling of present and future cyclones and will aid in minimising the devastating impacts of cyclones on lives and livelihoods in coastal communities.

Table of Contents

List of Figures

List of Tables

List of plates

1. Introduction

This chapter provides background information relevant to cyclones and the research field of paleotempestology. The research aims and objectives are stated, and a description of the study site is provided. The thesis structure is provided to show the links between the chapters and the research question.

Plate 1

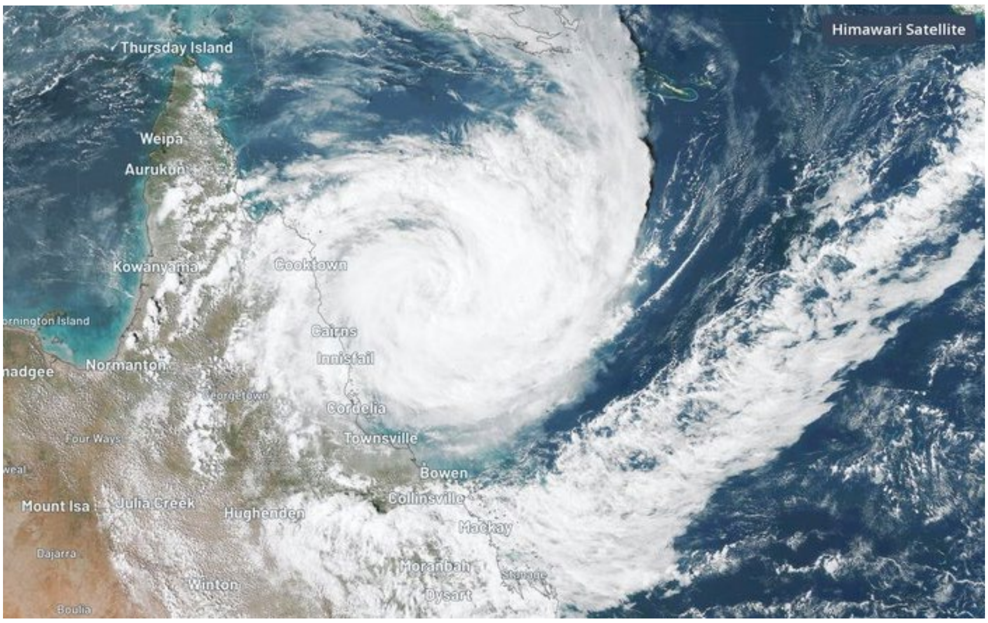

Note. Cyclone Jasper. From *weatherzone.com.au, 2023*

1.1 Cyclones and cyclone records

Tropical cyclones are low-pressure systems that originate over (sub)tropical waters (≥27°C), with surface wind speeds of at least 17 m s^{-1}. Once wind speeds exceed 33 m s^{-1}, the storms are referred to as 'typhoons' in the northwestern Pacific Ocean, 'hurricanes' in the North Atlantic Ocean and northeastern Pacific Ocean, or 'severe tropical cyclones' in the southwestern Pacific Ocean and southeastern Indian Ocean (cyclones in this thesis, regardless of geographic location) (Sharkov, 2012). Between 1960-2010 these intense storms, associated with extreme winds, heavy rainfall, storm surges and waves, caused the loss of 8,000 lives and AU$39 billion in damage each year on average (Bakkensen & Mendelsohn, 2019; Chang & Guo, 2007; Murnane & Liu, 2004; Sharkov, 2012; Wahiduzzaman et al., 2022) . Although devastating, cyclones are a natural occurrence and play an important role in coastal processes such as sediment transport and the development of coastal morphology.

Climate change is expected to cause an increase in cyclone *intensity* in the 21st century, although projected increases vary from 2% to >30% depending on the spatial resolution and the computer models used to mimic cyclone generation (Cheal et al., 2017; Chu & Murakami, 2022; Knutson et al., 2020; Walsh et al., 2016; Yoshida et al., 2017). Significant uncertainty still exists regarding cyclone *frequency* and *distribution*, and computer models indicate that changes might be ocean basin specific, e.g., increased cyclone activity in the Indian Ocean and the Pacific Ocean, but decreased activity in the Atlantic Ocean (Chu & Murakami, 2022; Yoshida et al., 2017). Whether these changes have a positive or negative impact on coastal settings is location-specific, which complicates modelling of coastal responses to climate change and future cyclone activity.

At least some of the variation between predictive models of future cyclone behaviour can be attributed to the scarcity of long-term instrumental records. The North Atlantic region has the longest instrumental record of cyclone occurrences, with records going back to the 1850s (Muller et al., 2017). Some scientists argue that these earliest records are incomplete due to equipment calibration inconsistencies and the inability of the earliest equipment to withstand the extreme conditions generated by cyclones (Landsea et al., 2008). The start of the 20th century is therefore considered to be the start of a reliable instrumental cyclone record (Chang & Guo, 2007). In other regions, such as Australia, the instrumental records only date back to the mid-1900s (Chand et al., 2019; Haig et al., 2014).These records are too short to distinguish between long-term variations in climate and cyclone formation (cyclogenesis) on one hand, and actual climatic trends such as human-induced (anthropogenic) climate change on the other (Knutson et al., 2010; Kumar, 2020). While historical records like ships' logs and newspapers extend back to the pre-instrumental age, they are too spatially biased and imprecise to be reliable (Murnane & Liu, 2004).

1.2 Paleotempestology

To overcome the limitations posed by historical and instrumental records, scientists examine biological, geomorphological, and geochemical archives for clues about past climates and past cyclone activity. These research activities are called paleoclimatology and paleotempestology, respectively. Paleoclimatology is the study of climate before the existence of instrumental records (Bradley, 2015). The interest in past climates received a boost in the 19th century, when the proven existence of Ice Ages in ancient times undermined the popular belief that climate and weather are stable, unchanging phenomena. The current global climate changes have caused the field of paleoclimatology to develop rapidly in recent decades, aided by technological improvements and scientific discoveries (Brönnimann, 2015). Within the field of paleoclimatology, paleotempestology focuses specifically on past cyclone activity and its scientific evidence (Oliva et al., 2018). Through increased understanding of past climates and their environmental drivers, current climate conditions can be better understood and possible consequences for the future under anthropogenic climate change can be inferred (Bradley, 2015; Fan & Liu, 2008; Strotz et al., 2016).

Evidence for past climates and past cyclonic activity is extracted from geomorphological, biological, geochemical, and sometimes historical archives, with specific parameters within the archives referred to as proxies (Fairchild & Baker, 2012). Paleoclimatology uses a range of archives and proxies, from ice cores and speleothems to microfossils and stable isotope ratios (Bradley, 2015; Jones et al., 2009). This thesis focuses on tropical paleotempestology (paleotempestology hereafter) and will therefore consider archives and proxies that develop and are best preserved in these regions. The most frequently used paleotempestological archives are overwash deposits, speleothems, and beach ridges, with microfossils and stable isotope ratios commonly used proxies within these archives. One of the reasons these archives and proxies are selected is because they contain material that can be radiometrically dated to determine absolute ages of extreme events (Liu, 2007a). The archives and proxies that are relevant for this research project, i.e., overwash deposits, beach ridges and microfossils, are discussed below.

Overwash deposits are sedimentary layers that have been deposited behind coastal barriers such as dunes or beach ridges. They also occur when sediments are deposited in marshes, mangroves or lakes that are situated behind beaches or rocky foreshores. Washover deposits are generated by storm surges and waves that are big enough to overtop the barriers or foreshore. They can be recognised as they are allochthonous, of foreign origin, compared to the sediments on which they are deposited. The allochthonous deposits, when compared to in-situ sediments, can differ in grain size, mineral or chemical composition, biological constituents, or a combination of these (Wang & Horwitz, 2007). If storm waves deposit coarse siliciclastic sand containing marine microfossils onto mangrove mud that is high in organic content and plant roots, the abrupt transition between sediment layers is a good indicator of this extreme event (Donnelly et al., 2006). The process of creating overwash deposits and the resulting sediment deposit stratigraphy is depicted in Figure 1.1.

Figure 1.1a

Overwash deposit process

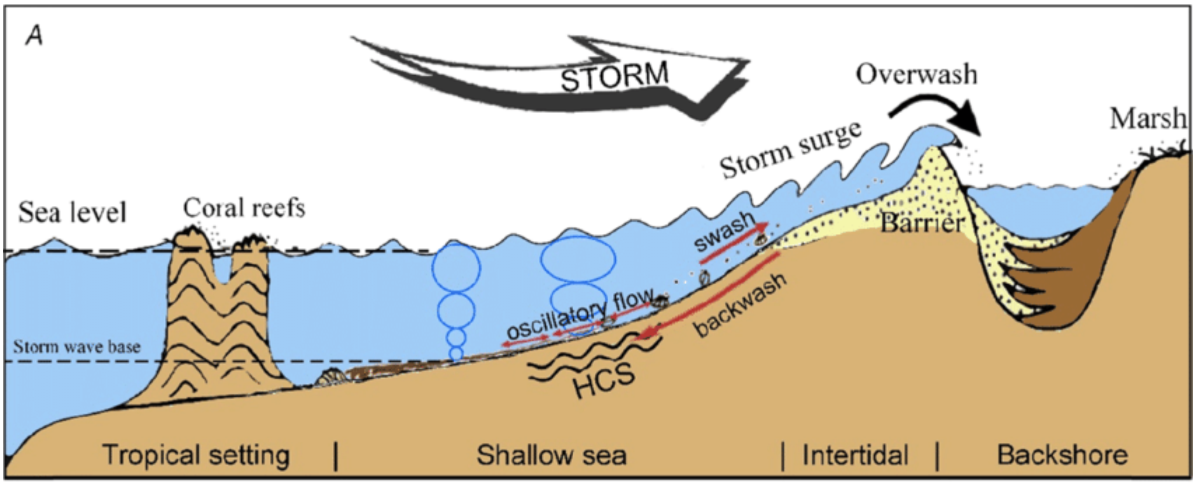

Note. Schematic representation of cyclonic conditions causing storm surge to overtop an existing barrier and deposit marine sediments in the back-barrier area. From *Xiong et al., 2018.*

b

Stratigraphy in sediment cores

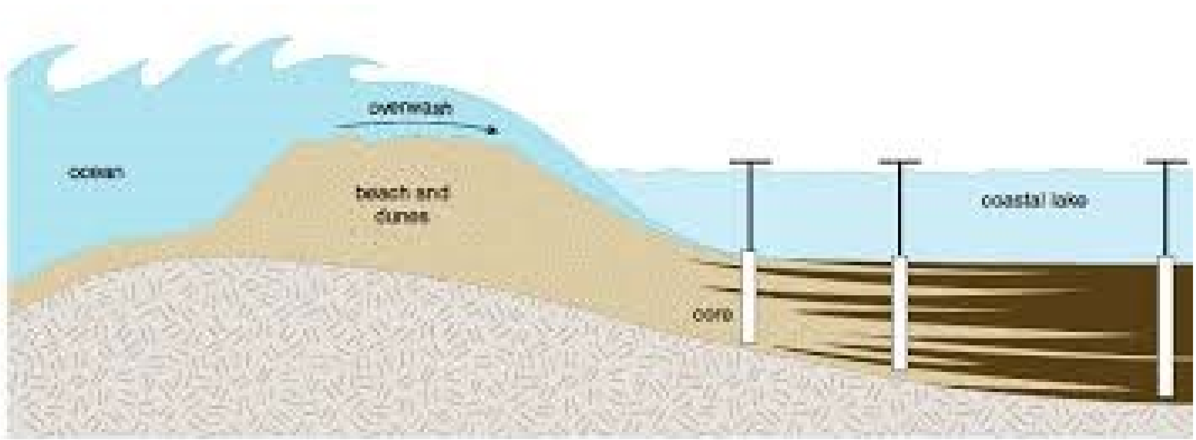

Note. Coring in the back-barrier lagoon would result in sedimentary cores with lagoonal/lacustrine sediments interspersed with beach/marine sediments. From *Liu, 2007.*

The term ‘beach ridge’ has been used to indicate a multitude of different landforms. For this thesis and for the use in paleotempestology, beach ridges are defined as intertidal and supratidal shore-parallel ridges composed of either sand or coral shingle. Beach ridges are primarily wave-deposited but can accumulate a top layer of wind-blown (aeolian) sediments after initial deposition (Nott, 2014; Tamura, 2012, 2014). Beach ridges are deposited above the fair-weather wave level, indicating they have been deposited by storm surges or waves that are of above-average height. A single beach ridge can consist of layers that were deposited by multiple events, and the height of the ridge influences subsequent deposits since only increasingly stronger cyclones can generate waves or surges that are big enough to overtop the existing ridge. The height of the ridge and the distance from the fair-weather water level are indicators of the strength of the storm and can therefore be used as archives in paleotempestology, although ridge height will introduce a preservation bias. Ridge height also depends on the specific environmental and hydrological conditions at the time of deposition (Nott et al., 2013).

Microfossils can either be whole organisms or parts of organisms, including shells or tests of microscopic organisms (e.g., foraminifera and diatoms); parts of macroscopic organisms (e.g., spicules and teeth); or reproductive parts of plants and fungi (e.g., pollen and spores). One of their common characteristics is the need for a microscope to study them (Beck Eichler & Barker, 2020a). Microfossils are highly specialised organisms that have very specific habitat requirements. They only tolerate a narrow range of environmental parameters such as temperature and salinity and live in narrowly constrained zones (Beavington-Penney & Racey, 2004; Javaux & Scott, 2003; Murray, 2006). Terrestrial microfossils can be deposited in coastal environments by a range of events including cyclones, seasonal rainfall events, landslides, and earthquakes. These microfossils are then considered allochthonous (Miller et al., 2013; Yao et al., 2021). The presence of allochthonous terrestrial microfossils in coastal or marine settings is therefore not necessarily indicative of cyclone activity.

Marine microfossils on the other hand can only be deposited in overwash deposits by storms and cyclones or tsunamis, as summarized by Pilarczyk and colleagues (2014). These processes differ in the footprints they leave behind in the sedimentological and microfossil record, making it possible to distinguish between the types of events. Tsunami deposits are generally uniform in thickness and form sheets, while storm deposits tend to form wedges that thin landwards. Tsunami deposits come from a range of environments and may consist of materials from across the continental shelf, while storm deposits only consist of nearshore sediments (Palmer et al., 2020; Pilarczyk et al., 2014). Once the type of deposit has been determined, microfossils can provide information about the location of origin (provenance) of the sediments. Based on the habitat zone and depth these microfossils normally occur in and on how far inland they have been deposited, conclusions can be drawn about the events that generated the overwash deposits containing microfossils. For example, Lane et al. (2011) used foraminifera to reconstruct the origin of storm deposits in a sinkhole in Florida. Based on the foraminiferal assemblages present and their known preferred habitats, the researchers were able to determine that some sediments originated from water depths up to 10 metres, which currently occur 3-5 km offshore (Lane et al., 2011) (Figure 1.2).

Figure 1.2a

Conceptual diagram of the distribution of foraminifera species in nearshore environments

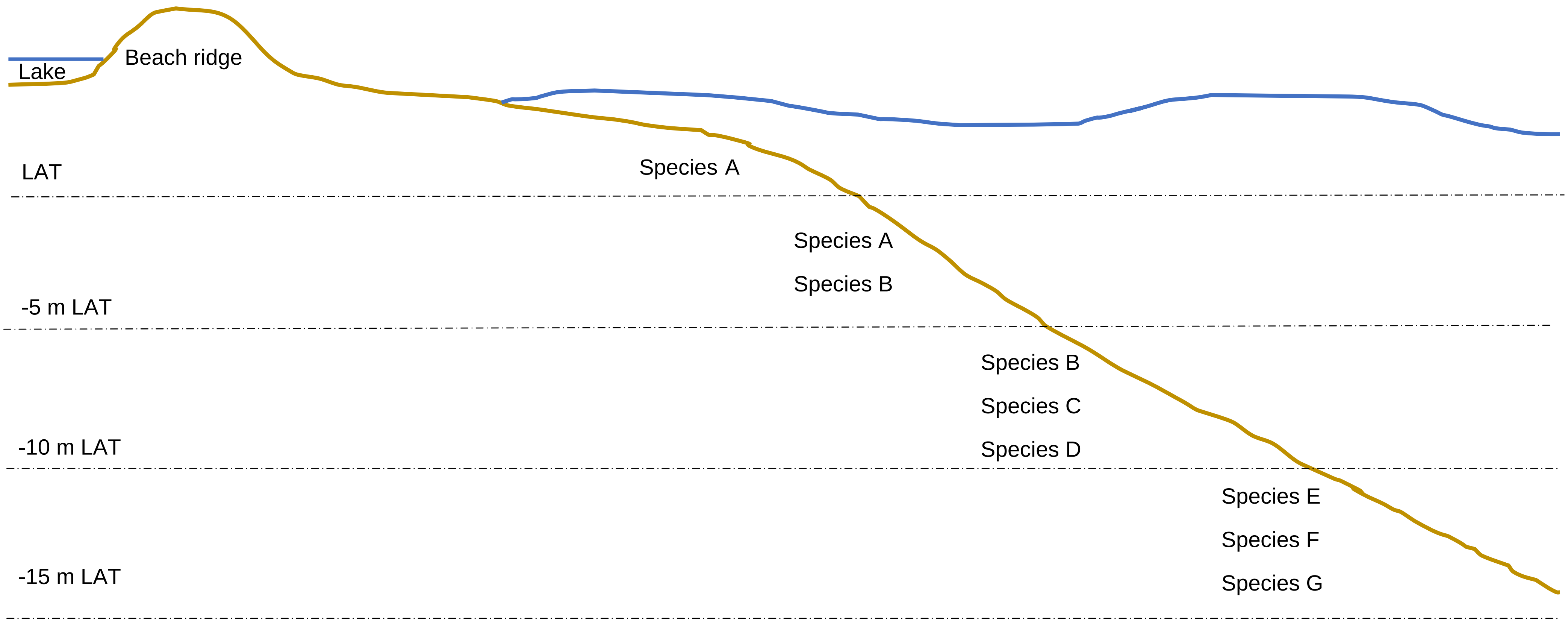

b

Impacts of cyclone-generated waves on nearshore sediments and foraminifera

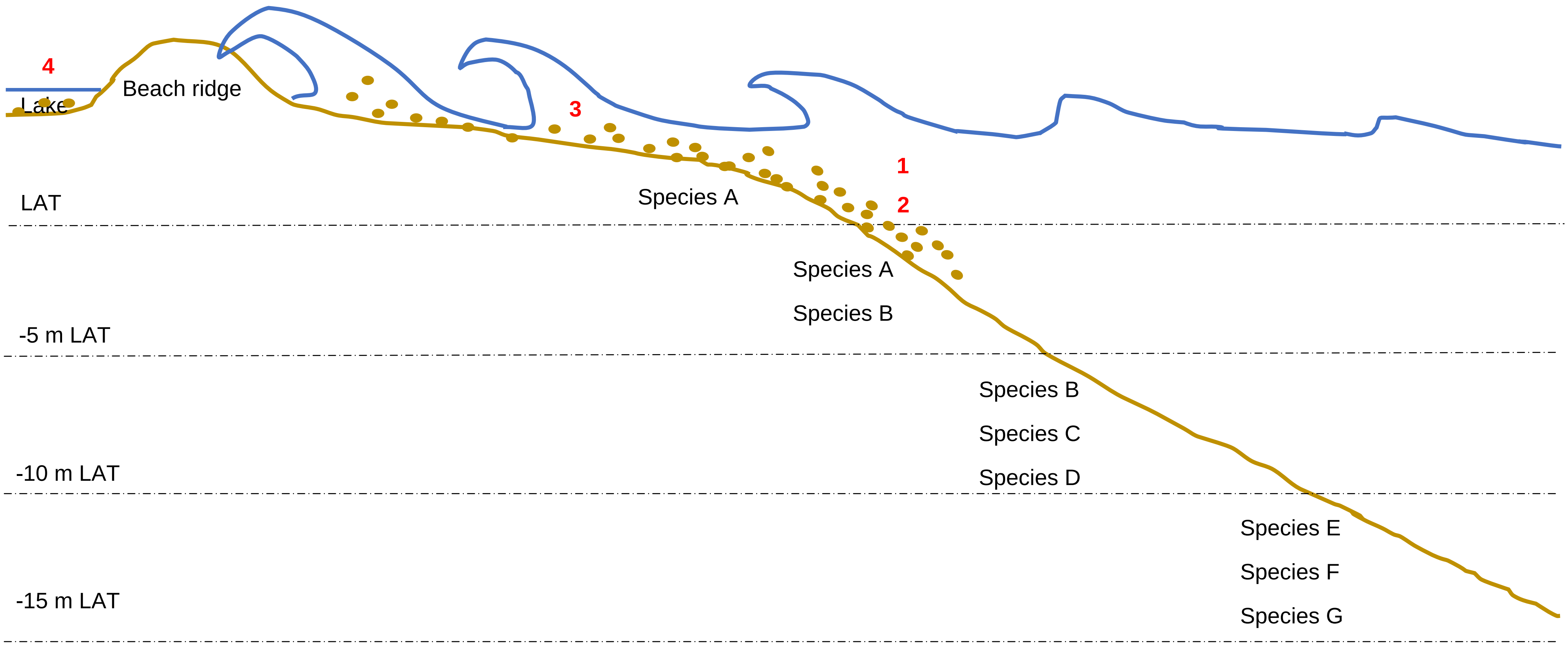

1. Cyclones generate waves, which interact with the ocean floor when water depth ≤ ½ wavelength
2. Wave interactions with the ocean floor entrain sediments containing foraminifera
3. Sediments and foraminifera are held in suspension and carried towards shore by the waves
4. Waves break across the beach ridge and deposit sediments and foraminifera in the lake

c

Impacts of severe cyclone-generated waves on nearshore sediments and foraminifera

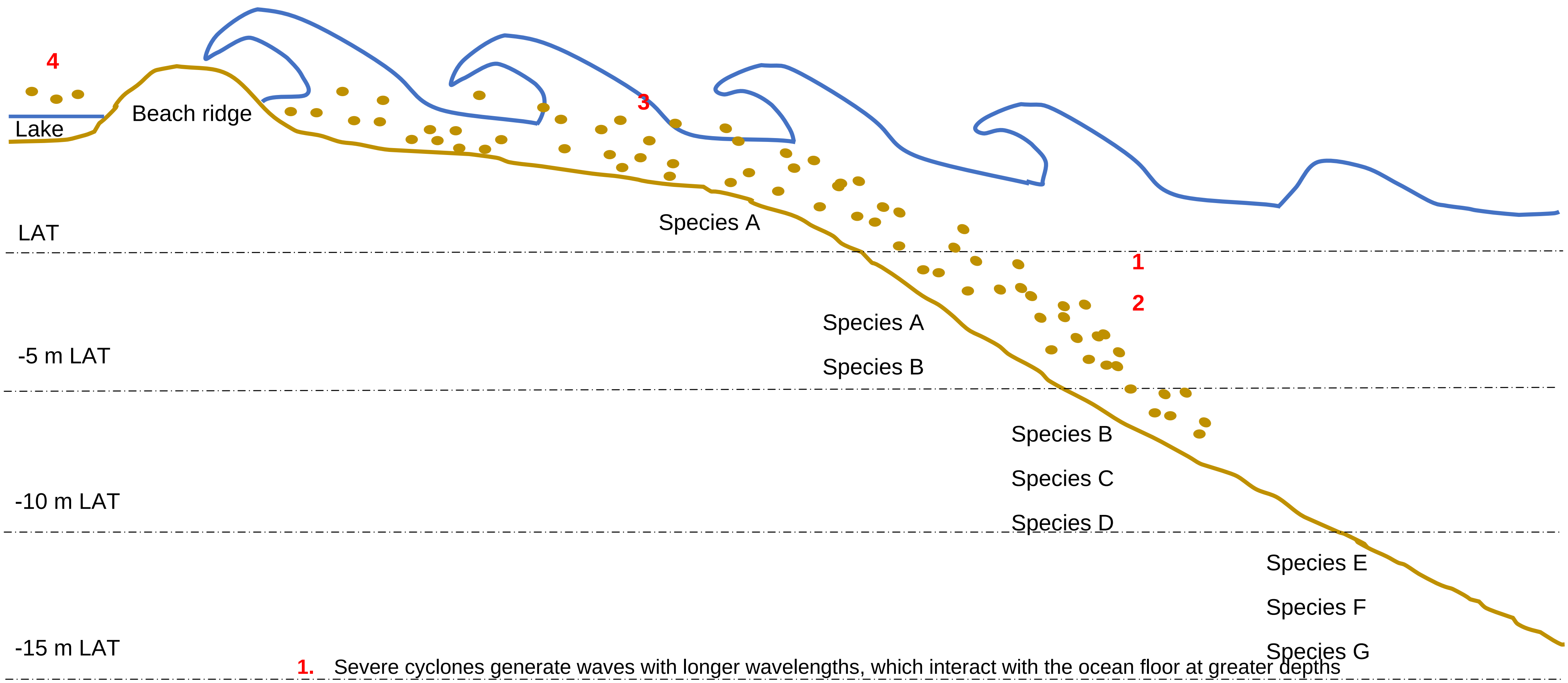

1. Severe cyclones generate waves with longer wavelengths, which interact with the ocean floor at greater depths
2. Sediments and foraminifera from these greater depths are entrained and transported to shore
3. Shallow-water sediments and foraminifera are also entrained and transported
4. Sediments and foraminifera are deposited in the lake

Regardless of which archives are used, they all have the potential to greatly extend beyond the past 70-120 years covered by instrumental records. Paleotempestological archives can record events that occurred centuries to millennia ago, improving knowledge of the natural climate variability and the influence of large-scale patterns such as the El Nino Southern Oscillation (ENSO) on cyclone occurrences and traits (Muller et al., 2017). Examples of paleotempestological research can be found all over the world: a 3,000-year cyclone record from the USA (Braun et al., 2017), a 5,000 year cyclone reconstruction for the Great Barrier Reef (GBR) (Nott & Hayne, 2001), a 3,000-year reconstruction of extreme events in Taiwan (Lallemand et al., 2016), and a paleocyclone reconstruction of the last interglacial period (125-130 KYA) from China (Du et al., 2016)

1.3 Foraminifera

While any paleotempestological archive can extend our instrumental record, microfossils have the potential to significantly improve the resolution of these reconstructions due to their species-specific depth- and habitat preferences. Two groups of microfossils that are present in coastal and shallow reef settings in cyclone-prone areas are diatoms and foraminifera. These microfossils occur from the poles to the tropics and different species live in habitats ranging from shallow lagoons to abyssal depths (Jain, 2020). Diatoms are unicellular photosynthetic algae that are mostly planktonic. Some species have cell walls made of silica, a material that is strong enough to withstand degradation after the organism's death. The planktonic nature of diatoms, and the fact that preservation of cell walls preferentially occurs in temperate to cold climates, make diatoms less suitable for tropical paleotempestology (Pilarczyk et al., 2014). This leaves benthic shallow-water foraminifera as the main microfossil archive used in paleotempestological research.

Foraminifera are unicellular organisms that have existed for at least 550 million years (Armstrong & Brasier, 2009; Jain, 2020). Their bodies consist of soft cytoplasm, enveloped by a hard outer shell called a test. These tests can be constructed of different materials, such as aragonite, calcite, silica or organic material (Saraswati, 2021). The carbonate tests are more durable than the silicate or organic tests, and it is the carbonate tests that are used for paleoclimatological and paleotempestological reconstructions. The chemistry of the tests provides information about environmental preferences of an organism, and keeps a record of environmental changes during its lifetime (Seears et al., 2012). While test morphology was initially used to distinguish between species, phenotypic plasticity, uncertainty about evolutionary pathways, and lack of taxonomists have seen an increase in the use of molecular technologies for identification (Sen & Bhadury, 2015). Despite technological advances, foraminifera taxonomy is far from resolved and is constantly being updated, with over 5,000 living (extant) benthic species classified to date (Roberts et al., 2016; Saraswati, 2021). Foraminifera range in size from µm to mm, with a few large benthic foraminifera reaching sizes of up to several cm. They are found in every part of the marine system, from beaches and shallow marine areas to the deep ocean floor (Armstrong & Brasier, 2009; Saraswati, 2021). Foraminifera occur worldwide, but different species tolerate narrow optimal ranges of environmental parameters such as salinity, temperature, and light intensity, making each species highly specialized and adapted to a particular environment (Beavington-Penney & Racey, 2004). The combination of parameters creates a niche in which the organism can thrive and to which they are morphologically adapted. The parameter that is closest to exceeding one of the organism's thresholds will determine its distribution, although foraminifera have been shown to be remarkably resistant to unfavourable conditions for several days or more (Murray, 2006).

Despite foraminifera having been well-studied, comprehensive reviews of species' distribution and habitat preferences are scarce. Researchers discuss the presence of species in sediments deposited by a specific event (Kosciuch et al., 2018; Pilarczyk et al., 2016; Prazeres et al., 2016; Strotz et al., 2016), species' abundance and occurrence in a specific geographical region (Delaine et al., 2015; Förderer et al., 2018; Haslett, 2001; Horton et al., 2007; Horton et al., 2003; Peters et al., 2020; Woodroffe et al., 2005), a subtype of foraminifera such as benthic or planktonic foraminifera (Beavington-Penney & Racey, 2004; Beck Eichler & Barker, 2020a; Kimoto, 2015; Roberts et al., 2016; Schiebel & Hemleben, 2005; Seears et al., 2012; Sen & Bhadury, 2015), or a combination of these topics. Some detailed reviews of specific species are provided by Mamo (2016), Debenay (2013), Nobes and Uthicke (2008), Hohenegger (1994, 1996) and Hohenegger et al. (1999), although these reviews still focus on a particular geographic location or a subset within foraminifera. John Murray's book *Ecology and applications of benthic foraminifera* discusses benthic foraminifera based on climate and habitat and provides a useful review of foraminifera used in paleotempestology (Murray, 2006). Table 1.1 provides an overview of shallow-water benthic foraminifera suitable for paleotempestology.

Table 1.1

Overview of benthic foraminifera found in nearshore environments

Genus	***Test type***	***Infaunal/ Epifaunal/ Epiphytic***	***Habitat***	***References***
Acervulina	Perforate (hyaline)	Epifaunal	Marine, temperate-warm water, 0-60 m depth, inner shelf	(Debenay, 2013; Javaux & Scott, 2003; Murray, 2006)
Alveolinella	Imperforate (porcelaneous)	Epifaunal	Marine, warm water (18-26 °C), 5-100 m depth, lagoons and inner shelf	(Beavington-Penney & Racey, 2004; Debenay, 2013; Murray, 2006; Nobes & Uthicke, 2008)
Ammonia	Hyaline	Infaunal	Brackish, marine, hypersaline, warm temperate-tropical water, 0-50 m depth, lagoons and inner shelf	(Berkeley et al., 2008; Debenay, 2013; Javaux & Scott, 2003; Murray, 2006; Nobes & Uthicke, 2008)
Amphisorus	Porcelaneous	Epifaunal	Marine, warm water (19-26 °C), 0-50 m depth, lagoons and nearshore	(Berkeley et al., 2008; Debenay, 2013; Javaux & Scott, 2003; Murray, 2006)
Amphistegina	Hyaline	Epifaunal	Marine, >20 °C, 0-130 m depth, coral reefs and lagoons	(Beavington-Penney & Racey, 2004; Debenay, 2013; Javaux & Scott, 2003; Murray, 2006; Nobes & Uthicke, 2008; Orpin et al., 1999)
Archaias	Porcelaneous	Epifaunal	Marine, >22 °C, 0-20 m depth, inner shelf	(Javaux & Scott, 2003; Murray, 2006)
Asterigerina	Hyaline	Epifaunal	Marine, (sub)tropical water, 0-100 m depth, inner shelf	(Javaux & Scott, 2003; Murray, 2006)
Asterorotalia	Hyaline	Epifaunal	Marine, (sub)tropical water, inner shelf	(Murray, 2006; Orpin et al., 1999)
Baculogypsina	Hyaline	Epifaunal	Marine, >25 °C, 0-10 m depth, coral reefs and lagoons	(Beavington-Penney & Racey, 2004; Debenay, 2013; Nobes & Uthicke, 2008; Strotz et al., 2016)
Borelis	Porcelaneous	Epifaunal	Marine, warm water (18-26 °C), 0-40 m depth, coral reefs and lagoons	(Beavington-Penney & Racey, 2004; Javaux & Scott, 2003; Murray, 2006)
Calcarina	Hyaline	Epifaunal	Marine, warm water (18-26 ° C) 0-70 m depth, coral reefs, lagoons and inner shelf	(Beavington-Penney & Racey, 2004; Debenay, 2013; Javaux & Scott, 2003; Murray, 2006; Nobes & Uthicke, 2008; Strotz et al., 2016)
Discorbis	Hyaline	Epifaunal	Marine, temperate-warm water, 0-50 m depth, inner shelf	(Javaux & Scott, 2003; Kitazato & M. Bernhard, 2014; Murray, 2006)
Elphidium	Hyaline	Infaunal/ Epifaunal	Brackish, marine, hypersaline, temperate-warm water, 0-70 m depth, lagoons and inner shelf	(Berkeley et al., 2008; Debenay, 2013; Javaux & Scott, 2003; Kitazato & M. Bernhard, 2014; Murray, 2006; Nobes & Uthicke, 2008; Orpin et al., 1999; Strotz et al., 2016)
Hanzawaia	Hyaline	Epifaunal	Marine, temperate-warm, inner shelf	(Debenay, 2013; Javaux & Scott, 2003; Kitazato & M. Bernhard, 2014; Murray, 2006)
Heterostegina	Hyaline	Epifaunal	Marine, warm water (18-26 °C), 0-130 m depth,	(Beavington-Penney & Racey, 2004; Debenay, 2013; Javaux &

			lagoons and shelf, seeks shadow	Scott, 2003; Kitazato & M. Bernhard, 2014; Murray, 2006; Nobes & Uthicke, 2008)
Homotrema	Hyaline	Epifaunal	Marine, temperate-warm water, coral reefs and inner shelf	(Debenay, 2013; Javaux & Scott, 2003; Murray, 2006)
Marginopora	Porcelaneous	Epiphytic	Marine, warm water (18-26 °C), 0-45 m depth, coral reefs, lagoons and inner shelf	(Beavington-Penney & Racey, 2004; Debenay, 2013; Murray, 2006; Strotz et al., 2016)
Massilina	Porcelaneous	Epiphytic	Marine, temperate-warm water, inner shelf	(Javaux & Scott, 2003; Murray, 2006)
Miliolinella	Porcelaneous	Epifaunal	Marine, hypersaline, 10-30 °C, 0-100 m depth, marshes, lagoons and inner shelf	(Debenay, 2013; Javaux & Scott, 2003; Murray, 2006; Nobes & Uthicke, 2008)
Neorotalia	Hyaline	Epifaunal	Marine, < 10 m depth, reef edges and reef flats, avoids high light levels	(Debenay, 2013; Nobes & Uthicke, 2008; Strotz et al., 2016)
Operculina	Hyaline	Epifaunal	Marine, hypersaline, warm water, 0-130 m depth, lagoon-shelf, medium light levels	(Beavington-Penney & Racey, 2004; Debenay, 2013; Murray, 2006; Nobes & Uthicke, 2008)
Operculinella	Hyaline	Epifaunal	Marine, warm water, 0-130 m depth, lagoon-shelf	(Beavington-Penney & Racey, 2004; Debenay, 2013; Murray, 2006)
Pararotalia	Hyaline	Epifaunal	Marine, warm water, inner shelf	(Debenay, 2013; Javaux & Scott, 2003; Murray, 2006; Nobes & Uthicke, 2008; Orpin et al., 1999)
Parasorites	Porcelaneous	Epifaunal	Marine, 0-70 m depth, protected settings	(Beavington-Penney & Racey, 2004; Debenay, 2013; Nobes & Uthicke, 2008)
Peneroplis	Porcelaneous	Epifaunal	Marine, warm water (18-27 °C), 0-70 m depth, lagoons and inner shelf	(Beavington-Penney & Racey, 2004; Debenay, 2013; Javaux & Scott, 2003; Kitazato & M. Bernhard, 2014; Murray, 2006; Nobes & Uthicke, 2008; Orpin et al., 1999; Strotz et al., 2016)
Planorbulina	Hyaline	Epifaunal	Marine, temperate-warm water, 0-50 m depth, inner shelf	(Debenay, 2013; Javaux & Scott, 2003; Murray, 2006; Nobes & Uthicke, 2008)
Poroeponides	Hyaline	Epifaunal	Marine, temperate-warm water, inner shelf	(Debenay, 2013; Murray, 2006)
Pyrgo	Porcelaneous	Epifaunal	Marine, temperate-warm water, inner shelf	(Debenay, 2013; Javaux & Scott, 2003; Kitazato & M. Bernhard, 2014; Murray, 2006; Nobes & Uthicke, 2008)
Quinqueloculina	Porcelaneous	Epifaunal	Marine, hypersaline, cold-warm water, lagoons, marshes and shelf	(Berkeley et al., 2008; Debenay, 2013; Javaux & Scott, 2003; Kitazato & M. Bernhard, 2014; Murray, 2006; Nobes & Uthicke, 2008; Orpin et al., 1999; Strotz et al., 2016)
Rosalina	Hyaline	Epifaunal	Marine, temperate-warm water, 0-100 m depth, lagoons, inner-mid shelf	(Berkeley et al., 2008; Debenay, 2013; Javaux & Scott, 2003; Kitazato & M. Bernhard, 2014;

				Murray, 2006; Nobes & Uthicke, 2008)
Sorites	Porcelaneous	Epiphytic	Marine, warm water (18-26 °C), 0-70 m depth, lagoons and nearshore	(Beavington-Penney & Racey, 2004; Debenay, 2013; Javaux & Scott, 2003; Murray, 2006; Nobes & Uthicke, 2008; Strotz et al., 2016)
Spirolina	Porcelaneous	Epiphytic	Marine, warm water (18-26 °C), lagoons and nearshore	(Debenay, 2013; Javaux & Scott, 2003; Murray, 2006)
Spiroloculina	Porcelaneous	Epifaunal	Marine, hypersaline, temperate-warm water, 0-40 m depth, lagoons and inner shelf	(Debenay, 2013; Javaux & Scott, 2003; Murray, 2006; Nobes & Uthicke, 2008)
Triloculina	Porcelaneous	Epifaunal	Marine, hypersaline, temperate-warm water, lagoons and inner shelf	(Berkeley et al., 2008; Debenay, 2013; Javaux & Scott, 2003; Kitazato & M. Bernhard, 2014; Murray, 2006; Nobes & Uthicke, 2008; Orpin et al., 1999)

1.4 Archive considerations

Archives used in paleotempestology have the potential to greatly increase our knowledge and understanding of cyclones in the past, present, and future, but there is an important factor that needs to be considered: the concept of uniformitarianism. This is the assumption that the same natural and geological processes that operated in the past, are still at work today. It is assumed that they operated at the same rate and intensity as the contemporary processes, and that they generated the same results that are visible today (Haywood et al., 2011; Hughes et al., 2011; MacDonald, 2017; Romano, 2015). Archives used in paleoclimatology have shown that these assumptions need to be reconsidered. Studies of tree ring characteristics (dendroclimatology/dendrochronology) by D'Arrigo and colleagues (2008), Hughes and colleagues (2011) and Schneider and colleagues (2014) discuss the 'divergence problem': tree ring measurements from recent years show a reduced sensitivity to temperature changes, impacting the assumed direct linear relationship between tree ring characteristics and temperature, and affecting temperature and climate reconstructions based on this relationship. The mechanisms behind this change in sensitivity are not yet understood, and suggestions range from decreased insolation to certain physiological thresholds being exceeded (D'Arrigo et al., 2008; Hughes et al., 2011; Schneider et al., 2014; Sheppard, 2010). Similarly, coral studies showed a positive relationship between temperature and coral calcification rates during the late 20th century (Bessat & Buigues, 2001; Lough & Barnes, 1997, 2000). During recent years however, some studies have found a seemingly inverted relationship. Warmer temperatures caused bleaching events with a reduction in calcification rates as a result, supporting the 'threshold hypothesis' (DeCarlo & Cohen, 2017; Tanzil et al., 2009; Van Oppen & Lough, 2009).

This ‘threshold hypothesis’ has consequences for archive calibration, which is the process of determining the relationship between measured parameters and the response of the archive or proxy to those parameters. Care must be taken in using current conditions to make inferences about the past, since current conditions seems to be the exception rather than the rule. An ‘inverse uniformitarianism concept’ seems to hold more merit; understanding the range of past climates and climate variability, and the drivers responsible, will provide the data for robust modelling of present and future climates (Bradley, 2015; Frank et al., 2010; MacDonald, 2017; Rosol, 2015). Despite this proposed reversal in thinking, the calibration problem remains; there is no other record to compare archives to besides our short instrumental record. As a result, the multi-proxy approach has gained popularity: cross-referencing multiple archives or proxies, preferably of a biological and non-biological nature, to minimise calibration errors and threshold sensitivity while increasing temporal resolution (Frank et al., 2010; Kiage & Liu, 2006; MacDonald, 2017). Confirming findings across a range of records will also increase the reliability of the findings, further reducing recording and preservation biases.

Although the previous considerations focus on paleoclimatological archives, they also apply to paleotempestology. The reconstruction of extreme events in paleotempestology is based on physical evidence deposited by hydraulic processes: the presence of overwash deposits or beach ridges, or the presence of sediments and foraminifera in environments they do not normally occur in. These physical processes can also be impacted by changes in environmental parameters. Sea level rise (SLR) can affect the deposition of sediments and foraminifera, since SLR causes storm surges or waves to deposit sediments higher up on shore or further inland without an increase in cyclone intensity (Woodruff et al., 2013). SLR also influences wave interaction with bottom sediments due to changes in water depth and tide range, causing changes in the types of foraminifera and sediments that are deposited as a result. A Category 3 cyclone that occurred when sea level was lower than present will therefore have a different signature in the sedimentary records compared to a contemporary Category 3 cyclone, despite having the same intensity. SLR of a few centimetres is not going to change the footprint noticeably, but a difference of 1-2 metres will (Yin et al., 2021). SLR can also affect other environmental parameters such as water temperature and light attenuation at a location, possibly causing foraminiferal habitat changes due to physiological threshold exceedance. (Milker et al., 2022). Along the same line, tides will also influence the footprint left behind by cyclones. Cyclone-generated waves and surges impacting the coast during low tide will not prograde as far inland as waves and surges generated during high tide or spring tide. Paleotempestologists therefore need a thorough understanding of the environmental conditions of the studied period and need to understand interactions between environmental processes.

Another consideration for paleotempestological research is location suitability since some environments record cyclone occurrences better than others. Locations selected for research need to experience minimal ‘background noise’: cyclones need to be extraordinary enough to leave an obvious footprint in the sedimentary records of that location. If a location experiences multiple winter storms every year as part of the natural conditions, sediments deposited during these storms can obscure or erase evidence of cyclones that are truly exceptional for that location. Ideal research locations would be those areas that experience stable climate and weather throughout the year, except for those occasional cyclone occurrences.

Preservation bias must also be considered: protected back-barrier lagoons and sinkholes are more conducive to retaining evidence of cyclones than sand beaches that are exposed to, and possibly disturbed by, human interference and natural processes (Brill et al., 2014; Pilarczyk et al., 2014). Besides environment type, the physical and geographical characteristics of a location also need to be considered. The orientation of the coast in relation to the cyclone plays a significant role in possible evidence retention. If waves are coming in perpendicular to shore, evidence might be retained since the waves have enough energy to deposit sediments onto or behind the beach. If waves come in at an angle to the coast or travel alongshore, wave energy is dissipated, and evidence might not be retained. Other characteristics such as bathymetry and sediment type also affect evidence preservation (Woodruff et al., 2013). It needs to be emphasised that not every cyclone will leave a trace in the sedimentary records, regardless of protected or open settings. As an example, Hippensteel & Garcia (2014) only found sedimentary evidence of up to 9 cyclones in North Carolina, USA, while the instrumental records show at least 17 cyclones impacting that location during the reconstructed period.

Taphonomic processes can affect evidence retention by changing the composition and preservation of foraminifera tests during their transition from living organism to fossil specimen (Murray, 2006). The main taphonomic processes are bioturbation and bioerosion, diagenesis and dissolution, and weathering (Berkeley et al., 2007). Bioturbation is the movement of organisms on sediment surfaces and through sediment layers. This movement causes mixing and unmixing of sediment layers, and changes in soil chemistry due to mucus excretion and pore water circulation (Murray, 2006). Bioturbation affects the position of foraminifera tests in the sediment, e.g., the upward movement of older tests through burrowing and waste product removal by infaunal organisms. These tests end up in the same sediment layer as younger or contemporary foraminifera, impacting the accuracy of dating and stratigraphic analyses used in paleotempestology. The changes in soil chemistry can also cause tests to be diagenetically altered or dissolved through bioerosion. Bioerosion is the actual degradation of tests through processes caused by organisms, e.g., predators boring holes in the test wall (Frozza et al., 2020). This can weaken the structural integrity of the test, reducing its chances of being preserved in sediment records. Since the narrow habitat range of foraminifera contributes to the precise determination of sediment provenance and cyclone intensity, loss of foraminifera tests from the sediments will significantly complicate precise event reconstructions. Bioerosion can also make the test look more degraded and therefore older than it is, which impacts visual dating analyses and the reconstruction of cyclone chronology.

Diagenesis and dissolution impact the structural integrity of tests through chemical alteration. Diagenesis is a change in the chemical composition of the test, e.g., alteration from one form of calcium carbonate (aragonite) to another (calcite) (Edgar et al., 2015). While aragonite is chemically less stable than calcite, it is more structurally robust. Diagenesis occurs after the death of an organism and is a result of the test trying to reach chemical equilibrium with the surrounding environment. Diagenesis from aragonite to calcite weakens the structural integrity of the test (Poirier et al., 2021). Dissolution has the same effect on foraminifera preservation as diagenesis, it weakens the test structure and reduces its chances of preservation in the record by physically dissolving the test and making it thinner and weaker. Weathering is the physical damaging and destruction of tests. This can happen through repeated burial, excavation and transport by waves, currents, and winds, as well as biological activity. These processes can cause the tests to crack, chip or fracture. Abrasion and scouring create depressions and grooves in the test which affect its structural integrity. These damaged areas on the test also give bioeroders a chance to drill into the test, further weakening it and reducing preservation (Beavington-Penney & Racey, 2004).

The advantage of these taphonomic processes is that they provide many clues about the processes that occurred after the death of an organism. As discussed by Murray, transport of foraminifera during storms results in abrasion of the test. The more abraded the test is, the further the test has been transported since the death of the organism (Murray, 2006). Severely abraded tests are an indication of long residence times in the environment between the death of the organism and the final deposition of the test, which means they are not directly related to the event that deposited them. If tests show little or no signs of abrasion on the other hand, the organisms were only transported over a short distance and were deposited soon after their death or died in-situ due to the studied event. These are the tests that need to be used in paleotempestological research and for dating purposes. The same applies to other forms of test alteration: significant bioturbation and bioerosion indicate disturbance and possible relocation of tests by other organisms, meaning that their place within the sediment is not an accurate representation of the actual deposition by an extreme event (Pilarczyk et al., 2014).

Timeframes are important to consider as well, particularly what part of the geological record is being studied. Paleoclimatological research and sea-level reconstructions have shown that sea levels around the world have only been at their current level for about 6,000-7,000 years, depending on the geographical region (Lewis et al., 2013). Before that, climates and sea levels differed too much from modern climates and sea levels to make any useful inferences about cyclogenesis and their impact on land. Paleotempestological research therefore needs to be constrained to the Holocene epoch and the past 6,000-7,000 years, with a particular focus on the mid- to late Holocene after sea levels stabilized (Woodruff et al., 2013).

Although the considerations stated above might complicate paleocyclone reconstructions and might reduce the preservation potential of foraminifera, it is unlikely that a contemporary foraminifera species, living in the clear and saline waters of a reef crest, used to live in the brackish and muddy waters of a marsh in the past. These habitats are too dissimilar and would require morphological and/or physiological adaptations (Beavington-Penney & Racey, 2004; Murray, 2013). It is therefore still acceptable to say that contemporary foraminifera species inhabit the same *type* of habitat as their historical counterparts, e.g., shallow marine, abyssal or brackish marsh habitats. Sediment type and grain size will also continue to provide information about cyclone activity, regardless of environmental conditions. If a coarse sand and gravel deposit containing marine foraminifera is found in a brackish, muddy marsh environment, cyclone deposition can still be inferred (Brill et al., 2016). Reconstructing the intensity of the cyclone depends on how much is known about the environmental parameters at the time of deposition. It can also be concluded that some environments are more conducive to preservation of cyclone evidence than others. Optimal preservation of overwash deposits will occur in an environment that experiences minimal disturbance: no frequent storms or waves to rework the sediments (except for the occasional cyclone that deposits the sediments and is the target of the research), little infaunal or epifaunal activity to minimize bioerosion and bioturbation, and stable chemical soil composition to minimize test dissolution and diagenesis. Hypersaline back-barrier lagoons or sinkholes are good examples of suitable environments (Pilarczyk et al., 2014). Relatively few organisms are adapted to the extreme environmental conditions of hypersaline lagoons and sinkholes, minimising bioerosion and bioturbation. Due to the waterlogged sediments in lagoons and sinkholes, the deposits are not subaerially exposed which limits weathering and prevents aeolian transport. Barriers will protect the deposits from being reworked by waves and tides, effectively preserving the sedimentary records for paleotempestological research.

1.5 Paleotempestological research to date

The research field of paleotempestology has received increased attention over the past few decades due to short instrumental records, climate change, increasing population sizes near the coast and therefore increasing costs and loss of life due to cyclones. Despite this increase in attention, certain tropical regions of the world are underrepresented in paleotempestological research, and particularly in foraminiferal paleotempestological research. There are several possible explanations for this underrepresentation: firstly, some tropical regions are remote and sparsely populated, and therefore costly and time-consuming to conduct research in. The low population numbers also reduce the urgency of creating an extensive cyclone record and accurate cyclone models, since cyclones in these areas have a relatively small impact on lives and livelihoods when they do occur. Examples of sparsely populated tropical regions are Western Australia and island nations in the Pacific Ocean such as Kiribati and Vanuatu. Secondly, some tropical regions are situated too close to the equator and the Intertropical Convergence Zone to experience cyclones on a regular basis, resulting in a lack of evidence in the sediment records (Smithers & Hoeke, 2014). Thirdly, the lack of foraminiferal research might be due to the unassuming and inconspicuous nature of the organisms: there are other, more visibly striking lines of cyclone evidence such as beach ridges, that preferentially attract the attention of paleotempestological researchers. Finally, another limitation is the preservation of foraminifera in overwash deposits. As discussed in section 1.4, the ideal depositional setting requires a combination of environmental conditions that is relatively rare in the tropics: a protected location that experiences no anthropological, hydrological, or geomorphological disturbances, little to no infaunal and epifaunal activity to minimize taphonomic alteration of tests, and stable chemical soil composition (Brill et al., 2014; Pilarczyk et al., 2014).

Most (sub)tropical paleotempestological research has been carried out in the Atlantic Ocean basin (Braun et al., 2017; Bregy et al., 2018; Collins et al., 1999; Hawkes & Horton, 2012; Hippensteel & Garcia, 2014; Horton et al., 2009; Lane et al., 2011; Martin & Muller, 2021; Mitchell et al., 2022; Peros et al., 2015; Scott et al., 2003; Williams, 2013). A comprehensive review of paleotempestological research in the western North Atlantic basin was published by Oliva and colleagues in 2018, although this also includes paleotempestological research that did not use microfossils as an archive (Oliva et al., 2018). The United States' and Caribbean coastlines are densely populated and on average suffer US$15.6 billion in damage each year due to cyclone impacts, explaining the proliferation of paleotempestological research projects in this area (Bakkensen & Mendelsohn, 2019).

The other ocean basins are significantly underrepresented in terms of tropical paleotempestology. In the Indian Ocean basin, only a few studies have generated paleotempestological reconstructions using foraminifera, due to the coastal areas being sparsely populated or situated too close to the equator. Hussain and colleagues used a multiproxy approach, including foraminifera, to show evidence of extreme wave events in sediment layers in India (Hussain et al., 2013). Brill and colleagues (2020) used the same method to reconstruct extreme events in the past 80 years in Myanmar. May and colleagues reconstructed cyclone and tsunami occurrences in the past 150 years in north-western Australia (May et al., 2015). Another research project reconstructed the Holocene sea-level history and extreme event occurrences just south of Broome in Western Australia using a multiproxy approach (Engel et al., 2015).

The Pacific Ocean basin has received more attention from paleotempestologists, but research is once again primarily concentrated around densely populated areas. Williams and colleagues reconstructed cyclones in the Gulf of Thailand over the past 8,000 years using a multi-proxy approach (Williams et al., 2016). To the north, in the Bohai Sea off the Chinese coast, Du and colleagues reconstructed extreme events from foraminifera evidence in aeolian deposits, focusing on the last interglacial period about 125,000-130,000 years ago (Du et al., 2016). Chen and colleagues examined sand cays on an island in the South China Sea to determine the occurrence of nine cyclones in the past 400 years (Chen et al., 2019). Some modern events have also been reconstructed: in the Philippines, Pilarczyk and colleagues and Soria and colleagues analysed overwash deposits generated by cyclone Haiyan in 2013 (Pilarczyk et al., 2016; Soria et al., 2018). Kosciuch and colleagues analysed the foraminiferal assemblages in overwash deposits in Vanuatu that are attributed to the 2015 cyclone Pam (Kosciuch et al., 2018). One research project was carried out in French Polynesia: Isaack and colleagues reconstructed paleocyclone occurrences in the past 5,000 years using sediments and foraminifera from Bora Bora (Isaack et al., 2016).

Since many of the cyclones that form over the warm waters of the Pacific Ocean track in a westerly direction due to the trade winds and the Coriolis effect, the tropical Australian east coast should receive considerable attention from researchers interested in foraminifera, but the opposite is true. Besides the few research projects in Western Australia mentioned earlier, microfossils have rarely been used to reconstruct cyclone occurrences in any other part of the country. According to the Australian Bureau of Meteorology (BoM), the Western South Pacific off Australia's east coast experiences cyclones on an annual basis, with an average of 4 cyclones occurring each year (2021). The paleotempestological research that has been conducted here has mainly focused on beach ridges: Forsyth analysed the morphology, sedimentology and luminescence chronology of three ridge plains in north-east Queensland, but didn't use microfossils as a proxy (Forsyth, 2013). Nott & Hayne (2001) and Nott (2003) analysed the morphology of beach ridges and combined their analysis with theoretical modelling to reconstruct paleocyclones. Other research includes the examination of a floodplain (Leonard & Nott, 2016), isotope analyses from speleothems and rainwater generated during a cyclone (Haig et al., 2014; Munksgaard et al., 2015; Nott et al., 2007), cyclone impacts on nearshore reefs (Perry et al., 2014; Puotinen, 2004), and reef growth on the central GBR during the Holocene period through coral core and microatoll analyses and Uranium-Thorium (U-Th) dating (Ryan, 2016; Ryan et al., 2016).

The only two research projects on the Australian east coast that have used microfossils as a proxy were carried out by Strotz and colleagues (2016) and Nott and colleagues (2013). Strotz and colleagues examined the foraminifera record on Heron Reef, before and after the passage of cyclone Hamish in 2009, to better understand changes in foraminifera assemblages due to cyclone impacts. Their findings indicated an increase in foraminiferal assemblage similarity between sampling sites directly after the cyclone, and a return to the original, diversified assemblage composition in subsequent samples. Nott and colleagues used a multiproxy approach, including foraminifera, to reconstruct cyclone Yasi and three other extreme events that impacted the northeast coast of Australia in the past 100 years. They concluded that marine diatoms and foraminifera in washover sediments are an indicator of deposition by cyclones but did not go into detail about depth or habitat preferences of specific species. Table 1.2 provides an overview of the tropical paleotempestological research carried out to date.

Table 1.2

(Sub)tropical paleotempestological research to date, using foraminifera as a proxy, sorted by ocean basin

Ocean Basin	***Location***	***Collection methods***	***Analyses***	***Resolution***	***Reference***
Atlantic	St. Catherine's Island, Georgia, USA	• 3 vibracores, paleomarshes • 1 vibracore, wetland	• Loss-on-ignition • X-ray fluorescence • Foraminiferal assemblages • Radiocarbon dating • Lead dating	• Max. penetration 475 cm • 3,300 yr before present (BP ~1950 AD) • 7 cyclones • Return period 471 years on average	Braun et al., 2017
Atlantic - Gulf of Mexico	Mississippi Sound, Mississippi, USA	• 3 hammer cores, coastal pond • 1 vibracore, beach	• Loss-on-ignition • Grain size distribution • Foraminiferal assemblages • Cesium dating • Radiocarbon dating	• Max penetration 113 cm • 2,500 yr BP • 12 cyclones • Return period variable	Bregy et al., 2018
Atlantic	McClellanville, South Carolina, USA	• 40 gouge-auger cores, beach ridge and pond	• Loss-on-ignition • Foraminiferal assemblages • Lead dating • X-radiographing	• Max. penetration 60 cm • 1845 AD • Cyclone Hugo, possibly 2 others	Collins et al., 1999
Atlantic – Gulf of Mexico	Galveston Island & San Luis Island, Texas, USA	• 31 gouge-auger cores, back-berms	• Loss-on-ignition • Grain size distribution • Foraminiferal assemblages	• Max. penetration 34 cm • Cyclone Ike	Hawkes & Horton, 2012
Atlantic	Onslow Bay, North Carolina, USA	• 10 gouge-auger cores, back-barrier and coastal marshes	• Wet sampling • Grain size distribution • Foraminiferal assemblages • Radiocarbon dating	• Min. penetration 300 cm • 1,500 yr BP • 5-9 cyclones, less than recorded cyclones (17)	Hippensteel & Garcia, 2014
Atlantic – Gulf of Mexico	Ocean springs, St. Andrews, Mississippi, USA, Dauphine Island, Alabama, USA	• Sediment samples from trenches in back-barrier marshes	• Grain size distribution • Foraminiferal assemblages	• Trench depth 50 cm • Cyclones Katrina and Rita	Horton et al., 2009
Atlantic – Gulf of Mexico	Apalachee Bay, Florida, USA	• 2 vibracores, coastal sinkhole • 2 piston cores, coastal sinkhole	• Loss-on-ignition • Grain size distribution • Foraminiferal assemblages • Radiocarbon dating	• Max. penetration 619 cm • 4,500 yr BP • 107-177 events • 7-year temporal resolution	Lane et al., 2011

			• Spectral analysis • Lead dating • Cesium dating	• 2.4-3.9 cyclones per century on average	
Atlantic – Gulf of Mexico	Estero Bay, Florida, USA	• 4 gouge-auger cores, back-barrier lagoon	• Loss-on-ignition • Grain size distribution • Foraminiferal assemblages • Lead dating	• Max. penetration 30 cm • 11.4 years old 0-5 cm depth • Cyclone Irma	Martin & Muller, 2021
Atlantic – Caribbean Sea	Anegada, British Virgin Islands, Caribbean	• 240 surface sediment samples, transects from dunes to reef crest	• Foraminiferal assemblages • Taphonomy	• Cyclone Irma	Mitchell et al., 2022
Atlantic – Caribbean Sea	Cuba, Caribbean	• Surface sediments, back-barrier lagoon • 4 Russian Peat cores, back-barrier lagoon	• Loss-on-ignition • Grain size distribution • Charcoal analysis • Foraminiferal assemblages • Radiocarbon dating • Cesium dating	• Max. penetration 211 cm • 3,500 yr BP • Cyclone resolution not specified	Peros et al., 2015
Atlantic	Singleton Swash, South Carolina, USA	• 3 vibracores, marsh	• Loss-on-ignition • Foraminiferal assemblages • X-radiography • Radiocarbon dating	• Max. penetration 358 cm • 5,700 yr BP • 12 cyclones • Return period variable	Scott et al., 2003
Atlantic – Gulf of Mexico	Louisiana's Chenier Plain, Louisiana, USA	• Gouge-auger cores, chenier/beach ridge plain	• Loss-on-ignition • Foraminiferal assemblages • Radiocarbon dating • Cesium dating	• Max. penetration 150 cm • 600 yr BP • Return period 1.2 cyclones per century on average but variable	Williams, 2013
Indian Ocean	Velanganni, India	• 1.2 m x 1.2 m trench, beach ridge	• Oven dried • Grain size distribution • Foraminiferal assemblages	• Max. penetration 120 cm • 2 cyclones • Age and return period unknown	Hussain et al., 2013
Indian Ocean	Rakhine coast, Tanintharyi coast Myanmar	• Trenches, back-barrier area, beach ridge, coastal plain	• Grain size distribution • Carbon content • Foraminiferal assemblages • Radiocarbon dating • Lead dating • Cesium dating	• Max. penetration 50 cm • 700 yr BP • 4 cyclones • Resolution unreliable due to shoreline retreat	Brill et al., 2020

			• Optically stimulated luminescence (OSL) dating		
Indian Ocean	Onslow, Western Australia, Australia	• 1 percussion core, back-barrier washover plain • 6 gouge-auger cores, back-barrier washover plain	• Loss-on-ignition • Grain size distribution • Foraminiferal assemblages • Magnetic susceptibility • X-ray fluorescence • X-ray diffraction • OSL dating • Radiocarbon dating	• Max. penetration 900 cm • 7,700 yr BP • 3 cyclones • 2 tsunamis • Return period 50 years on average (cyclones only)	May et al., 2015
Indian Ocean	McKelson Creek, Western Australia, Australia	• 4 percussion cores, mudflat • 15 sediment profiles, foredunes	• Loss-on-ignition • Grain size distribution • Foraminiferal assemblages • Radiocarbon dating	• Max. penetration 830 cm • 8,350 yr BP • 3-5 events, cyclones or tsunamis inconclusive • Resolution unreliable due to erosional setting	Engel et al., 2015
Pacific Ocean – Gulf of Thailand	Cha-am, Kui Buri, Thailand	• 8 vibracores, marsh • 4 vibracores, beach ridge swale	• Oven dried/air dried • Grain size distribution • Foraminiferal assemblages • Radiocarbon dating	• Max. penetration 208 cm • 8,000 yr BP • 19 cyclones • Return period variable	Williams et al., 2016
Pacific Ocean – Bohai Sea	Miaodao Archipelago, China	• Coring technique unknown	• Air dried • Grain size distribution • Foraminiferal assemblages • Radiocarbon dating • OSL dating	• Max. penetration 650 cm • Resolution 0-130 KA • 15 cyclones between 73-88 KA	Du et al., 2016
Pacific – South China Sea	Guangjin Island, China	• 2 m deep pit, sediment samples every cm and every 2 cm as control, back-beach area	• Air dried • Grain size distribution • Foraminiferal assemblages • Radiocarbon dating • Uranium-Thorium (U/Th) dating	• Max. penetration 200 cm • 450 yr BP • 9 cyclones • Return period variable	Chen et al., 2019
Pacific – Leyte Gulf	Samar Island, Leyte Island, Philippines	• 41 gouge-auger cores, back-beach area • 3 shallow trenches, back-beach area	• Wet sampling • Foraminiferal assemblages • Taphonomy	• Cyclone Haiyan	Pilarczyk et al., 2016

Pacific – Leyte Gulf	Hernani, Philippines	• 24 gouge-auger cores, beach and back-beach area • 4 shallow trenches, beach and back-beach area	• Loss-on-ignition • Carbonate content • Grain size distribution • Foraminiferal assemblages • Taphonomy	• Cyclone Haiyan	Soria et al., 2018
Pacific – Coral Sea	Efate Island, Tanna Island, Vanuatu	• 53 samples walking, diving, Ekman grab sampler, bay area • 5 trenches	• Wet and dry sampling • Grain size distribution • Foraminiferal assemblages • Taphonomy	• Cyclone Pam	Kosciuch et al., 2018
Pacific	Bora Bora, French Polynesia	• 7 vibracores, reef lagoon	• Wet and dry sampling • Grain size distribution • Carbonate content • Foraminiferal assemblages • X-ray fluorescence • Radiocarbon dating	• Max. penetration 460 cm • 10,000 yr BP • Cyclone frequency not specified	Isaack et al., 2016
Pacific – Coral Sea	Heron Island, Queensland, Australia	• 18 surface samples, reef flat • 1 Ponar grab sample, channel	• Oven dried • Grain size distribution • Foraminiferal assemblages • Taphonomy	• Cyclone Hamish	Strotz et al., 2016
Pacific – Coral Sea	Cowley Beach, Tully Heads, Cardwell, Queensland, Australia	• 14 pits, across beach ridges	• Dried samples • Grain size distribution • Foraminiferal assemblages • X-ray fluorescence	• Max. penetration 90 cm • 1900 AD • 4 cyclones	Nott et al., 2013

Based on this review, it can be concluded that, despite its long tropical coast and exposure to tropical cyclones, Australia is underrepresented in paleotempestological research compared to other continents. Furthermore, the use of foraminifera for paleotempestology in Australia has been restricted to four research projects, with two projects carried out in Western Australia and two research projects conducted in Queensland. The two projects in Queensland only looked at cyclone occurrences within the instrumental record period, which means that foraminifera have never been used to reconstruct a high-resolution paleocyclone history for Queensland.

1.6 Conclusion

Cyclones can be devastating natural disasters that impact (sub)tropical regions and cause significant loss of lives and livelihoods. The ability to accurately model cyclogenesis and future cyclone behaviour under climate change is constrained by short and spatially biased instrumental cyclone records and limited insights into the response of cyclone intensity, frequency, and distribution to climate variability (Knutson et al., 2010; Kumar, 2020) The research field of paleotempestology aims to extend cyclone records by examining biological, geomorphological, and geochemical archives and proxies to infer the occurrence of cyclones prior to the start of the instrumental records. The most frequently used paleotempestological archives are overwash deposits and beach ridges, with microfossils commonly used as proxies within these archives. Dating techniques are used to provide cyclone and depositional chronologies, expressed in absolute ages. Each archive and proxy has advantages and shortcomings that need to be considered, in combination with general considerations such as the validity of the uniformitarianism concept. Due to these considerations, researchers have adopted a multi-proxy approach when conducting paleotempestological research, to minimize recording and preservation biases and negate other possible limitations to research techniques.

One of the proxies that has the potential to reconstruct paleocyclones with great precision is microfossils. The microfossils most suitable for paleocyclone reconstructions are benthic shallow-water foraminifera, since they occur in abundance in (sub)tropical regions and each species has a narrow range of optimal environmental parameters in can tolerate and will therefore live in. To use foraminifera as a paleotempestological proxy, preservation is key and is most likely to occur in protected settings free from anthropological and geomorphological processes. Despite the potential advantage of using foraminifera as a paleotempestological proxy, relatively little is known about foraminifera species and their preferred habitats, and reviews are scarce. Foraminifera are also underrepresented in tropical paleotempestology research conducted outside the Atlantic Ocean basin, as shown by the summary of foraminiferal paleotempestological research carried out to date. There are several possible reasons for this underrepresentation, such as remoteness of research locations and low population numbers, inconspicuousness of foraminifera compared to other paleotempestological archives and proxies, and the relative scarcity of locations conducive to foraminifera preservation. Despite these possible shortcomings of foraminifera as a proxy, it has been shown that there are tropical locations that provide protected settings conducive to paleotempestological foraminifera research.

1.7 Aims and objectives

The aim of this research project is to test the following hypothesis: *Foraminifera exhibit species-specific depth preferences and can be used to reconstruct Holocene cyclone occurrences at Middle Island on the central GBR, Queensland, Australia.*

To test the hypothesis, the objectives of this research project are:

1) To describe and quantify the distribution, habitat, and depth preferences of contemporary foraminifera from Middle Island on the central GBR.
2) To analyse sediment cores from the ephemeral lake on Middle Island for overwash deposits and foraminiferal presence
3) To reconstruct Holocene cyclone occurrences at Middle Island based on the collected data
4) To assess the strengths and limitations of a novel research method that uses species-specific depth preferences of foraminifera to reconstruct paleocyclone occurrences

1.8 Research location

Both the deposition and the preservation of paleotempestological archives and proxies are vital for paleocyclone reconstructions. Furthermore, details about present and past hydrological, geomorphological, and environmental parameters at the depositional location need to be understood to correctly interpret the paleocyclone record. Due to these requirements, Middle Island was chosen as the location for this research project (Figure 1.3).

Figure 1.3

Location of Middle Island on the central Great Barrier Reef

Note. From *Koci, 2024.*

Middle Island (19°59'S, 148°21'E), is a 1.2 km long and 500 m wide island that is situated in Edgecumbe bay, ~10 km off the coast of Bowen, Queensland, Australia. It is situated in the dry tropics and experiences a stable climate with temperatures ranging from 19.5-28.6 °C and an average annual rainfall of 895 mm (averaged over 1987-2015) (Bureau of Meteorology, 2024b). Most of the rainfall occurs during the Austral summer, which lasts from December to March. During fair-weather conditions, the island is sheltered from the prevailing south-easterly trade winds by Cape Gloucester and Gloucester Island to the east. Its sheltered position reduces the length of water over which winds can blow (fetch), which limits the impact of fair-weather waves on the island's shorelines. Due to its stable climate, absence of seasonal storms and protection from fair-weather waves, the cyclones that periodically form in the region are the only cause of possible overwash deposits on Middle Island. A readily available source for these overwash deposits is the fringing reef on the island's southwestern side, with a reef flat that is ~300 m wide at its widest and reef slopes that are near-vertical. Both the reef flat and reef slopes provide overwash deposit material, as well as habitats for marine organisms and microfossils such as foraminifera.

In addition to providing a suitable location for possible archive deposition, Middle Island also has good preservation potential. Due to its sheltered setting and the difference in magnitude between fair-weather conditions and cyclonic conditions, overwash deposits can be preserved on the island once deposited. This preservation potential is shown by the shingle ridge that is located behind the beach on the southwestern side of the island. Previous research in this location has shown that the shingle ridge is the result of deposition by cyclone-generated waves (Ryan, 2016). The ridge height was measured at 6.3 m above lowest astronomical tide (LAT) and its width varies between ~50-70 m. The ridge has been stable long enough for vegetation to establish and grow on it, which supports the preservation potential of overwash deposits on the island. An ephemeral lake has formed behind the ridge and is hypothesised to have been an embayment with an open connection to the ocean. The deposition of the shingle ridge severed the connection between the ocean and the bay, transforming the latter into an inland lake (Figure 1.4).

Figure 1.4a

Middle Island features relevant to this research project

Note. From *Geonadir, 2024.*

b

Vegetated shingle ridge on the southwestern side of Middle Island

The lake is ephemeral and primarily contains water during the wet season, partially due to runoff from the surrounding hillslopes. The lake's surface is vegetated by grasses and a few dispersed trees and lies ~2.5 m above LAT. Because of the vegetation in the lake and the periodical runoff from the surrounding hillslopes, the sediments in the lake are mostly composed of organic material and siliciclastic grains. Any marine sediments that are washed into the lake as overwash deposits will leave a recognisable footprint in the sediment stratigraphy due to their different chemical composition, presence of marine organisms and coarser grain size. When overwash deposits are deposited in the lake, they are protected from being reworked by waves and wind and are therefore likely to be preserved. Furthermore, Middle Island is uninhabited, and a permit is required to access the island for research purposes or other invasive activities. Absence of anthropogenic influences minimises the disturbance of sediments and overwash deposits and increases their preservation potential.

Previous studies at Middle Island have provided insights into the geomorphological history of the island. Ryan and colleagues (2016) collected reef cores from the reef flat and reconstructed a chronostratigraphic reef record based on U-Th dates. The reef at Middle Island was shown to have initiated around ~7,900 yBP (years before present, present being 1950), with reef growth continuing until around ~6,500 yBP. After this period, reef framework ages showed a hiatus of ~5,000 years, which Ryan et al., interpreted to be the result of repeated cyclone impacts that stripped the reef flat. This conclusion was supported by a radiocarbon date that was obtained from the shingle ridge on the southwestern side of the island. The date of 4,555 ± 140 yBP that was obtained for the ridge provides a temporal constraint regarding its placement and coincides with the hiatus in reef flat ages retrieved from the cores. The height of the ridge and the amount of material needed to deposit the ridge indicate cyclonic conditions, and the age of ridge combined with the reef age hiatus showed that this material originated from the reef flat. In addition to reef growth reconstructions, Ryan and colleagues determined sea level histories for Middle Island. Fossil microatolls on the reef flat indicate that sea level was around ~1 m higher when the reef flat reached sea level around 6,500 yBP, which is supported by other studies that have reconstructed sea level histories for Australia (Lewis et al., 2013; Ryan et al., 2016). The previously collected information supports the hypothesis that Middle Island is a suitable research location for paleocyclone reconstructions, due to the excellent deposition and preservation potential of overwash deposits, as well as age constraints for paleocyclone reconstructions.

1.9 Project significance

This research project is significant for several reasons. Firstly, a new method for use in paleotempestological research will be developed and tested. Species specific depth preferences of foraminifera have the potential to greatly improve the resolution of paleocyclone reconstructions but have never been used as a paleotempestological proxy. Instead of being able to only infer cyclone frequency based on the number of overwash deposits, depth preferences are hypothesised to provide information about sediment provenance, cyclone intensity and wave height. Secondly, this research project will increase the knowledge about foraminifera species and their species-specific habitat- and/or depth preferences around Middle Island. A detailed foraminiferal database with location-specific assemblage information does not currently exist, which restricts the use of foraminifera as a proxy for ecological and environmental reconstructions. Lastly, extending our cyclone records and increasing their resolution will provide greater insight into cyclone variability throughout the Holocene, which can then be linked to possible drivers of this variability. An improved understanding of the links between cyclogenesis and drivers will advance the performance of current cyclone models and will better inform the modelling of cyclone occurrence, frequency, and intensity in the future under anthropogenic climate change. It will also provide a better framework for coastal management decisions, and for coastal communities to minimise the damage to lives and livelihoods caused by current and future cyclones.

1.10 Thesis structure

This thesis is divided into four chapters and is centred around the hypothesis*: <u>Foraminifera exhibit species-specific depth preferences and can be used to reconstruct Holocene cyclone occurrences at Middle Island on the central GBR, Queensland, Australia</u>*.

Chapter 2 describes and quantifies contemporary foraminiferal assemblages found on the reef flat and reef slopes around Middle Island. This addresses the knowledge gap concerning the paucity of location-specific foraminiferal assemblage descriptions. Statistical analyses were used to determine whether species can be assigned to specific depth ranges, which was identified as another knowledge gap of particular importance to paleotempestological research.

Chapter 3 analyses overwash deposits in sediment cores that were retrieved from the ephemeral lake on Middle Island. The sediment core stratigraphy was documented, and sediment samples were analysed for grain size distribution and foraminiferal content. Based on the results from chapter 2, foraminifera in the sediment cores were assigned to provenance depth where possible. This enabled the reconstruction of wavelengths that deposited the sediments and foraminifera in the lake, and the overwash deposits were used to draw conclusions about cyclone occurrences and frequency at Middle Island during the Holocene.

Chapter 4 provides a discussion of the findings from the previous chapters and presents the answer to the research hypothesis. This chapter also provides suggestions and recommendations for future research, based on the results from the previous thesis chapters (Figure 1.5).

Figure 1.5

Schematic thesis chapter overview

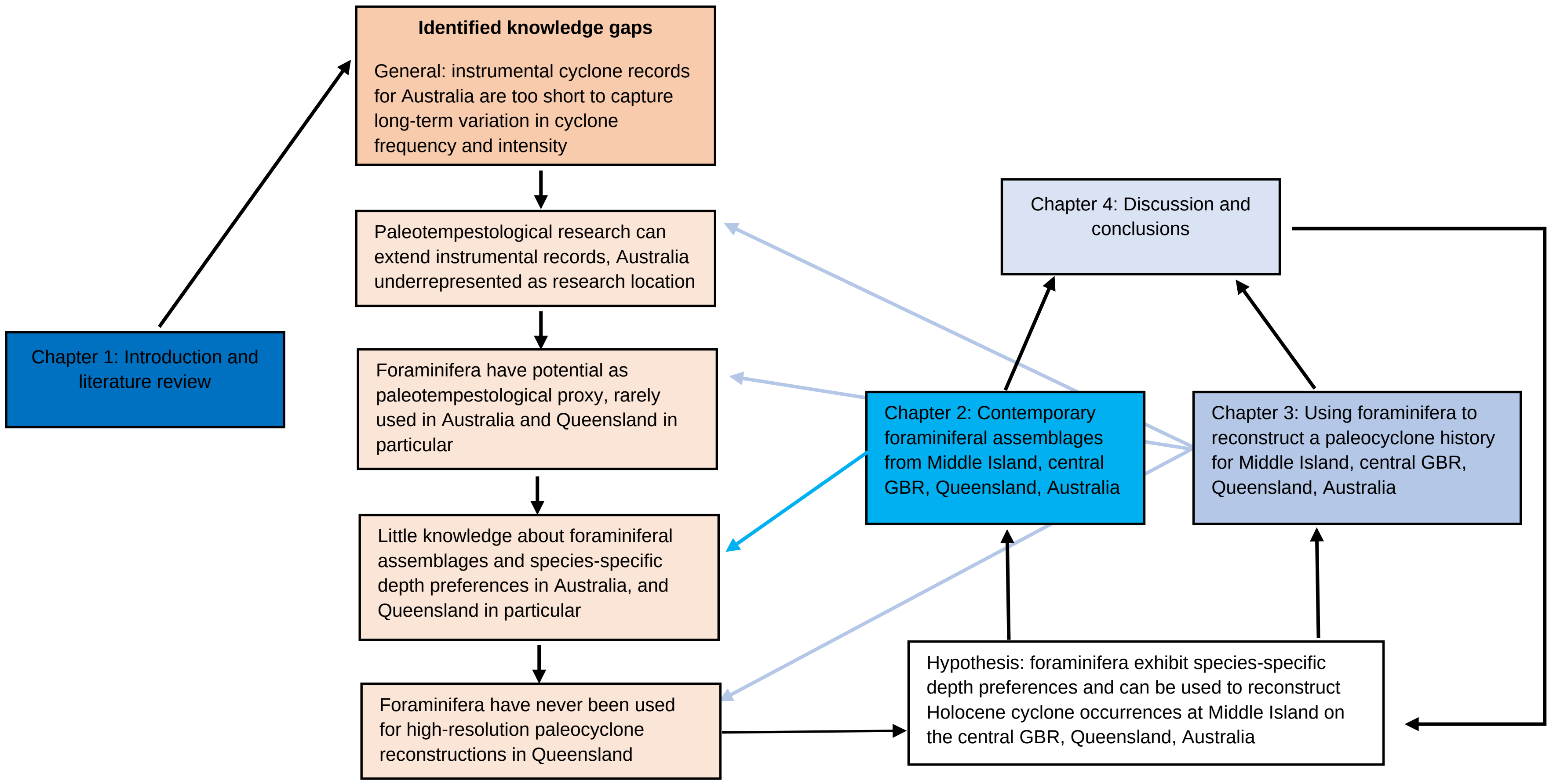

2. Contemporary foraminiferal assemblages from Middle Island on the central Great Barrier Reef, Queensland, Australia

This chapter describes and quantifies the foraminiferal assemblages from the reef flat and reef slopes around Middle Island on the central Great Barrier Reef, Queensland, Australia. Statistical analyses are performed to determine whether foraminifera exhibit species-specific depth preferences at this location.

Plate 2

Note. Spiroloculina elegans.

2.1 Introduction

Cyclones, associated with extreme winds, heavy rainfall, storm surges and waves, have caused the loss of 8,000 lives and AU$39 billion in damage on average each year since 1960 (Bakkensen & Mendelsohn, 2019; Sharkov, 2012; Wahiduzzaman et al., 2022) Despite the threat to lives and livelihoods, accurately predicting cyclone formation (cyclogenesis) and behaviour remains difficult due to the multitude of climatic and environmental variables that influence these complex systems. Additionally, short instrumental records of 70 years (Pacific Ocean basin) to 120 years (Atlantic Ocean basin) provide a limited frame of reference for computer models that are now widely used to predict cyclone behaviour (Muller et al., 2017). Anthropogenic climate change is expected to influence future cyclone frequency and intensity, but our short instrumental records fail to capture long-term variability in cyclogenesis due to climatic and environmental changes. As a result, future cyclone projections are accompanied by a considerable amount of uncertainty. (Cheal et al., 2017; Chu & Murakami, 2022; Knutson et al., 2020; Walsh et al., 2016; Yoshida et al., 2017). Simultaneously, as global populations increase, more people rely on coastal areas for their lives and livelihoods, and are exposed to the devastating impacts of cyclones (Sengupta et al., 2023). The paucity of long-term records and growing populations in coastal areas emphasize the need for a better understanding of cyclones, the impacts of climate change on their formation and behaviour, and the risks they pose to coastal communities.

Geological records contain a wealth of information about past climatic variations, the occurrence of extreme events such as volcanic eruptions, earthquakes and cyclones, and the responses of the biotic and abiotic environments to these variations and events (e.g., Brill et al., 2020; Jeong et al., 2022). Geological, chemical, and biological archives and proxies within geological records can be used to extend our instrumental records by reconstructing past conditions with excellent spatial and temporal resolution, if they are preserved in geological records (Bradley, 2015; Jones et al., 2009). For paleotempestological purposes, archives and proxies such as overwash deposits, beach ridges and stable isotope ratios can be used to extend the instrumental cyclone records and increase our understanding of cyclone frequency and variability in the past under varying climatic scenarios (Frappier et al., 2007; Liu, 2007a; Muller et al., 2017). An improved understanding of the effects of climatic variations on cyclone characteristics will contribute to the development of more accurate models for cyclogenesis in the present and into the future under anthropogenic climate change. In turn, improved models will better inform coastal managers and communities about the potential impacts of cyclones on lives and livelihoods, enabling the development of more effective management plans and damage minimisation strategies.

Paleotempestological archives and proxies can yield evidence of cyclone occurrences (e.g., Braun et al., 2017; Lases-Hernández et al., 2020; Tamura et al., 2018; Yap et al., 2021), but are limited in their ability to provide details about cyclone characteristics such as intensity or resulting wave height. Benthic foraminifera are marine microfossils that are considered as a proxy with the potential to provide information about cyclone specifics. Foraminifera are protists, found in marine sediments all over the world, from the poles to the tropics. Foraminifera display species-specific habitat- and depth preferences and are abundant in marine environments from nearshore settings to deep abyssal plains

(Beavington-Penney & Racey, 2004; Javaux & Scott, 2003; Murray, 2006). Because foraminifera are abundant, distributed in species-specific zones and produce tests with high preservation potential, they can greatly improve the temporal and spatial resolution of paleotempestological reconstructions if they are preserved in overwash deposits. Overwash deposits are wave-deposited sediments that have been deposited on land, above the reach of fair-weather waves and water levels, indicating extreme weather events such as cyclones (Wang & Horwitz, 2007). Identification of foraminiferal species in overwash deposits could provide information about their habitat- and depth preferences and therefore which part of the marine environment they originated from (their provenance) (Barbieri et al., 2006). The depth associated with sediment provenance could then be used to calculate wave height, based on relationships established through wave theory. Resulting wave height could then be linked to cyclone intensity, by using cyclone modelling in combination with local bathymetric data.

To date, the majority of paleotempestological studies using foraminifera as a proxy, have been carried out in the USA and the Caribbean (e.g., Braun et al., 2017; Bregy et al., 2018; Hippensteel & Garcia, 2014; Lane et al., 2011). The other ocean basins are underrepresented in terms of paleotempestological foraminiferal research, and most of the research has been concentrated around densely populated areas such as Thailand, India, and China (e.g., Chen et al., 2019; Hussain et al., 2013; Williams et al., 2016). Only four paleotempestological studies have used foraminifera to reconstruct cyclone history in Australia (Engel et al., 2015; May et al., 2015; Nott et al., 2013; Strotz et al., 2016). All the research projects to date used foraminifera as general indicators of overwash deposits and marine provenance, but no conclusions were drawn about foraminifera assemblages and cyclone specifics such as intensity or resulting wave height. The lack of foraminiferal use is likely because little is known about foraminiferal community assemblages at specific locations. Similar foraminiferal assemblages occur in locations with similar geographical and environmental conditions, but site-specific variations in parameters can cause changes in composition. Environmental parameters such as salinity, oxygen availability, temperature, substrate type, food availability, light intensity and pH influence species-specific habitat suitability (Capotondi et al., 2022; Murray, 2006; Singh et al., 2022). Since these environmental parameters are location-specific, foraminiferal assemblages will need to be characterised for a specific location before they can be used to make inferences about cyclone specifics such as intensity or resulting wave height. Because sediment collection is already an integral part of most paleotempestological studies, foraminiferal assemblages will automatically be collected with sediment samples if they are present. Adding foraminifera identification to paleotempestological research will therefore only require a few extra steps in the analyses but could result in much higher resolution and specificity of the paleocyclone histories developed for a location.

This chapter will determine whether foraminifera exhibit species-specific depth preferences at Middle Island. Testing this statement involves: 1) Collecting nearshore marine sediment samples from around Middle Island on the central Great Barrier reef near Bowen, Queensland, Australia, 2) Documenting habitat types and depths of sediment source zones, 3) Identifying foraminifera species and foraminiferal assemblages associated with these depths and habitat types, 4) Performing analyses to determine statistically significant differences between assemblages, 5) Determining whether foraminifera species can be linked to specific habitats or depth ranges.

2.2 Methods

2.2.1 Surficial sediment samples

Surficial sediment samples containing foraminiferal assemblages were collected from the reef flat and reef slopes flanking the southern side of Middle Island during field trips in March and August 2023 (see Chapter 1 for detailed site description). The sediment samples were collected from a range of depths, starting on the reef flat and terminating on the sea floor seaward of the reef slopes at ~10 m below LAT (Figure 2.1).

Figure 2.1

Surficial sediment collection locations

Note. From *Google Earth, 2024.*

Samples from the reef flat were collected at low tide, along a transect perpendicular to the shoreline. The reef flat is situated at ~1 m above LAT near the shoreline and slopes down to around LAT near the reef crest. Water depths on the reef flat were ≤ 0.2 m at the time of collection and some of the fossil microatolls and elevated areas of the reef flat were subaerially exposed, while lower-lying areas of the reef flat experienced ponding of seawater. Six sediments samples (<20 grams dry weight each) were collected from these ponds by hand and stored in plastic containers, and the coordinates were recorded using a hand-held GPS. To obtain sediment samples from the reef slopes, a Van Veen grab sampler with a volume of 1 litre was deployed from the JCU research vessel 'Terapon II'. The research vessel's onboard GPS system was used to record sediment sampling depths, which were then converted to depths relative to LAT. Five sediment samples were obtained from the southern half of the western reef slope, one sample from each of the following depths below LAT: ~0.5 m, ~2m, ~4m, ~6m and ~10 m. The amount of retrieved sediment varied between 20-50 grams dry weight per sample, depending on substrate type, sediment availability on the substrate, and retention in the grab sampler during retrieval. Despite repeated attempts, no sample could be recovered from a depth of ~8 m below LAT at this sampling location. Sampling of the reef slope north of the initial location did yield a sediment sample from a depth of ~ 9 m below LAT, as well as an additional sample from ~5.5 m. Despite repeated attempts, no samples could be retrieved from the southeastern reef slopes. In total, 13 sediment samples were recovered: six from the reef flat, five from the southern part of the western reef slope and two from the northern part of the western reef slope. All recovered samples were transferred to plastic containers for transport and subsequent storage in the sediment laboratory refrigerator at JCU.

2.2.2 Reef habitats

Reef habitat characteristics at the sediment sampling locations were recorded during the fieldtrips using a SeaViewer drop camera launched from the research vessel. The drop camera was lowered over the side of the vessel until it hovered ~ 0.5 m above the reef/sea floor, and footage was recorded as the vessel slowly moved along the transect (~1 km/hour). At 0.5 m elevation above the sea floor, the substrate could be observed despite the turbid water conditions at the time of recording. The drop camera was connected to a video screen onboard the vessel, showing the footage being recorded. To prevent the camera contacting the bottom and stirring up sediment that would obscure benthic observations, imagery relayed to the onboard screen was carefully monitored and used to adjust camera depth by raising and lowering the camera on the attached cable. The drop camera recorded the date and time the footage was taken, together with the coordinates of the video transects via an integrated GPS input. The research vessel's onboard navigation system was also used to record depths and corresponding time stamps, to enable correlation of video footage with habitat depth during video processing. Video footage was obtained for all the sediment sample locations on the western side of the reef. Some additional footage was obtained from similar depth transects on the south-eastern side of the reef, to characterise reef habitat zones across the full extent of the reef (Figure 2.2). The video transects covered depths ranging from 0.4 m above LAT to 13.9 m below LAT.

Figure 2.2

Drop camera transect locations

Note. From *Google Earth, 2024.*

2.2.3 Foraminiferal assemblages

To identify foraminiferal assemblages from the reef flat and reef slopes, collected sediment samples were split into two subsamples. One of the subsamples was wet sieved to minimise damage to the foraminiferal tests, while the other subsample was retained for archive purposes. Since tests of common tropical foraminifera species range in size from ~250 µ up to ~ 2 mm, subsamples were processed through stacked sieves with apertures of 500 µ and 250 µ. Any grains ≥500 µ were retained on the top sieve, while any grains between 250-500 µ were retained on the bottom sieve. The grains that were retained by the sieves were oven dried at low temperatures (~45°C), to remove water from the samples without damaging foraminiferal tests that might be present in the sediments. The dried samples were transferred to sealed and labelled plastic containers until they could be sorted under a microscope.

To separate foraminifera from sediment grains, dried samples were transferred to a petri dish and placed under a Nikon SMZ1500 stereoscopic microscope, with an AmScope MU1003B digital camera attached to the eyepiece. The camera was connected to a computer and the microscope image was projected onto the computer screen, which facilitated the sorting and identification process. Foraminiferal tests were separated from sediment grains by hand, using a fine paint brush. Identification was performed using 'A guide to 1000 Foraminifera from Southwestern Pacific New Caledonia' by Jean-Pierre Debenay, supplemented by the World register of Marine Species website (Ahyong et al., 2024;

Debenay, 2013). Species' names and absolute counts for each sample were recorded in Excel spreadsheets. In addition to species counts, the average level of taphonomic degradation for the sample was assessed, to provide an indication of the post-mortem history of observed tests. The following categories were assigned to indicate taphonomic degradation: 'Pristine', 'Little taphonomic degradation', 'Moderate taphonomic degradation' and 'Significant taphonomic degradation'. Foraminifera tests that could not be identified to species level because they were too degraded were not included in the counts. Foraminiferal identification to species level is dependent on a significant amount of detail still visible on the test, and 'Significant taphonomic degradation' is therefore a relative definition that did not exclude identification. To account for varying sample sizes, samples were analysed until a total count of 300 foraminifera was reached for that sample. If this count could not be reached, the entire sample was sorted, and all foraminifera were counted and identified where possible. Based on the abundance of foraminifera in the sediment sample and the amount of sediment collected, sorting and identification times varied from an hour to several hours per sample. After identification, foraminifera tests were transferred to a separate labelled container, while the remaining sediment grains were returned to their original container.

2.2.4 Analyses

To determine habitat characteristics, video footage was reviewed in the VideoLAN media player (VLC v. 3.0.20, 'Vetinari'), Time stamps and depths from the research vessel's onboard navigation system were compared with the time stamps recorded by the drop camera, and screenshots for each sampling depth were taken from the video footage. Subsequently, the screenshots were loaded into the Coral Point Count program with Excel extensions (CPCe, v4.1, Kohler & Gill, 2006). The screenshots were overlayed with 25 randomly distributed points, and the type of cover under each point was assigned to one of the following categories: 'Algae (AL)', 'Ascidians (AS)', 'Coral rubble (CR)', 'Dead hard corals (DHC)' 'Live hard corals (LHC)', 'Soft corals (SC)', 'Substrate (SU)' and 'Unknown/Unidentifiable (UN)'. Due to high turbidity and limited visibility at the time the drop camera footage was recorded, image quality was too low to identify coral and algae down to genus or species level. Habitat type descriptions were therefore restricted to general cover type.

To determine whether foraminiferal communities exhibited statistically significant differences along a depth gradient, count data were analysed using R Statistical Software (v4.3.3; R Core Team, 2024) and the RStudio interface (v2024.04.1+748). In addition to the built-in packages in R, the 'dplyr' (v1.1.4; Wickham et al., 2023), 'indicspecies' (v.1.7.14, Miquel et al., 2023), plot3d (v1.4.1; Soetaert, K., 2024), 'rgl' (v1.3.1; Adler & Murdoch, 2023), 'vegan' (v2.6-4; Oksanen et al., 2022), and 'vegan3d' (1.3-0; Oksanen et al., 2024) packages were installed and loaded into the library to perform the necessary statistical analyses. Foraminifera counts for all samples were converted to proportional data, to standardise the dataset and reduce the impact of sample size differences. The dataset was loaded into R, and the 'vegdist' function from the 'vegan' package was used to produce a dissimilarity matrix with Bray-Curtis indices. The dissimilarity matrix compared the foraminiferal assemblage in each sample to the assemblages from all other samples and determined the degree of dissimilarity between samples. The Bray-Curtis indices were used for the following reasons: ecological community data generally contain zeroes when species are not present in a particular sample. Linear (Euclidean) indices tend to give more weight to abundance differences than to the presence or absence of a species, which produces dissimilarity matrices based on abundance dissimilarities, not on species dissimilarities (Ricotta & Podani, 2017). Bray-Curtis indices were developed to overcome this limitation. Additionally, Bray-Curtis indices can determine which specific species are responsible for the dissimilarities between samples, which is particularly relevant for this research project (Ricotta & Podani, 2017).

Once the dissimilarity matrix was produced, the potential effect of spatial autocorrelation on foraminiferal assemblage dissimilarity needed to be assessed. Assemblages that are close together in geographical space are expected to be more similar than assemblages that are further removed from one another (Luo et al., 2022). Foraminiferal assemblages from adjacent locations and depths might therefore be similar due to their geographical proximity, not because they exhibit specific depth- or habitat preferences. To account for potential spatial autocorrelation, the sample depths were divided into three depth groups: 5-0 m above LAT (reef flat samples), 0-5 m below LAT and 5-10 m below LAT. The geographical location of each sediment sample was entered into R, using latitude and longitude coordinates. Dissimilarity matrices for the depth groups and the geographical locations were produced using Euclidean indices, since depth and geographical locations are physical, metric distances. A partial Mantel test was performed, which compared the dissimilarity matrices of foraminiferal assemblages and depth ranges, while accounting for the geographical locations of the samples using the dissimilarity matrix for the coordinates. The test results include two statistics: an r-value that ranges between -1 and 1 and indicates the direction and the strength of the relationship between the compared dissimilarity matrices, and a p-value that indicates whether the null hypothesis of no correlation should be retained or rejected. The test was performed using an alpha significance level of 0.05 and a Kendall correlation index, since this index does not make any assumptions about the distribution of the dataset and tends to be more robust than the Spearman correlation index (Croux & Dehon, 2010). A total of 99,999 permutations were performed to strengthen the outcome of the Mantel test.

To identify which species were responsible for the dissimilarities between samples, indicator species for each depth range were determined using the ‘multipatt’ function from the ‘indicspecies’ package, using an alpha significance level of 0.05 and a group-equalised phi coefficient. This coefficient was chosen because the foraminiferal assemblages varied in size between samples, which tends to produce skewed results when other indices are used. The group-equalised phi coefficient negates this limitation by standardising the relative frequencies within and outside of the target site groups (Tichy & Chytry, 2006). The results include a species statistic, which is a combination of ‘specificity’ and ‘fidelity’. The specificity is the mean abundance of a species in a specified depth interval, as a proportion of its mean abundance in all depth intervals. The fidelity is the proportion of samples within the depth interval that the species occurs in. The species statistic ranges from 0-1, and values close to 1 therefore indicate a high specificity combined with a high fidelity. The null hypothesis for indicator species assumed that there was no relationship between foraminifera species and the depths they occurred in.

2.3 Results

2.3.1 Reef habitats

The video footage analyses showed that the western reef slope was primarily covered by algae and coral rubble to a depth of ~8 m below LAT, interspersed with patches of bare substrate. The only exception was the northern part of the western reef slope where a narrow band of live hard coral was present at a depth of ~1 m below LAT, although there were patches of coral rubble and bare substrate visible between the corals. On the southern part of the western reef slope, soft corals/algae dominated the ~8 m isobath, interspersed with dead hard coral and some ascidians. No bare substrate was visible on this part of the reef slope. Further north along the western reef slope, the ~8 m isobath was characterised by bare substrate without any other cover present. Past the 8 m isobath, the reef slope levelled out and transitioned into the ocean floor at a depth of 11-12 m below LAT, which was characterised by bare substrate with a few small patches of coral rubble on both the northern and southern part of the western reef slope (Table 2.1 and Figure 2.3).

Table 2.1

Habitat type and cover as a proportion of the total cover at that depth. Empty cells indicate absent habitat types

Site	*Depth (m) (LAT)*	Algae	Ascidians	Coral Rubble	Dead hard coral	Live hard coral	Soft coral	Soft coral/algae	Substrate	Unknown
T1 (W)	***0.4***	0.40		0.32					0.24	0.04
South.	***-0.2***	0.36		0.64						
half	***-0.7***			0.88					0.08	0.04
	-1.7	0.44		0.28					0.20	0.08
	-4.9			0.60					0.36	0.04
	-6.3			0.60						0.40
	-7.9		0.08		0.20			0.68		0.04
	-9.1			0.08	0.08				0.68	0.16
	-13.9								1.00	
T4 (W)	***-1.9***	0.96								0.04
South.	***-6.4***			0.40		0.04			0.36	0.20
half	***-9.5***			0.20				0.04	0.76	
T5 (W)	***-0.9***			0.20	0.04	0.28			0.28	0.20
North.	***-2.3***	0.56						0.28		0.16
half	***-4.4***			0.36					0.56	0.08
	-6.9								0.92	0.08
	-7.9								1.00	
	-10.9			0.12					0.88	
T2 (SE)	***-0.1***	0.36			0.48					0.16
	-1.5			0.16	0.56	0.16				0.12
	-2.9							0.96		0.04
	-3.2	0.88								0.12
	-5.9				0.08			0.40	0.08	0.44
	-7.4				0.04			0.72	0.20	0.04
	-8.9				0.72	0.16				0.12
	11.9							0.36	0.64	
T3 (SE)	***-1.9***					0.52		0.12	0.16	0.20
	-2.9			0.32				0.64		0.04
	-5.4							0.84		0.16
	-7.0			0.24		0.20		0.44		0.12
	-10.9							0.52	0.48	

Figure 2.3

Reef cover screenshots

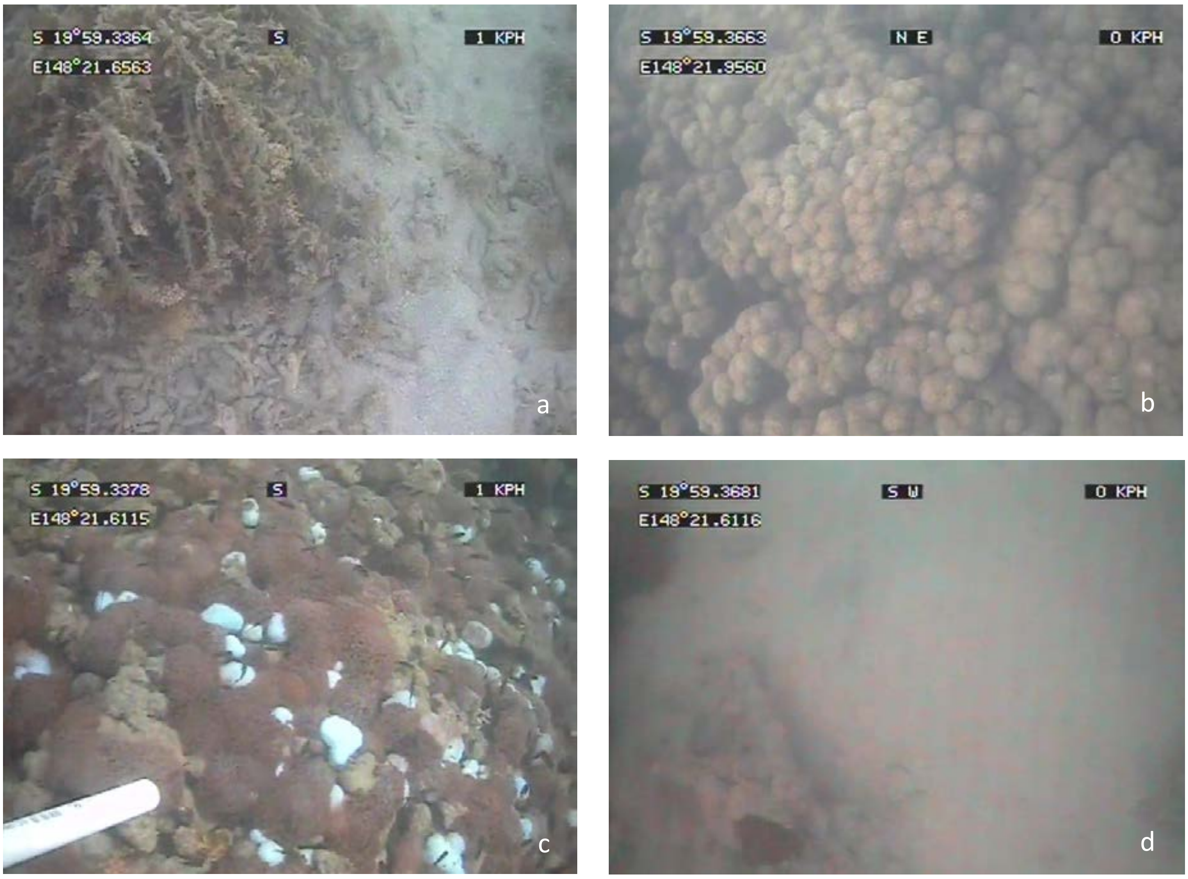

Note. a) 0.4 m above LAT, b) 3 m below LAT, c) 8 m below LAT, d) 9.5 m below LAT.

On the south-eastern side of the reef, a mix of live and dead hard corals covered the reef slope to a depth of ~ 3 m below LAT, with a few patches of algae growing on or between the corals. Between 3-8 m below LAT, soft corals and algae dominated the reef slope, with small patches of coral rubble present but hardly any visible substrate. Past the 9 m isobath, the ocean floor levelled out at similar depths compared to the western side of the reef (11-12 m below LAT) and was characterised by a mix of soft coral/algae and substrate. The 9 m isobath formed an exception, as it was characterised by dead hard corals with a few live coral colonies visible between the dead colonies.

2.3.2 Foraminiferal assemblages

A total of 3,706 foraminifera tests were counted, and identification resulted in 61 genera and 146 species (Appendix 1). The tests showed varying degrees of taphonomic degradation, ranging from ‘pristine’ to ‘significantly degraded’. Since taphonomic degradation is a result of long residence times in the environment, combined with possible transport, the degraded tests were not considered to be autochthonous to the depth they were collected from. A total of 2,724 tests that were labelled ‘pristine’ or ‘little taphonomically degraded’ were retained for statistical analyses. Of the 61 genera that were identified, 40 genera were represented by a single species, while the other 21 genera were represented by as little as two species (e.g., *Operculina, Peneroplis* and *Sahulia)*, or as many as 21 species (*Quinqueloculina)*. Of the 40 genera with a single species, 16 genera were only identified once, with only one specimen belonging to that genus: *Adelosina, Ammomassilina, Caronia, Cymbaloporella, Fijiella, Flintina, Flintinoides, Globorotalia, Massilina, Paratrochammina, Pseudolachlanella, Siphonina, Spirillina, Spirotextularia, Tretomphalus* and *Varidentella*. In terms of abundance across all samples, *Elphidium* was the most abundantly occurring genus with 623 specimens, followed by *Amphistegina* with 363 specimens and *Quinqueloculina* with 282 specimens. The genera *Amphistegina, Elphidium* and *Peneroplis* were represented in all samples by at least one species. The genus *Quinqueloculina* was present in all but one sample. *Calcarina, Heterostegina* and *Neorotalia* were present in all but two samples, and *Eponides, Epistomaroides* and *Triloculina* in all but three samples (Figure 2.4).

Figure 2.4

Microscope images of common foraminifera genera from Middle Island

Note. a) Elphidium craticulatum., b) Quinqueloculina auberiana, c) Amphistegina lessonii, d) Peneroplis planatus

Of the 146 species, *Elphidium craticulatum* occurred most frequently with 331 specimens identified, followed by *Peneroplis pertusus* with 192 individuals and *Amphistegina lobifera* with 185 individuals. Three species were present in all samples: *Amphistegina lessonii, A. lobifera* and *Elphidium craticulatum*. Both *Peneroplis pertusus* and *P. planatus* were present in all but one sample. *Calcarina hispida, Neorotalia calcar* and *Quinqueloculina auberiana* were identified in all but two samples, and *Elphidium crispum, Epistomaroides polystomelloides, Eponides (cribro)repandus* and *Triloculina barnardi* occurred in all but three samples.

On the reef flat, species diversity was lowest in the reef flat 3 sample, which was taken from the reef flat about halfway between the reef crest and the beach. Test abundance was lowest on the reef flat area closest to the beach (reef flat 6), although the number of tests was similar throughout all reef flat samples. Highest species diversity occurred in the reef flat 4 sample, and highest test abundance in the reef flat 5 sample. On the reef slopes, species diversity was highest at 5.5 m below LAT and lowest at 4.0 m below LAT. Test abundance was highest at 10 m below LAT and lowest at 6.0 m below LAT (Table 2.2).

Table 2.2

Species diversity and test abundance in sediment samples from Middle Island

	Reef flat 1	**Reef flat 2**	**Reef flat 3**	**Reef flat 4**	**Reef flat 5**	**Reef flat 6**	**-0.5 m LAT**	**-2.0 m LAT**	**-4.0 m LAT**	**-5.5 m LAT**	**-6.0 m LAT**	**-9.0 m LAT**	**-10 m LAT**
Number of species	10	13	8	27	22	24	45	52	37	98	43	95	63
Test abundance	68	71	66	82	84	62	225	195	368	371	181	433	518

Based on the statistical analyses performed in R, dissimilarities between foraminiferal assemblages ranged from ~0.17 (comparison between reef flat samples 1 and 2) to ~0.87 (reef flat sample 3 compared to the reef slope sample from 0.5 m below LAT). Dissimilarity values range from 0-1, with 0 indicating that samples are identical in terms of community assemblage, and 1 indicating there are no common species between the two compared samples. The resulting table is 'halved'; comparing sample 1 to sample 2 is the same as comparing sample 2 to sample 1, and samples are not compared to themselves (Table 2.3).

Table 2.3

Dissimilarity matrix for foraminiferal assemblages from Middle Island

	Reef flat 1	**Reef flat 2**	**Reef flat 3**	**Reef flat 4**	**Reef flat 5**	**Reef flat 6**	**-0.5 m LAT**	**-2.0 m LAT**	**-4.0 m LAT**	**-5.5 m LAT**	**-6.0 m LAT**	**-9.0 m LAT**
Reef flat 2	0.17											
Reef flat 3	0.25	0.17										
Reef flat 4	0.58	0.57	0.64									
Reef flat 5	0.58	0.61	0.70	0.41								
Reef flat 6	0.73	0.74	0.78	0.45	0.46							
-0.5 m LAT	0.72	0.80	0.87	0.58	0.52	0.69						
-2.0 m LAT	0.76	0.81	0.85	0.70	0.69	0.69	0.55					
-4.0 m LAT	0.47	0.57	0.67	0.62	0.54	0.69	0.57	0.60				
-5.5 m LAT	0.69	0.70	0.78	0.66	0.50	0.72	0.47	0.61	0.52			
6.0 m LAT	0.68	0.76	0.82	0.67	0.66	0.74	0.43	0.53	0.38	0.57		
-9.0 m LAT	0.72	0.76	0.82	0.68	0.58	0.76	0.56	0.64	0.59	0.24	0.60	
-10 m LAT	0.56	0.73	0.68	0.71	0.59	0.77	0.60	0.65	0.48	0.44	0.58	0.46

Foraminiferal assemblages followed the general trend of increasing dissimilarity with increasing distance/depth. The partial Mantel test returned an r-value of 0.3109 and a p-value of 0.0035 and indicated that there was a significant and positive relationship between assemblage composition dissimilarity and depth, and that this was unrelated to spatial autocorrelation.

Because the relationship between assemblage composition and depth was shown to be significant, the indicator species function was used to determine which species were responsible for the differences between assemblages. The resulting list showed species that were associated with each depth range. Group 1 (reef flat samples) contained one unique species: *Amphistegina lobifera*. Group 2 (0-5 m below LAT) did not contain any indicator species. Group 3 (5-10 m below LAT) contained 15 indicator species: *Ammonia aoteana, Clavulina pacifica, Elphidium advenum, Elphidium excavatum, Elphidium hispidulum, Operculina ammonoides, Parasorites orbiculus, Quinqueloculina crassicarinata, Quinqueloculina parvaggluta, Quinqueloculina polygona, Sahulia conica, Sigmoihauerina involuta, Siphonaperta arenata, Spiroloculina communis and Textularia dupla. Elphidium crispum* was associated with any depth other than the reef flat, as it was an indicator species for the combination of group 2 and group 3 (Table 2.4).

Table 2.4

Indicator species based on depth ranges, with their respective species statistic values and p-values

Depth	Species	Species statistic	p-value (99,999 permutations)
Reef flat (5-0 m above LAT)	*Amphistegina lobifera*	0.785	0.00888
5-10 m below LAT	*Ammonia aoteana*	0.772	0.01744
	Clavulina pacifica	0.770	0.01750
	Elphidium advenum	0.751	0.01750
	Elphidium excavatum	0.806	0.01750
	Elphidium hispidulum	0.750	0.01709
	Operculina ammonoides	0.635	0.02043
	Parasorites orbiculus	0.751	0.01750
	Quinqueloculina crassicarinata	0.774	0.01750
	Quinqueloculina parvaggluta	0.793	0.01040
	Quinqueloculina polygona	0.667	0.04545
	Sahulia conica	0.936	0.00136
	Sigmoihauerina involuta	0.793	0.01750
	Siphonaperta arenata	0.764	0.01750
	Spiroloculina communis	0.694	0.01750
	Textularia dupla	0.753	0.01750
0-5 m below LAT + 5-10 m below LAT	*Elphidium crispum*	0.817	0.00552

2.4 Discussion

This study provides the first description of contemporary foraminiferal assemblages from the reef flat and reef slopes around Middle Island and identifies the habitat types on the reef slopes. Most importantly however, this study statistically shows that foraminifera at Middle Island exhibit species-specific depth preferences.

2.4.1 Foraminifera identification

Foraminifera were shown to be abundantly present around Middle Island, with 3,706 identified foraminifera belonging to 146 species and 61 genera. Sediment samples were collected in March and August during the Austral autumn and winter, and tests were identified regardless of whether the organism was alive or dead upon collection. The resulting foraminiferal assemblages were therefore a time-averaged representation of species present in the environment and were unaffected by seasonal reproduction cycles. Since no distinction was made between dead and alive foraminifera, test preservation was used to infer residence times in the environment, as well as potential transport from the original habitat to the collection zone. Long residence times in the environment, or transport from one location to another, result in taphonomic degradation of the test (Berkeley et al., 2009; Murray, 2006). The degree of taphonomic degradation can therefore be used to determine if a foraminiferal test is autochthonous to the location and depth it was collected from. Of the 3,706 foraminifera that were identified, 2,724 individuals showed minimal taphonomic degradation and could be linked to Middle Island and their collection depth with a high level of confidence.

The correct identification of foraminifera to species level in this study is supported by studies from similar geographical locations (e.g., Berkeley et al., 2008; Johnson, 2017; Mamo, 2016), which identified a large proportion of the same species in their assemblages. Of the 16 genera that were represented by only one species and one specimen in this study, *Adelosina, Cymbaloporella, Fijiella, Paratrochammina, Spirillina* and *Varidentella (*as *Quinqueloculina)* were also identified in some of the other studies previously mentioned. This supports the correct identification of these genera and species and indicates that they represent genuinely rare foraminifera for Middle Island. The other 10 genera with only one specimen present at Middle Island could have been misidentified but could also represent genuinely rare species. Nevertheless, 10 potentially misidentified foraminifera do not affect the outcomes of this research project, since they constitute <1% of the foraminiferal tests that were retained for statistical analyses.

2.4.2 Foraminiferal assemblages and habitats

The foraminiferal assemblages from Middle Island showed considerable variation in species diversity and test abundance. The low abundance of foraminifera on the reef flat is likely due to a combination of two factors: adverse environmental conditions and reduced preservation potential. The reef flat at Middle Island is exposed during low tides, and water depths only reach ~2 m during the highest tides. Some ponding of water occurs in reef flat areas with lower elevation, but even these ponds experience significant fluctuations in environmental parameters such as salinity, irradiation, and hydrodynamic conditions due to tidal influences (Murray, 2006). This makes the reef flat unsuitable for most foraminiferal species due to an exceedance of their preferred range of environmental parameters. The few species that were present in the reef flat samples confirmed the current knowledge about foraminiferal distributions and parameter preferences. For example, *Amphistegina lobifera* is known to have a high light tolerance and to shelter under boulders or coral rubble in extreme hydrodynamic settings (Hohenegger, 2004). The same applies to *Heterostegina depressa*, as this species has been shown to live in rock pools and tolerate light intensities up to 70% (Beavington-Penney & Racey, 2004). Certain *Quinqueloculina* and *Triloculina* species are known to tolerate hypersaline environments such as lagoons, although environmental tolerances vary between species (Debenay, 2013). In addition to adverse environmental conditions, preservation potential on the reef flat is reduced compared to the reef slopes. The fluctuations in environmental parameters promote taphonomic processes such as dissolution and diagenesis, and water movement and currents due to the tides increase weathering and breakage of the tests (Murray, 2006). Some foraminiferal species can survive the adverse conditions on the reef flat, but their tests are unable to withstand taphonomic degradation after the death of the organism. Adverse environmental conditions therefore result in low species diversity, and taphonomic degradation results in low species abundance on the reef flat.

A variety of habitats were identified on the reef slopes between 0-10 m below LAT, which resulted in an increase in species diversity compared to the reef flat. The western reef slope habitats consist of algae, coral rubble, and bare substrate, which is reflected by the foraminiferal species that were present in the sediment samples. As an example, *Calcarina* species live in environments below the fair-weather wave base and are considered epifaunal species, or epiphytic on algae (Murray, 2006). *Calcarina* species were abundantly present across all reef slope depths and virtually absent from the reef flat, which confirms their habitat preferences. The genus *Peneroplis* is known to cling to plants or hard substrates and to live at depths between 0-70 m (Beavington-Penney & Racey, 2004). *Peneroplis* was abundantly present at all reef slope depths due to the presence of algae and hard substrates such as dead hard coral or coral rubble. Due to a lack of bare substrate availability on the southeastern reef slopes, no sediment samples were collected from this side of the reef. Sediment availability is also the cause of the differences in test abundances on the western reef slopes. Depths with a high proportion of bare substrate and coral rubble yielded more sediment and therefore higher test abundance totals for that sample. Slope depths that were dominated by algae or soft coral yielded little sediment, which resulted in lower foraminifera test counts. To improve sediment collection success in future studies, reef slope samples could be collected by hand using SCUBA. Small patches of bare substrate are easily recognised and accessed by divers, which allows the sampling of reef slope areas with low proportions of bare substrate. If dives are executed along multiple transects across the full width of the reef, replicate samples from the same depths can be collected, and collection depths can be determined with greater precision than was managed in the present study. These more detailed results also include a potential increase in the resolution of species-specific depth preferences, where the preferences might be restricted to a 1-2 m interval instead of the current 5 m interval.

Even though the foraminiferal assemblages in the reef flat samples contained far less individuals than the assemblages from the reef slopes, all samples are an accurate representation of the total population. Forcino and colleagues. (2015) statistically analysed the effect of sample size on abundance-based, ecological, multivariate statistical analyses. They concluded that sample sizes of ≥ 58 individuals per sample were sufficient to perform community-based statistical analyses, such as determining the influence of environmental gradients on community composition. Increasing the population size beyond this number did not change the outcome of the analyses. The only caveat is that small sample sizes of 58 individuals might not capture the full species diversity in a community (Forcino et al., 2015). The lowest recorded test abundance at Middle Island was 62 tests in the reef flat 6 sample, which is above the threshold determined by Forcino and colleagues. This sample also contained the second highest number of species on the reef flat. The lowest number of species was recorded in reef flat sample 5, which contained four more tests than reef flat sample 6. This demonstrates that higher test abundance does not result in higher species diversity, at least not at this research location. As a result, all samples were treated as accurate representations of the population at each sampling location, and the statistical analysis results were considered significant and representative. Lowering the threshold for foraminiferal counts in future studies will significantly reduce research time and effort and will increase the quantity of foraminiferal studies that can be performed for a given budget and research period.

While this study aimed to identify and describe the foraminiferal assemblages and habitats around Middle Island, it was beyond the scope of this research project to measure all the environmental parameters that influence the distribution of foraminifera species. As a result, no conclusions can be drawn about the response of foraminifera species to changes in environmental parameters such as salinity, water temperature and light intensity. Furthermore, the quality of the recorded drop camera footage was suboptimal due to high turbidity and limited visibility, which prohibited the identification of corals or algae to species level. The composition of foraminiferal assemblages followed the general trends of species-specific preferences for habitat types, but any relationships between foraminifera species and coral or algal species could not be identified. Using a hand-held underwater camera and SCUBA in future studies would improve the quality of the resulting footage. The proximity of the diver to the reef or substrate would minimise the influence of water turbidity and limited visibility on footage quality. As a result, habitat analyses and foraminiferal assemblage analyses could be performed with greater precision and would yield more detailed results.

2.4.3 Species-specific depth preferences

Of the 146 foraminifera species from Middle Island, 17 species were shown to exhibit species-specific depth preferences. It is important to note that depth itself is not an environmental parameter that influences the distribution of foraminiferal species. Rather, environmental parameters such as salinity, light intensity, and water temperature, are subjected to changes along a depth gradient and it is these parameters that the foraminifera species respond to. As such, depth is a proxy for the combined effects of all the environmental parameters that influence foraminifera distribution, and the changes in these parameters along a depth gradient. On one hand, using depth as a proxy means that individual environmental parameters do not need to be measured to quantify changes in foraminiferal assemblage composition. On the other hand, the obtained depth preferences for foraminifera species at Middle Island are only representative of the conditions at this location. Environmental parameters at other locations are likely to differ, both in their absolute values and in their relative changes along a depth gradient. As an example, consider a nearshore environment that experiences fluvial discharge from a nearby river delta. Even if the hypothetical location's reef flat width, reef slope gradient, and habitat types and distribution are identical to those of Middle Island, the freshwater influx from the river delta will reduce salinity levels in the nearshore environment and alter the distribution of foraminifera species due to their salinity preferences (Beck Eichler & Barker, 2020b).

Samples were collected from a range of depths between 0.5 and 10 m below LAT, but depths were grouped together in 5 m intervals. This grouping is a result of the sampling method that was used to collect the sediment samples from the reef slopes. A Van Veen grab sampler was deployed from the research vessel, which was not anchored to the reef or the sea floor. This meant that the vessel was affected by swell and currents around Middle Island and was therefore never fully stationary. The vessel's onboard depth sounder was used to infer water depths below the vessel, but the measurements fluctuated due to the vessel's movements. Sampling depths are therefore an estimate of the true depth, which needed to be considered before statistical analyses were performed. It was therefore decided to group depths together in 5 m intervals, to account for the differences between estimated depths and actual depths.

Of the 146 identified species, 17 species or ~12% were assigned to a specific depth based on their species' statistic values, which are a combination of specificity and fidelity. These 17 indicator species therefore occur most frequently in the specified depth range and are present in the majority of, or in all the samples within that depth range. The remaining 88% of the species are therefore either evenly distributed across all samples, or they are variable in their occurrence in the samples within a depth range. If species are evenly distributed across all samples, they can be considered generalists that are adapted to a wide range of environmental parameters. *Elphidium craticulatum* was present throughout all samples and can therefore be considered a generalist. If species are variable in their appearance within a depth range, it can indicate that species are rare and recorded test abundance was low. It can also indicate that test preservation was low and that their tests were either not present, or they were taphonomically too degraded to be included in the counts. *Spiroloculina* species are an example of foraminifera with a thin, fragile test morphology that is easily degraded (Figure 2.5).

Figure 2.5

A pristine Spiroloculina elegans *test (left) versus a degraded*

Spiroloculina *species test (right)*

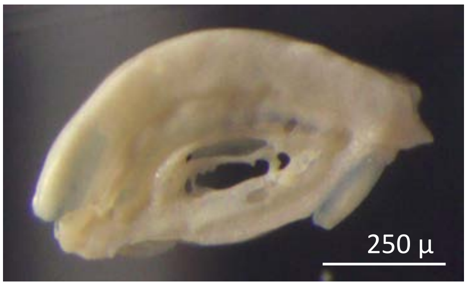

Variable appearances in samples within depth ranges can also indicate that species have a narrower species-specific depth preference than what was tested here. It could be that species are specific to a 1-2 m depth range, but that this preference was not recognised due to the coarser depth intervals that were decided upon. This indicates that future studies might be able to restrict depth preferences to even narrower ranges than presently achieved.

The results of this study have several significant implications for future foraminiferal and paleotempestological research. Currently known depth preferences of foraminifera are limited to a general range that mostly applies to the whole genus: *Peneroplis* species occur between 0-70 m water depth, *Heterostegina* species are found anywhere between 0-130 m and *Spiroloculina* species occur at depths between 0-40 m (e.g., Beavington-Penney & Racey, 2004; Murray, 2006; Nobes & Uthicke, 2008). These ranges are based on idealised environments and the associated hypothesised environmental parameters, and data to support these depth ranges are sparse (Beavington-Penney & Racey, 2004). Some genera such as *Amphistegina* are already known to exhibit species-specific depth preferences, but these ranges still cover 10-50 m. Based on the results from this study, future studies can be used to reduce the known range of species-specific depth preferences. By employing the same method that was tested here, foraminiferal assemblages for a range of locations can be identified and described, including depth preferences. The resulting database can be used to compare species-specific depth preferences between locations and can aid in narrowing down the known depth ranges. If future projects also incorporate the measurement of specific environmental parameters such as salinity or water temperature, these parameters can also be used to make further inferences about species' environmental preferences. The resulting database can then be used to increase the resolution of all paleo- and contemporary ecological and environmental studies that use foraminifera as a proxy.

Findings from this study clearly indicated that foraminifera at Middle Island exhibit species-specific depth preferences and can therefore be used as a proxy for paleotempestological research at this location. Evidence of cyclone occurrences is contained in overwash deposits, which are marine sediments that are deposited beyond the reach of fair-weather waves. If these overwash deposits, and any foraminifera contained therein, are preserved after deposition, they can provide detailed information about the provenance of the marine sediments. Presence of foraminifera has already been used to infer marine provenance, but now these foraminifera can be used to determine the provenance depth of marine sediments. Once the provenance depth is known, these depths can be used to model the wave height that was responsible for deposition of the sediments, since wave height and water depth are related and quantifiable. The wave height can then be used to infer cyclone strength, which will greatly improve the resolution of future paleocyclone reconstructions compared to current studies.

2.5 Conclusion

This study provides the first description of foraminiferal assemblages and reef habitats from Middle Island on the central Great Barrier Reef, Queensland, Australia. Foraminifera were abundantly present on the reef slopes and reef flat around the island, and foraminiferal assemblages generally increased in species diversity and test abundance with greater depths below LAT. Foraminifera at Middle Island also conformed to the general knowledge about species-specific habitat preferences, although the quality of the obtained drop camera footage prohibited an in-depth analysis. Using a novel research approach, this study also shows that foraminifera at Middle Island exhibit species-specific depth preferences and can be assigned to depths within a 5 m interval. Even though the statistically derived depth-preferences are particular to Middle Island, future studies can employ the same technique that was used here to determine species-specific depth preferences for their location of interest. By comparing the obtained datasets, known depth ranges for foraminifera species can be constrained to smaller ranges, which will improve the resolution of paleo- and contemporary ecological and environmental studies that use foraminifera as a proxy. Species-specific depth preferences of foraminifera are also useful for the reconstruction of paleocyclone occurrences at Middle Island. Foraminifera are already used as a proxy to infer marine provenance of preserved overwash deposits in coastal locations. Species-specific depth preferences can now be used to determine not just marine provenance, but also provenance depth. Since water depth and wave height are related, this information can be used to model wave height and therefore the strength of the cyclone that was responsible for generating the waves. This will greatly increase the resolution of paleocyclone reconstructions compared to the current level of resolution. Reconstructing paleocyclone occurrences will extend our current instrumental cyclone records and will provide insights into cyclone variability throughout the Holocene, which can then be linked to possible drivers of this variability. An improved understanding of the links between cyclogenesis and drivers will advance the performance of current cyclone models and the modelling of cyclone occurrence, frequency, and intensity in the future under anthropogenic climate change. It will also provide a better framework for coastal management decisions, and for coastal communities to minimise the damage to lives and livelihoods caused by cyclones in the future.

3. Using foraminifera to reconstruct Holocene cyclone occurrences at Middle Island on the central Great Barrier Reef, Queensland, Australia

This chapter uses evidence from percussion cores to reconstruct a paleocyclone history for Middle Island, Queensland, Australia. Sedimentary analyses, foraminifera identification and radiocarbon dates are used to determine the age, frequency, and depth provenance of overwash deposits recorded in the stratigraphy of the lake at Middle Island

Plate 3

Note. Percussion core PC3.3.

3.1 Introduction

3.1.1 Cyclones in Australia

Tropical cyclones are one of the most destructive natural disasters and are associated with extreme winds, intense rainfall, storm surges and waves. In Australia, cyclones caused AU$26 billion in damage in the period 1966-2017 (McAneney et al., 2019) and resulted in 192 deaths in the period 1970-2015 (Coates, 2017). Accurately predicting cyclone frequency and intensity is vital for the protection of lives and livelihoods, but our current cyclone models are based on instrumental records with lengths that vary per ocean basin (Muller et al., 2017). The instrumental record for the Australian region is one of the shortest records available, only covering the period from 1970-present (Nott, 2009). According to these instrumental records, 11 cyclones form in the Australian region on average each year, with four of these cyclones crossing the coast. When further dividing the Australian region into subregions, the Western Australian region sees the formation of seven cyclones on average each season, with four cyclones forming in the Queensland region (Bureau of Meteorology, 2024a). The most cyclone-prone area is the north-western coast of Western Australia, between Broome and Exmouth. According to the Australian Bureau of statistics (ABS), this stretch of coast is sparsely populated (~50,000 inhabitants), reducing the risk to lives and livelihoods (Australian Bureau of Statistics, 2022). The Queensland coast is much more densely populated, with major population centres like Cairns (~167,000 inhabitants), Townsville (~193,000 inhabitants) and Mackay (~122,000 inhabitants) all at risk of experiencing the devastating impacts of cyclones (Australian Bureau of Statistics, 2022).

To quantify risks associated with cyclones, recurrence intervals of cyclones of a specific category can be calculated. Cyclone categories are based on mean wind speeds and maximum wind gust speeds (Table 3.1).

Table 3.1

Cyclone categories used by the Australian Bureau of Meteorology

Category	Central pressure (hPa)	Mean wind speed	Maximum gust speed
Category 1	986-995	63-88 km/h	≤ 125 km/h
Category 2	971-985	89-117 km/h	125-164 km/h
Category 3 (severe)	956-970	118-159 km/h	165-224 km/h
Category 4 (severe)	930-955	160-199 km/h	225-279 km/h
Category 5 (severe)	<929	≥200 km/h	≥279 km/h

Recurrence intervals can be expressed as a probability (0.01 or 1%) or a return period (1 in 100 years), indicating the probability of a cyclone of a specific category occurring during any given year. These recurrence intervals are then used to inform governments about disaster management and building codes for coastal properties (Nott & Jagger, 2013). Based on our instrumental records, a Category 5 cyclone is expected to impact the Queensland coast once every 1000 years on average (Henderson & Harper, 2003). When looking at severe cyclones in general (Category 3-5), one of these is expected to impact Queensland every ~90 years on average (Mortlock et al., 2023). However, our instrumental records fail to capture long-term variations in cyclone frequency and intensity that are due to interannual and interdecadal climatic variations and external influences such as volcanic eruptions and solar activity (Mortlock et al., 2023; Nott, 2009). Climate change is also expected to influence the frequency and intensity of cyclones in the future, but without a good understanding of the physical mechanisms that underlie cyclone formation and variability, current cyclone models are unable to adequately incorporate these expected changes (Knutson et al., 2020).

3.1.2 Paleocyclone reconstructions and considerations

To extend our instrumental records and produce paleocyclone reconstructions, scientists use archives and proxies that are preserved in the geological records. Contrary to instrumental records that only provide cyclone information for the past ~100 years, geological archives and proxies such as storm deposits and stable isotope ratios can provide information about several thousands of years of cyclone occurrences (Liu, 2007a). However, to correctly interpret the geological record, paleotempestologists need to know if environmental, hydrological, and geomorphological processes in the studied period differed from the present-day processes. To reconstruct paleocyclone histories for the Queensland region, the following aspects need to be considered.

Coastal processes and the impacts of cyclones on coastal regions are a result of sea level at the time of occurrence. Relative sea level, which is sea level relative to the adjacent landmass, is a result of ocean water/ ice volume (eustatic) and tectonic (isostatic) processes at a particular location, and has fluctuated throughout Earth's history (Shennan et al., 2015). Research has shown that sea levels were around ~125 meters lower during the Last Glacial Maximum (LGM), which occurred ~20,000 years ago (Lewis et al., 2013). When temperatures increased and the climate shifted towards our current interglacial stadial, thermal expansion and the melting of glaciers and ice caps caused a rapid increase in global sea levels, until they reached a new equilibrium known as the Mid-Holocene Highstand (Lewis et al., 2013). The exact timing of the Highstand varies per ocean basin due to local and regional bathymetry and tectonic activity. For Australia, and Queensland in particular, research has shown that the Highstand occurred around 6,000 years ago and reached a level that was ~1.5 m higher than current sea levels (Lewis et al., 2013). It is unclear whether the Highstand continued for several thousand years before dropping rapidly or whether sea levels fell smoothly to current levels, but relatively stable sea levels have only occurred since the mid-Holocene (Lewis et al., 2013). Higher sea levels during the Highstand meant that coastal processes such as wave action and erosion could occur at higher elevations on shore compared to the present day. This also applies to cyclone impacts on coastal areas, since waves could reach further inland and storm deposits could be deposited at higher elevations relative to the present. Falling sea levels after the Highstand caused most of Australia's coastline to extend seawards (prograde), preserving landforms from the Highstand period and changing the impact zone of subsequent hydrological and geomorphological processes. It is therefore essential that paleotempestologists know the age of landscapes and landforms that are being used for paleocyclone reconstructions, since the omission of sea-level changes in cyclone modelling can result in an overestimation of past wave height and cyclone intensity.

During the mid-Holocene, the energy conditions on the Great Barrier Reef also differed from current conditions. The Great Barrier Reef (GBR) started developing on the continental shelf off Australia’s east coast when sea levels stabilised during the mid-Holocene. On the northern and southern GBR, reefs developed on substrates that were 15-20 m below sea level at the time while the central GBR reefs initiated on substrates 20-25 m below sea level (Perry, 2011). Due to the transgression after the LGM and the Highstand during the mid-Holocene, vertical reef growth lagged behind the rapid rise in sea levels. Reefs on the GBR therefore did not play a role in wave dispersal during the mid-Holocene, and this period is known as the Holocene High Energy Window. This meant that high-energy waves generated by cyclones could propagate across the continental shelf and onto shore, depositing sediments at much higher elevations than currently possible (Perry, 2011). This also results in an overestimation of paleocyclone intensity if not taken into consideration.

Besides changes in relative sea level, temporary changes in sea level due to cyclones also need to be considered. Storm tide refers to the tide level at the time of the cyclone impacting the coast, combined with waves (wave set up) and elevated water levels due to strong onshore winds (wind set up) (Unnikrishnan et al., 2022). The height of the storm tide is a result of many factors, such as cyclone intensity, its size, the angle of approach relative to the coastline and the local bathymetry (Siahsarani et al., 2021). The inundation level, i.e., the total amount of flooding of the coastal area, is a combination of the storm tide, current relative sea level and wave run up (Forsyth et al., 2010). Inundation levels caused by a cyclone during low tide will not be as high as the inundation caused during high tide and will leave a different signature in the landscape. A cyclone approaching perpendicular to the coast will generate higher storm surges than a cyclone that approaches the coast at an angle (Unnikrishnan et al., 2022). As a result, two cyclones of the same intensity can leave different signatures in the landscape, depending on specific conditions at the time they occurred. Paleocyclone reconstructions are therefore always paired with an error margin and are likely to be conservative estimates of cyclone intensities since they assume the ‘optimal’ conditions (e.g., high tide and perpendicular approach) (Nott et al., 2009).

It is important to note that storm deposits such as beach ridges provide a conservative estimate of both the frequency and intensity of paleocyclones. Existing beach ridges can be washed away by subsequent events of a higher magnitude, erasing any evidence of the smaller events (Forsyth, 2013). This will result in an underestimation of paleocyclone frequency, since only the high magnitude events are preserved in the record. If subsequent events don’t erase the original ridge but increase its height by adding sedimentary layers, the resulting ridge height will introduce a preservation bias since only progressively larger events are able to overtop the accumulated ridge (Nott, 2009). Once a ridge is too high to be overtopped by subsequent events, a new ridge will be deposited on the seaward side of the original ridge. This ridge will record smaller events unless washed away, and will only record events until its height introduces preservation bias (Nott et al., 2009). This impacts the frequency and intensity estimate of paleocyclones, with the record selectively skewed towards the more extreme events.

Additionally, deposition of a beach ridge will provide information about the minimum water level required to deposit it, but does not place any limits on the maximum water level reached during the event (Nott, 2009). This will result in an underestimation of paleocyclone intensity.

3.1.3 Cyclone modelling

Total inundation during cyclones is a combination of storm surge, tide, wave set up, wind set up, current sea levels and wave run up. To accurately model inundation during cyclones, the relationship between these components needs to be understood and quantified to use them as variables in computer-generated cyclone simulations. Local bathymetry and coastal morphology also play an important role in cyclone modelling, and need to be taken into account (Nott et al., 2009). Based on bathymetry data for the Queensland coast just north of Cairns, Nott (2003) determined that wave set up is equivalent to ~10% of the significant wave height (average of the highest 1/3 of experienced waves) and wave run up equivalent to ~30% of the significant wave height. Nott et al. (2009) later calculated that the combined wave set up and run up for Cowley Beach near Mission Beach was only ~12%, emphasising the importance of local bathymetric differences. Once inundation components and local bathymetry data are known for a specific location, model-generated cyclones can be compared to cyclones recorded during the instrumental record period to test the accuracy of the computer model.

Using this method, Nott et al. (2009) produced a 6,000 year paleocyclone record based on a series of beach ridges at Cowley Beach, which is situated between Innisfail and Mission Beach in Queensland. Forsyth et al. (2010) performed a similar analysis on beach ridges found at Rockingham Bay, south of Cowley Beach. In both cases, ridge heights were measured in meters above Australian Height Datum (AHD), which is approximately equal to mean sea level. Sediment samples were dated to obtain absolute ages for the ridges. To calculate wave heights necessary to deposit these ridges at their current height above AHD, a range of parameters was entered into computer models. Changes in sea level were taken into account, as well as tidal ranges and local bathymetry data. Both studies concluded that, based on the results generated by the models, the wave heights necessary to deposit these ridges are associated with severe Category 4 and Category 5 cyclones. According to the number of ridges found in both locations, the frequency of intense paleocyclones was much higher than the instrumental records suggest (Forsyth et al., 2010; Nott et al., 2009). Instead of a Category 5 cyclone having a return interval of 1 in 1000 years, the average return period was calculated to be around 200 years instead. Forsyth et al. (2010) furthermore concluded that cyclone intensities and frequencies have varied in the past, with an active period of high-intensity cyclones occurring between 130-1,500 years ago, and another period occurring between 3,300-5,000 years ago. This variability was based on the spacing of the ridges, their heights, and their respective ages.

These two studies demonstrate that current instrumental records fail to capture long-term variations in both cyclone frequency and intensity in Queensland. However, the method used to reconstruct the paleocyclone record has a few limitations. One of the main limitations, which is particularly relevant to governments in terms of disaster management and building codes for coastal properties, is the likely underestimation of cyclone intensities and total inundation levels. Cyclone modelling showed that a Category 5 cyclone with a central pressure of 920 hPa was linked to an inundation level of 5.3 m above AHD, while a Category 5 cyclone with a central pressure of 880 hPa was associated with an inundation level of 7 m above AHD (Nott et al., 2009). While the highest ridge at Cowley Beach measured 5.5 m above AHD, the total inundation levels could have been closer to the 7 m above AHD generated by the models. It is precisely these maximum inundation levels that are important for disaster management groups and coastal construction companies, since they need to base their policies and codes on 'worst-case scenarios'.

A discussed in Chapter 1, foraminifera are microfossils that exhibit species-specific depth preferences. Chapter 2 described and quantified the contemporary microfossil assemblages from around Middle Island, situated on the central GBR. Statistical analyses showed that foraminiferal assemblages vary with depth, and that specific species can be assigned to specific depth ranges at this location. This chapter will use that information to test the second part of the research hypothesis: *Foraminifera can be used to reconstruct Holocene cyclone occurrences at Middle Island on the central GBR, Queensland, Australia.* If foraminifera in overwash deposits can be linked to specific depth ranges, the wave height responsible for depositing these foraminifera can be calculated. When this wave height is combined with the other factors that influence total inundation levels (i.e., relative sea level and local bathymetry), the total inundation levels for paleocyclones can be reconstructed with greater precision than currently possible.

3.2 Methods

3.2.1 Hand auger cores

Hand auger sediment cores were collected from the ephemeral lake on Middle Island in October 2023. The cores were retrieved to collect information about the sediment composition and stratigraphy in the lake, as well as the depth of the underlying reefal matrix from when the lake was an embayment with an open connection to the ocean. Hand auger corers are portable and easy to use but are limited in their penetration potential by the manual strength of the operator. They also cause mixing/smearing of sediment layers due to the rotation required to retrieve the corer, which can affect the accuracy of stratigraphical and sedimentary analyses. Hand auger cores are therefore useful for preliminary investigations but less suitable for sediment collection. The hand corer used for this research project was a 1 m long, semicircular, hollow metal pipe with sharp edges and a handle attached to the top (Figure 3.1).

Figure 3.1

Hand auger corer with retrieved sediment cores

For core collection, the pipe was pushed into the ground until refusal, and core extensions were used to increase penetration depth where the sediments allowed penetration past 1 m depth. Where possible, the cores were extended until terminating in the reefal matrix below the lake sediments, to retrieve the full stratigraphy since the formation of the lake. Upon twisting the corer, the sharp edges of the metal pipe cut a semicircular core out of the sediments, which was captured in the hollow pipe. The hand auger was removed from the sediment and the collected core was inspected for sediment stratigraphy, texture and colour of soil layers, and evidence of marine provenance such as coral clasts. A total of 14 sediment cores were collected, varying in length from 45-160 cm depending on soil composition, presence of impenetrable clasts and the depth of the reefal matrix. The cores were retrieved along four transects, which started at the landward edge of the shingle ridge on the southwestern side of the island, extended towards the middle of the lake, and covered the width of the lake (Figure 3.2).

Figure 3.2

Hand auger core collection

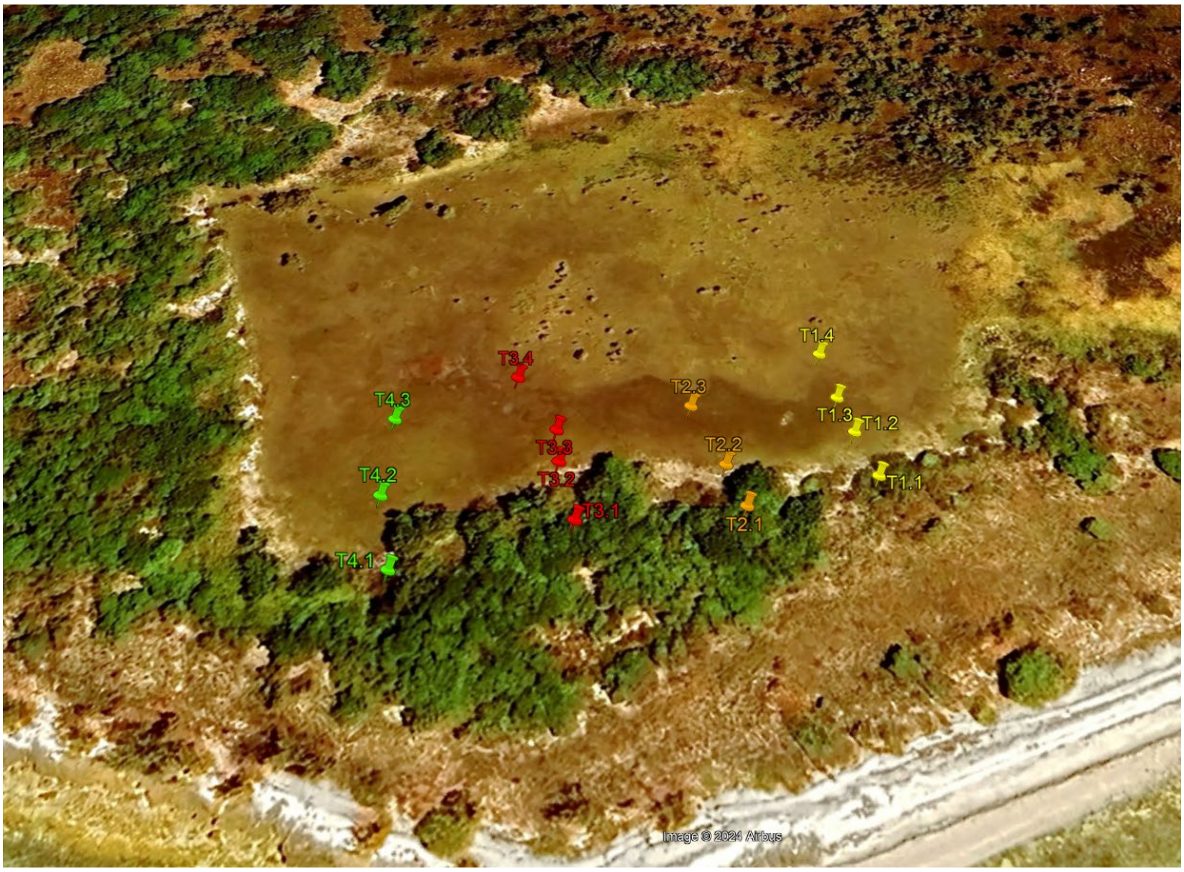

Note. From *Google Earth, 2024.*

All collected cores were photographed and features of interest were described. A total of three sediment samples were collected from cores 3.1 and 4.3, to be analysed for sediment composition and foraminifera presence. These samples were collected from sediment layers that were deemed to be of marine origin, which occurred at 50 cm and 75 cm downcore in core 3.1 and at 45 cm downcore in core 4.3. The samples were stored in labelled plastic containers for transport and storage in the sediment laboratory refrigerator at JCU. After the cores were described and photographed, the core sediments were redeposited in their original position. All core collection locations were recorded using a hand-held GPS.

The collected core samples were wet sieved to minimise damage to fragile foraminifera tests. The samples were sieved through stacked sieves with 500 µ and 250 µ apertures, since common tropical foraminifera are known to grow to these sizes. After sieving, the size fraction samples were dried in an oven at low temperatures (~45°C) to evaporate the water from the samples without damaging foraminifera tests. The dried samples were transferred to a petri dish and studied under a Nikon SMZ1500 stereoscopic microscope, with an AmScope MU1003B digital camera attached to the eyepiece. The camera was connected to a computer and the microscope image was projected onto the computer screen, which facilitated the sorting and identification process. Foraminiferal tests were separated from sediment grains by hand, using a fine paint brush. Identification was performed using ‘A guide to 1000 Foraminifera from Southwestern Pacific New Caledonia’ by Jean-Pierre Debenay, supplemented by the World register of Marine Species website (Ahyong et al., 2024; Debenay, 2013). When present, foraminifera were placed in a separate container, while the remaining sediment grains were returned to their original container.

3.2.2 RTK-GPS

To determine the topography and elevation of the reef flat, the shingle ridge and the lake surface above LAT, a Real Time Kinematic Global Positioning System (RTK-GPS) with a vertical and horizontal precision of ~0.01-~0.005 m was deployed. The RTK-GPS base station was set up on top of the shingle ridge, and its height above the ground was measured and programmed into the device. The RTK-GPS rover was used to measure the elevation of a range of points across the lake’s surface, the shingle ridge, and the reef flat (Figure 3.3). A measurement of the stillwater level was also recorded, together with the time it occurred. This information, in combination with the tide data from the nearby tide gauge at Abbott Point and the correction for the height of the base station, was used to convert elevation data to heights relative to LAT. Elevation relative to LAT is needed to reconstruct wave heights and inundation levels of overwash events, and to reconstruct a high-resolution paleocyclone history for Middle Island.

Figure 3.3

RTK-GPS elevation measurements

Note. From *Google Earth, 2024.*

3.2.3 Percussion cores

Percussion cores were collected from the ephemeral lake on Middle Island in November 2023. Once again, the lake did not contain any water at the time of core collection. Percussion coring requires more cumbersome equipment than hand auger coring but has the advantage of reaching greater penetration depths and collecting more sediments due to the diameter and length of the pipes used. Percussion coring also reduces smearing compared to hand auger coring. Coring was performed by manually hammering aluminium pipes (3 m length, 9.5 cm diameter and 2 mm walls) into the sediment until refusal. The penetration depth of the pipe was measured, as well as the depth of the sediments in the pipe to calculate compaction. Each coring pipe was then filled with water and sealed to create a partial vacuum. Wrenches were used to rotate the pipe and lift it out of the sediment, after which the bottom end of the pipe was capped to prevent sediment loss. After draining the water, excess pipe was cut using a pipe cutter and the pipe was labelled and sealed for transport and storage in the sediment laboratory refrigerator at JCU.

Because the previously collected hand auger cores managed to penetrate down to the reefal matrix in most cases, the percussion cores were collected along the same transects that were used for the hand auger cores. Due to time constraints and the amount of manual labour involved, percussion cores were collected along the full length of two of the transects, while core collection was limited to the back of the ridge along the other two transects (Figure 3.4).

Figure 3.4

Percussion core collection

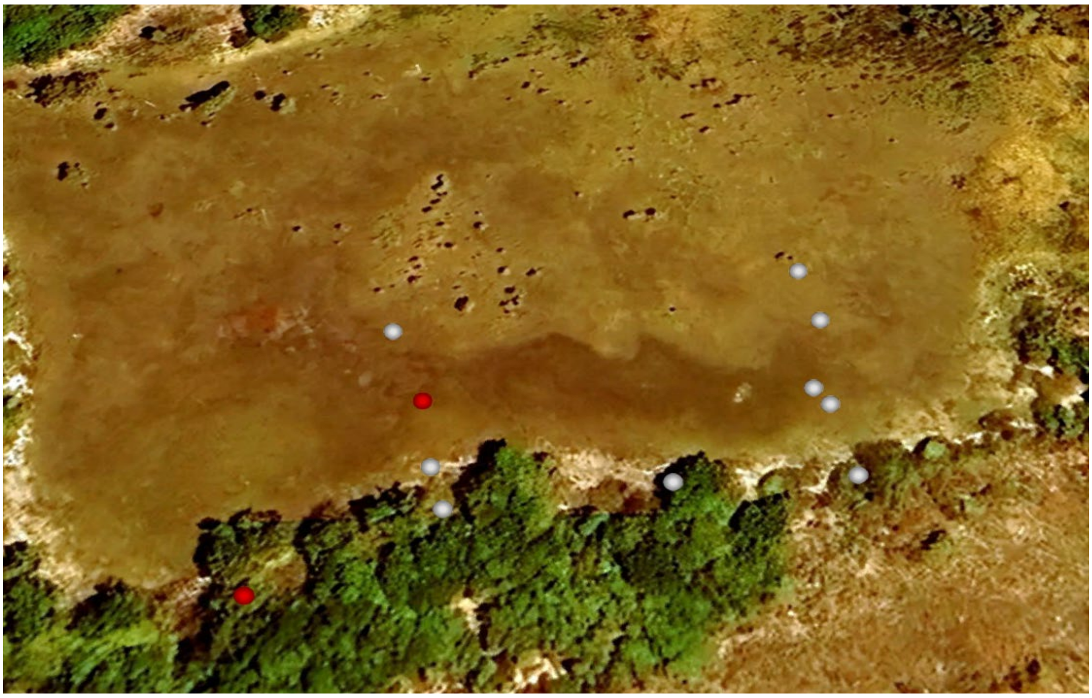

Note. The two cores marked in red were used for sedimentary and foraminiferal analyses.

From *Google Earth, 2024.*

Washover events are most likely to be recorded in the sediments directly behind the ridge since the ridge introduces friction and causes washover waves to decelerate. Washover waves might therefore lose their energy too quickly to reach the middle of the lake, which is why the majority of the percussion cores were collected adjacent to the ridge. Percussion coring resulted in the collection of 11 cores, ranging in length from 0.28-1.57 m, with cores PC3.1 and PC1.3 failing to reach the reefal matrix. The location of each percussion core was recorded using a handheld GPS.

3.2.4 Analyses

All 11 percussion cores were cut in half using a circular saw and the halves were photographed. One half of the core was retained for archive purposes, while the working half was used for analysis. For each core, the visible stratigraphy was recorded along with the boundary depths, and Munsell's colour charts were used to classify the colour of each visible layer. Soil texture was recorded for the layers, as well as the presence of material that indicated either marine or terrestrial provenance (i.e., coral clasts, grass roots, peat). Coral clasts with good preservation were recorded, along with their depth downcore, as potential radiocarbon dating samples. Four coral clasts were selected: a *Goniastrea* clast from PC1.1 at 70 cm downcore, a *Goniopora* clast from PC3.3 at 60 cm downcore, a piece of branching *Seriatopora* coral from PC3.4 at 110 cm downcore, and another *Goniopora* clast from PC4.1A at 55 cm downcore. The clasts were removed from the cores and placed in an ultrasonic device to remove any contaminants or encrusting materials. These allochthonous materials can be much younger than the coral clasts upon which they are found, which will distort the generated radiocarbon date. Dissolution and degradation of coral skeletons also affects the accuracy of returned radiocarbon dates. The two clasts from PC3.3 and PC3.4 were deemed to be in the best condition, without visible signs of coral skeleton dissolution or degradation. A small subsample of <5 grams was removed from each clast using a handheld grinder. These subsamples were cleaned in the ultrasonic device once more and weighed after air-drying. The samples were sent to the Waikato Radiocarbon Laboratory in New Zealand for radiocarbon dating. The remainder of the coral clasts was retained as backup material for potential future dating.

Once all the cores were described and photographed, two percussion cores were selected for further analysis: PC3.3 (132 cm) and PC4.1A (127 cm). PC4.1 was retrieved from the lake directly behind the ridge, while PC3.3 was retrieved from a location further towards the centre of the lake. Their selection was based on the length of the cores, their varying locations along the transects, the presence of visible stratigraphic layers, the presence of reefal material throughout the bottom part of the core, and the presence of potential radiocarbon dating samples. All these characteristics made the two chosen cores suitable candidates for containing evidence of overwash deposits. From each of the two selected cores, sediment samples of 1 cm thick were collected at 5 cm intervals throughout the full length of the core, resulting in 26 samples from core PC3.3 and 25 samples from core PC4.1A. The sampling interval was chosen to get a high-resolution stratigraphical reconstruction of the cores, without the analysis being prohibitively time-consuming. The obtained sediment samples were split into two subsamples, with one subsample retained as archive subsample. The other subsamples were dried in an oven at low temperatures (~45°C) to evaporate the water while preventing damage to foraminiferal tests and other fragile carbonate material. The subsample's dry weights were recorded, to be able to later calculate the proportion of grain size fractions for each sample. Grain size distribution can provide information about sediment provenance and can be used as an indicator of overwash deposits if the grains are coarser than the in-situ sediments onto which they are deposited. Samples for core PC3.3 varied in weight from 6.03-47.53 grams and PC4.1A core samples varied in weight from 3.93-16.53 grams. After weighing, the samples were submerged in water and placed in an ultrasonic machine for dispersion. Once the samples were rehydrated and dispersed, the sediments were sieved through a stack of sieves with the following apertures: 1 mm, 500 μ, 250 μ, 125 μ and 63 μ. These size fractions were chosen to determine grain size distribution of the samples while simultaneously capturing any foraminifera present in the samples. A pan was placed underneath the 63 μ sieve, to collect the sediments <63 μ. The sediment fractions >63 μ were returned to the oven to dry, while the <63 μ fraction was analysed in a Malvern Mastersizer 3000 to determine grain size distribution within this smallest size fraction. Once the size fractions >63 μ had dried, the weight of each size fraction was recorded and subtracted from the total weight of the subsample, to determine the weight of the <63 μ fraction. The 500 μ and 250 μ size fractions were analysed for foraminiferal presence using the same methods that were used for the hand auger samples.

To analyse the <63 μ fractions in the Mastersizer, the samples were returned to the ultrasonic device after sieving to prevent flocculation. The Mastersizer was cleaned with the pre-programmed cleaning cycle, using distilled water. The following settings were used for the sample analyses: non-spherical particles, kaolinite constitution, water as the medium, obscuration rate of 5-20% and three replicates per sample. Non spherical particles and kaolinite constitution most closely resembled the particles in the sediment samples, and distilled water was used to minimise background scatter. Obscuration of 5-20% was set to minimise reading error due to too little/too much sample added to the machine. Three replicates were chosen to obtain an average reading over three samples and to strengthen the results of the readings. After confirming the settings, the Mastersizer was initialised, and the background readings were completed. The sediment sample was added to a beaker with distilled water using a pipet, until the obscuration reached ~12% (halfway between 5% and 20%). The sample was analysed, and the results were checked for data quality and consensus between replicates. If the analyses were accepted, results were saved as a CSV file for use in Excel. If an error occurred due to low data quality or differences between replicates, the machine was cleaned, and the sample was re-analysed.

3.3 Results

3.3.1 Hand auger cores

The 500 μ and 250 μ fractions from core 3.1 at 50 cm downcore both consisted of predominantly siliciclastic material, with a few organic (grass) roots present. No coral clasts, shells or shell fragments were identified, and no foraminifera were present in the sample. The 500 μ and the 250 μ size fractions from core 3.1 at 75 cm downcore mainly consisted of coral clasts and coral- and shell fragments, interspersed with a few siliciclastic grains and organic (grass)roots. The 500 μ fraction did not contain any foraminifera, but three *Elphidium craticulatum* species were identified in the 250 μ fraction. The 500 μ and 250 μ fractions from core 4.3 at 45 cm downcore both consisted of a mix of carbonate material and siliciclastic grains. In the 500 μ fraction, coral clasts were present, but no shells or shell fragments were identified, and no foraminifera were found. In the 250 μ fraction, coral clasts, shells, and shell fragments were present, but no foraminifera were identified.

3.3.2 RTK-GPS

The landward side of the shingle ridge on the southwestern side of the island starts at an elevation of 2.53 m above LAT and increases to 6.21 m above LAT, at which point the ridge is ~50 m wide. The shingle ridge then decreases in height towards the beach to 3.78 m above LAT, to reach a width of ~65 m. The large shingle ridge is fronted by the contemporary berm crest, which is the swash limit under fair-weather conditions, and reaches an elevation of 4.18 m above LAT. The beach then slopes down steeply and transitions into the reef flat, which is elevated about 1 m above LAT. At ~100 m from the shoreline, where the stillwater level was measured, the reef flat still has an elevation of ~0.9m which indicates a very gentle slope. The ephemeral lake's surface shows very little relief and is situated between 2.38-2.56 m above LAT (Figure 3.5)

Figure 3.5

Elevation profile for topographic features on Middle Island

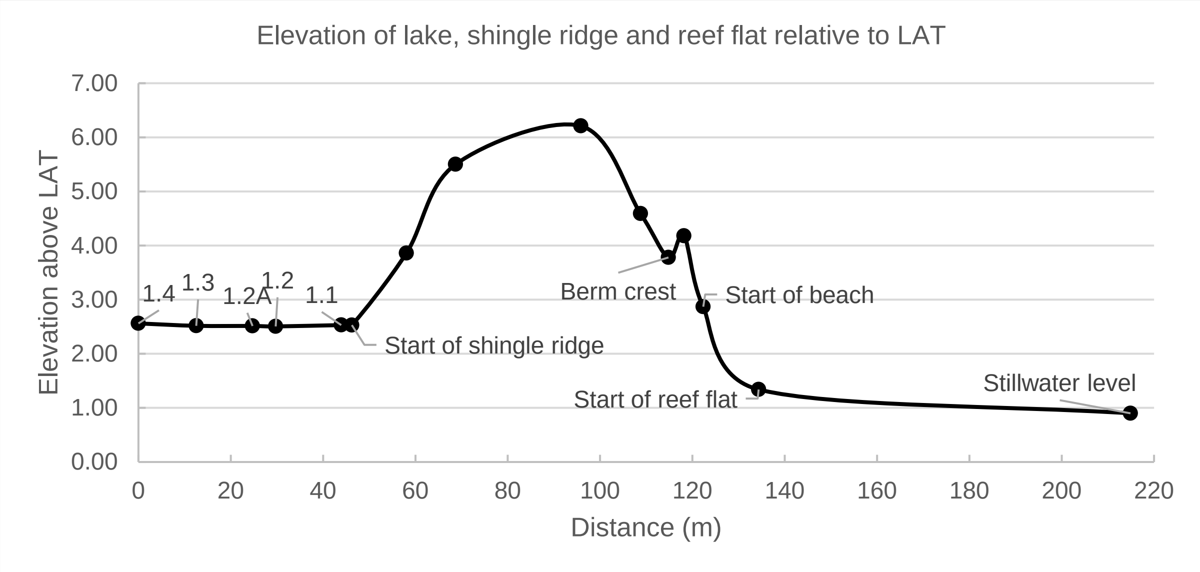

3.3.3 Percussion cores

The 11 percussion cores collected from the lake at Middle Island varied in length from 0.28-1.57 m and in compaction from 6.7-53.8%. The cores with lengths of ~1 m or longer showed similar compactions ranging from 19.9-27.4%. The two shortest cores, PC1.3 and PC3.1, were 6.7% and 10.0% compacted, while PC1.4 showed 14.1% compaction. Core PC4.1, even though it only measured 60 cm, had the highest compaction of all the cores: 53.8% (Table 3.2).

Table 3.2

Percussion core lengths and compaction rates

Core	Core length (m)	Penetration (m)	Compaction (%)
PC1.1	*1.38*	*1.75*	*21.1*
PC1.2A	*0.92*	*1.20*	*23.3*
PC1.3	*0.28*	*0.30*	*6.7*
PC1.4	*0.67*	*0.78*	*14.1*
PC2.1	*0.93*	*1.22*	*23.8*
PC3.1	*0.36*	*0.40*	*10.0*
PC3.2	*1.29*	*1.61*	*19.9*
PC3.3	*1.32*	*1.78*	*25.8*
PC3.4	*1.57*	*2.05*	*23.4*
PC4.1	*0.60*	*1.30*	*53.8*
PC4.1A	*1.27*	*1.75*	*27.4*

The number and thickness of stratigraphic layers differed per core, but all cores had a black, organic sediment layer at the top that was 5-15 cm thick. All cores, except cores PC1.3, PC3.1 and PC3.4, recorded a change in sediment from organic fine mud to a coarser sandy layer around 40-50 cm downcore. Coral clasts also started appearing in the cores at depths of 30-40 cm, although PC3.4 was an exception and did not record coral clasts until 75-85 cm depth. Cores PC1.1, PC3.3 and PC3.4 displayed an orange/yellow sediment layer around 85 cm downcore. Sediments generally lightened in colour from black to light grey/greenish grey with increasing depth downcore, and all cores that penetrated past 1 m depth terminated in a greenish-grey, muddy, wet sediment layer. This layer contained organic material as well as coral clasts with crustose coralline algae (CCA) attached to their surfaces.

RTK-GPS measurements at the core collection locations revealed that the lake's surface exhibits very little relief, and the uppermost sedimentary layers in all 11 cores were situated at 2.38-2.56 m above LAT. Cores PC1.3 and PC3.1 only penetrated the upper 30 cm of the lake sediments before terminating on impermeable material, and these two cores were not retained for stratigraphic analysis. The other nine cores showed similar stratigraphic zones and indicate that PC3.3 and PC4.1A, which were chosen for further analyses, are representative of the stratigraphy across the full extent of the lake (Figure 3.6).

Figure 3.6

Percussion core stratigraphy

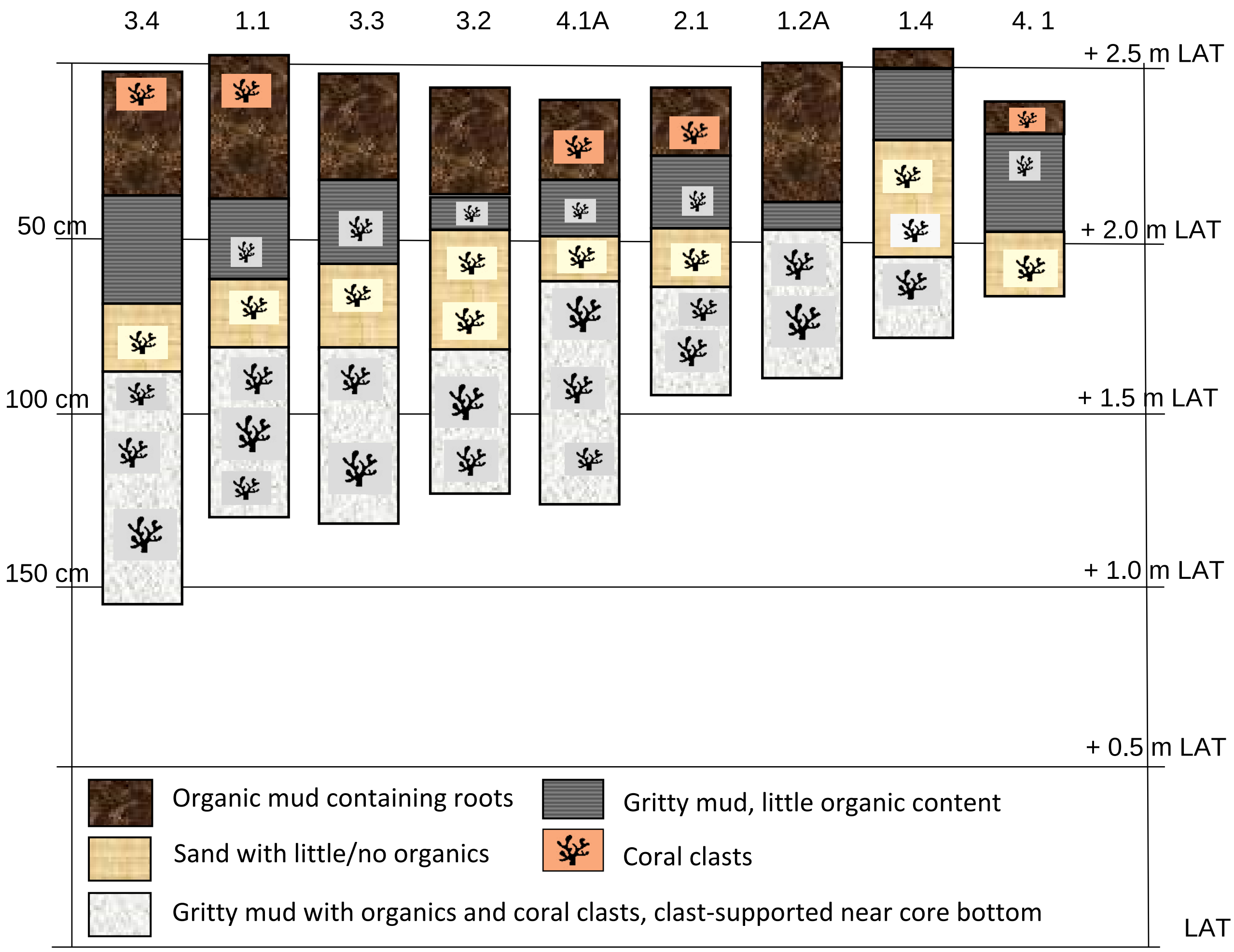

Note. *Left axis indicates core length, right axis indicates elevation above LAT. Core tops reflect elevation changes in the lake's surface. Core numbers ending in .1 were collected directly behind the shingle ridge, core numbers ending in .4 were recovered from the middle of the lake.*

The grain size distribution analyses for cores PC3.3 and PC4.1A resulted in 51 depth interval samples and six size fractions (1 mm, 500 μ, 250 μ, 125 μ, 63 μ and <63 μ) per sample, providing a total of 306 subsamples. After drying and weighing the subsamples, the weight of each size fraction was calculated as a percentage of the total sample weight (Figure 3.7)

Figure 3.7

Percussion core size fraction distribution

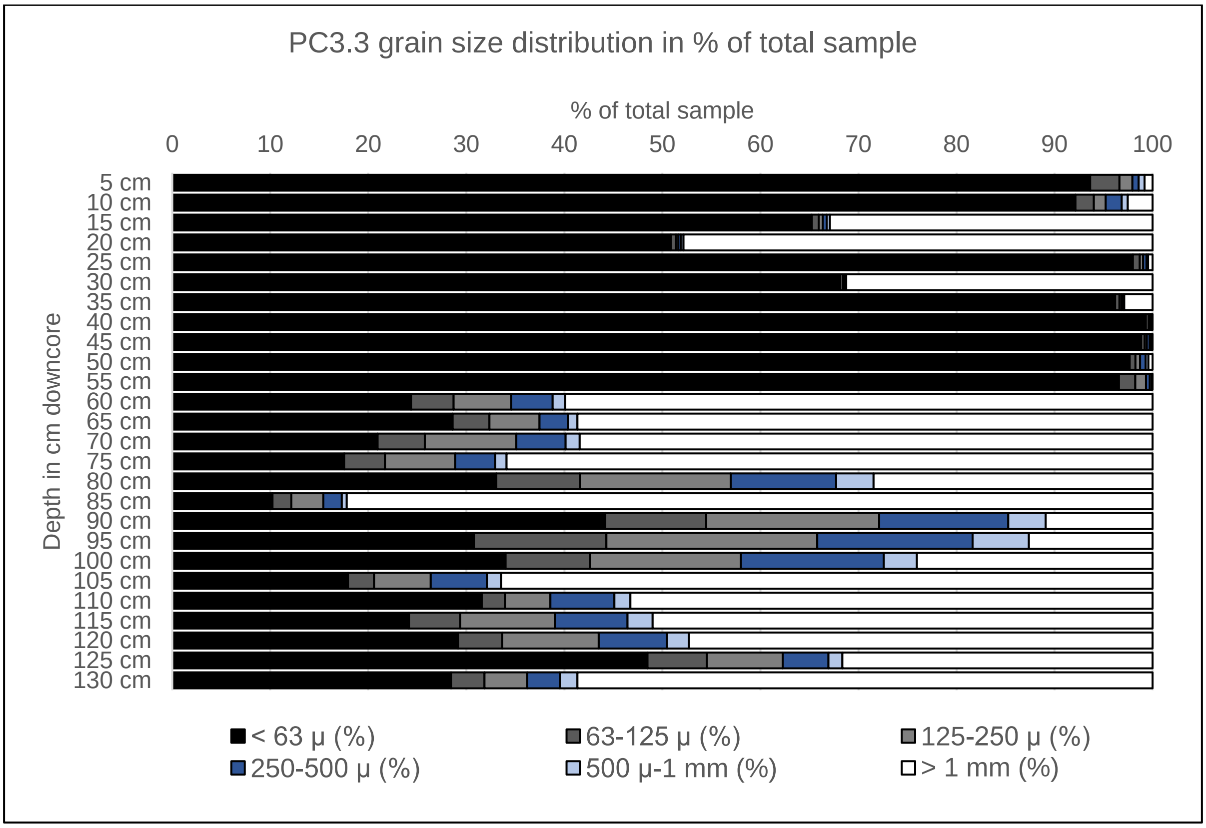

Note. Size fractions that correspond to foraminifera test sizes are highlighted in blue.

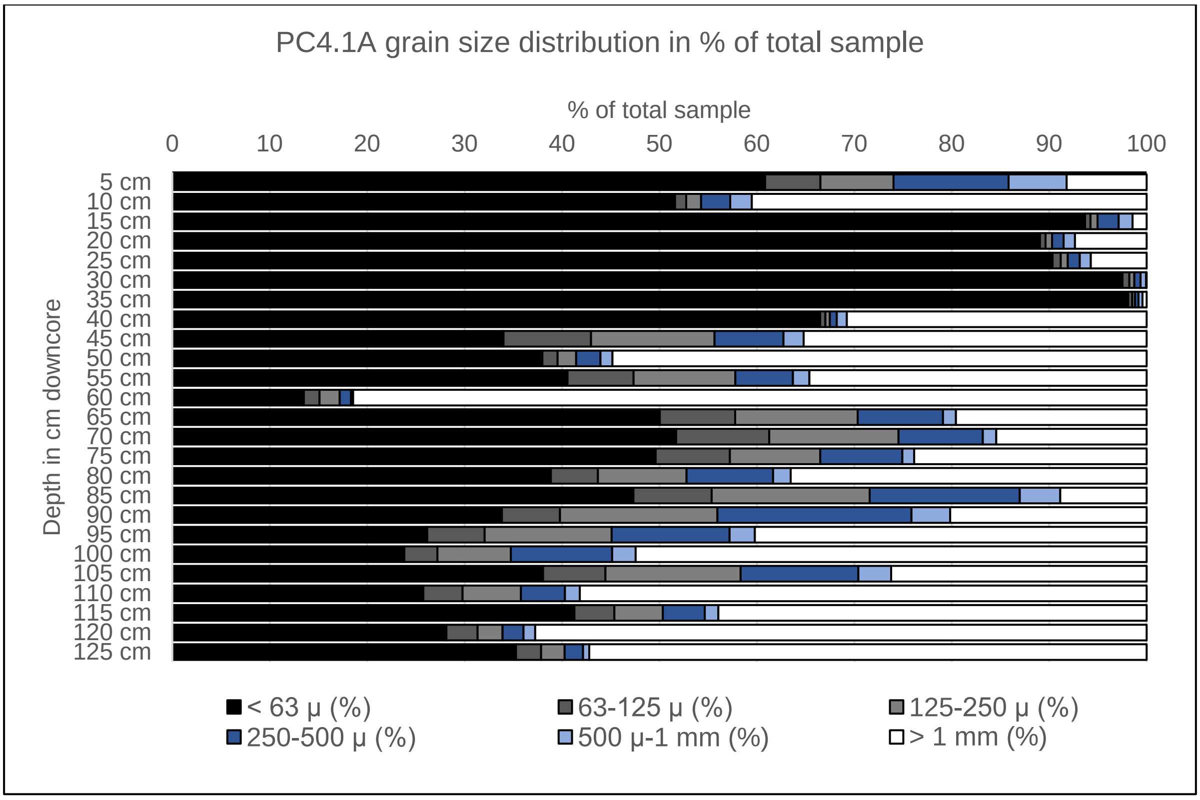

Note. Size fractions that correspond to foraminifera test sizes are highlighted in blue.

The top 55 cm of the PC3.3 core were dominated by the <63 µ size fraction, which constituted ≥50% of the total sample weight. At 5, 10, 25 and 35-55 cm downcore the <63 µ size fraction was responsible for >90% of the weight of the total sample. The sediments in the remaining layers were composed of both the <63 µ size fraction (up to ~68%) and the 1 mm fraction (up to ~48%). Past 55 cm downcore, the sediments became more varied and were composed of a range of size fractions. In most sediment layers in the bottom half of the core, the 1 mm size fraction was dominant, with weight percentages ranging from ~45-85%. Exceptions were seen at 80, 90-100 and 125 cm downcore, where the <63 µ fraction dominated once again. The remaining size fractions (63-500 µ) had minor contributions to the sample weight throughout the whole core but did increase past 55 cm downcore.

The top 5 cm of the PC4.1A core showed a varied composition, with all size fractions contributing to the sample weight. The <63 µ fraction still dominated this layer, contributing 60% to the total sample weight. The 10 cm layer was a mix of the <63 µ fraction (~52%) and the 1 mm fraction (~40%). From 15-35 cm downcore the <63 µ fraction dominated, contributing >85% to the total sample weight. From 40 cm downcore the sediments became more varied, although all samples were either dominated by the <63 µ sample (up to ~50%) or the 1 mm sample (up to ~80%).

The sediment size fraction distribution of the <63 μ samples were analysed in the Mastersizer. Three replicates were produced for each sample, and the averaged results are shown in figure 3.8.

Figure 3.8

Distribution of size percentiles in the 63 μ sediment size fraction

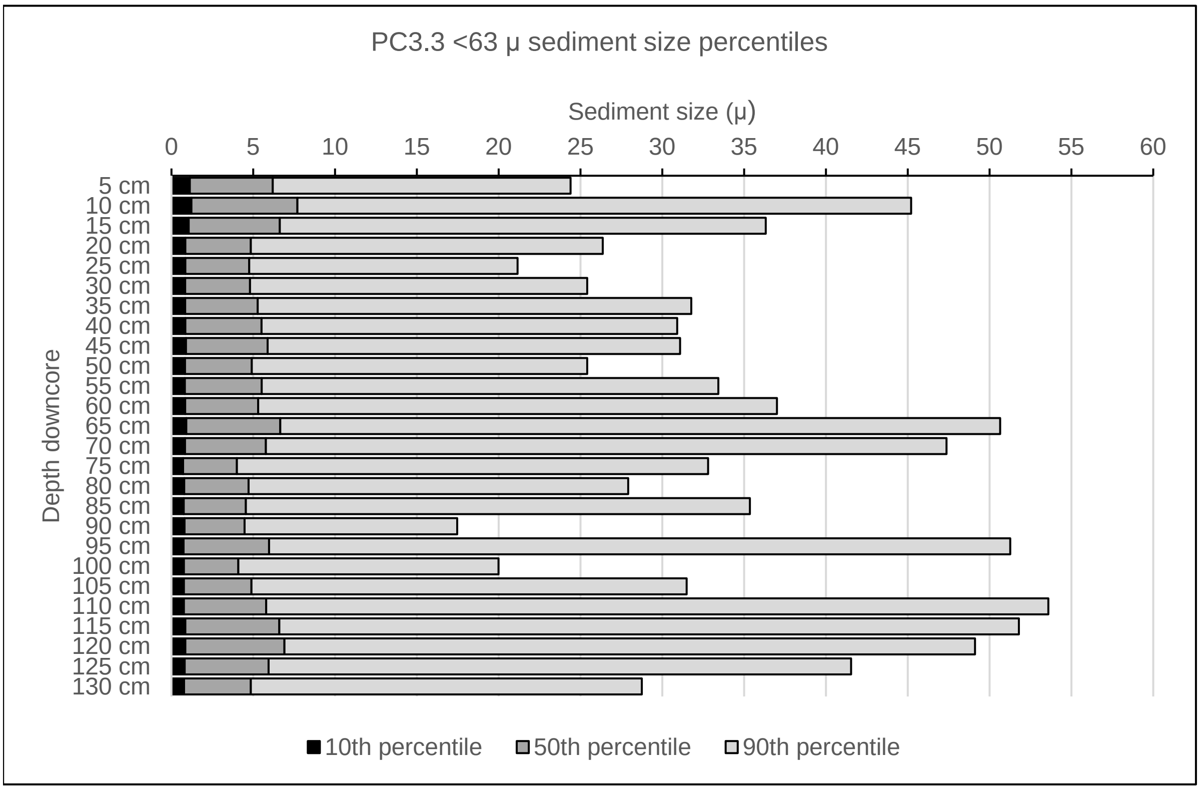

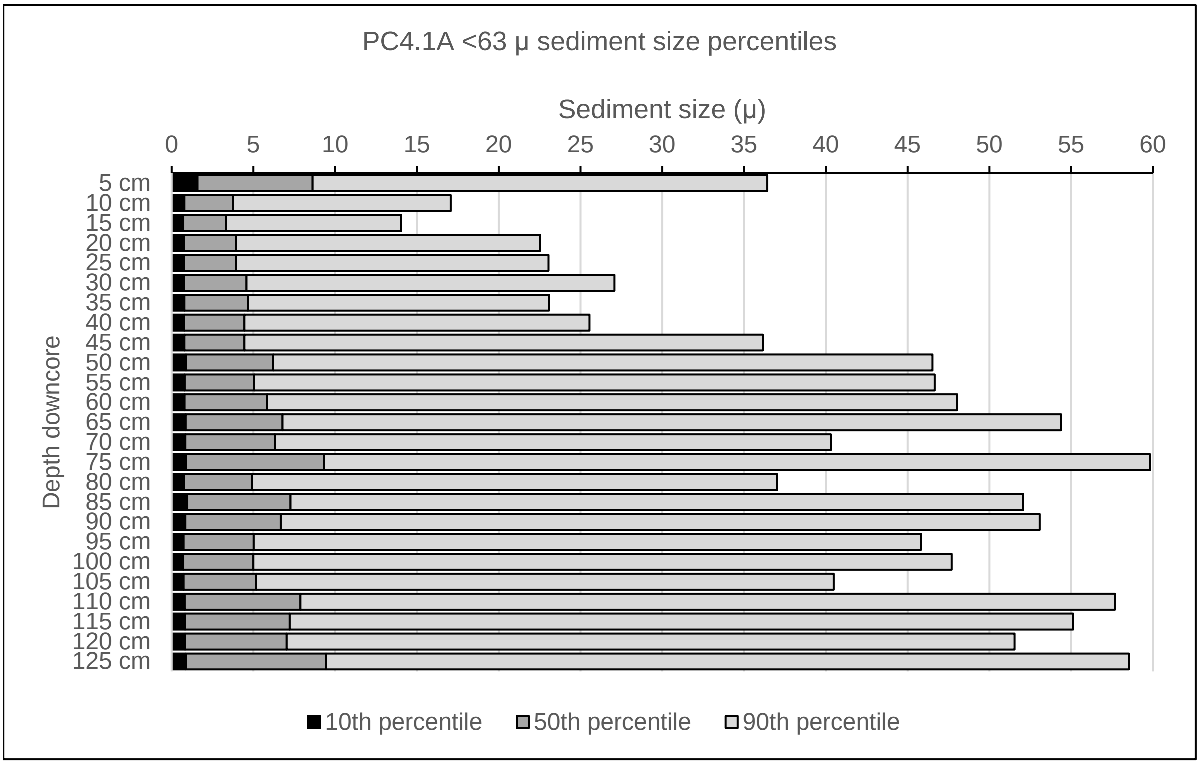

PC3.3 showed a variable size distribution within the <63 μ size fraction, although the majority of the sediment grains measured between 5-55 μ across all samples. The smallest grain sizes belonged to the sediment sample from 90 cm downcore, followed by the sediments from 100 cm downcore. The largest grains were found at 110 cm downcore, followed by the sediments from 115 cm downcore. No clear patterns in size distribution were visible in this core. PC4.1A also showed a variable size distribution within the 63 μ size fraction and the largest proportion of sediment grains measured between 5-60 μ across all samples. The size fractions in PC4.1A showed a general increase in size with increase in depth downcore, although the sediments from 5, 70 and 105 cm downcore are notable exceptions.

3.3.4 Foraminifera

The 250 μ and 500 μ size fractions from the 51 depth samples from cores PC3.3 and PC4.1A were analysed for foraminiferal content. In PC3.3, foraminifera were found throughout most the core. From 15-40 cm downcore, *Ammonia* was the only genus present in the samples and all foraminifera were found in the 250 μ size fraction. From 50-90 cm downcore, the foraminifera almost exclusively belonged to the genus *Elphidium*, with one specimen of *Textularia* identified as well as one specimen of the genus *Reussella*. *Elphidium* species occurred in both the 250 μ and the 500 μ fraction, the other two foraminifera were found in the 250 μ size fraction. The sample from 90 cm downcore contained a diverse foraminiferal assemblage, mainly present in the 250 μ size fraction. Due to the time-consuming nature of the sorting and identification processes, the sediment samples from 95-130 cm downcore were not analysed for foraminifera.

PC4.1A contained a more diverse assemblage of foraminifera, and the top 10 cm of the core contained foraminifera that were tentatively identified as *Paratrochammina* species. The foraminifera between 10-60 cm mainly belonged to the genus *Elphidium*, which were present in both size fractions. Starting at 65 cm downcore, foraminifera species were abundantly present in the sediments and assemblages were counted until a count of 100 foraminifera was reached, based on the previously discussed paper by Forcino and colleagues (2015). The samples between 80-115 cm were not analysed due to time constraints. The samples from 115-125 cm downcore were analysed to determine if foraminifera were still abundant throughout this part of the core, which was the case for the 115 cm sample but not for the 120 and 125 cm samples (Appendix 2).

Both cores contained foraminifera species that were determined to be depth-specific in the previous chapter. All the foraminifera in the cores belonged to the 5-10 m below LAT depth interval, except for two *Elphidium crispum* specimen which occur anywhere on the reef slopes below LAT. All depth-specific foraminifera belonged to the 250 μ size fraction (Table 3.3).

Table 3.3

Depth-specific foraminifera in PC3.3 and PC4.1A

	PC4.1A	***PC3.3***
Depth	**250 µ**	**250 µ**
45 cm	*Elphidium hispidulum (2)* - 5-10 m below LAT	
50 cm		*Textularia dupla (1)* - 5-10 m below LAT
65 cm	*Clavulina pacifica (1)* - 5-10 m below LAT	
	Elphidium hispidulum (9) - 5-10 m below LAT	
	Quinqueloculina crassicarinata (1) - 5-10 m below LAT	
70 cm	*Elphidium crispum (1)* - 0-10 m below LAT	*Elphidium hispidulum (6)* - 5-10 m below LAT
	Elphidium hispidulum (4) - 5-10 m below LAT	
	Quinqueloculina crassicarinata (1) - 5-10 m below LAT	
	Spiroloculina communis (1) - 5-10 m below LAT	
	Textularia dupla (1) - 5-10 m below LAT	
75 cm	*Elphidium hispidulum (1)* - 5-10 m below LAT	
	Spiroloculina communis (1) - 5-10 m below LAT	
80 cm	*Elphidium excavatum (1)* - 5-10 m below LAT	
	Elphidium hispidulum (1) - 5-10 m below LAT	
90 cm		*Elphidium hispidulum (5)* - 5-10 m below LAT
115 cm	*Elphidium crispum (1)* - 0-10 m below LAT	
	Sahulia conica (1) - 5-10 m below LAT	

Note. The numbers in brackets indicate the quantity of identified tests, followed by their specific depth ranges as determined in chapter 2.

3.4 Discussion

This study identified three overwash deposits in percussion cores collected from Middle Island, and used species-specific depth preferences of foraminifera to determine a sediment provenance depth of at least 5-10 m below LAT.

3.4.1 Evidence of washover events

Based on the sediment characteristics and the presence of depth-specific foraminifera in the core, PC3.3 recorded washover events at depths of 50 cm downcore, 70 cm downcore and 90 cm downcore. PC4.1A showed similar evidence of overwash deposits at 45 cm downcore, 65-80 cm downcore and 115 cm downcore (Figure 3.9)

Figure 3.9

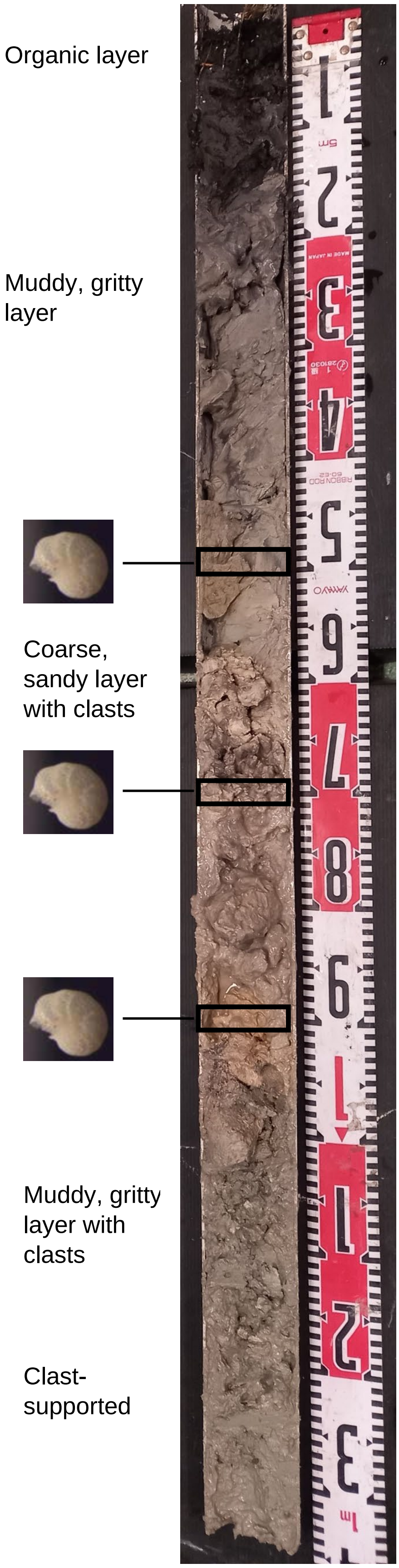

Note. PC3.3.

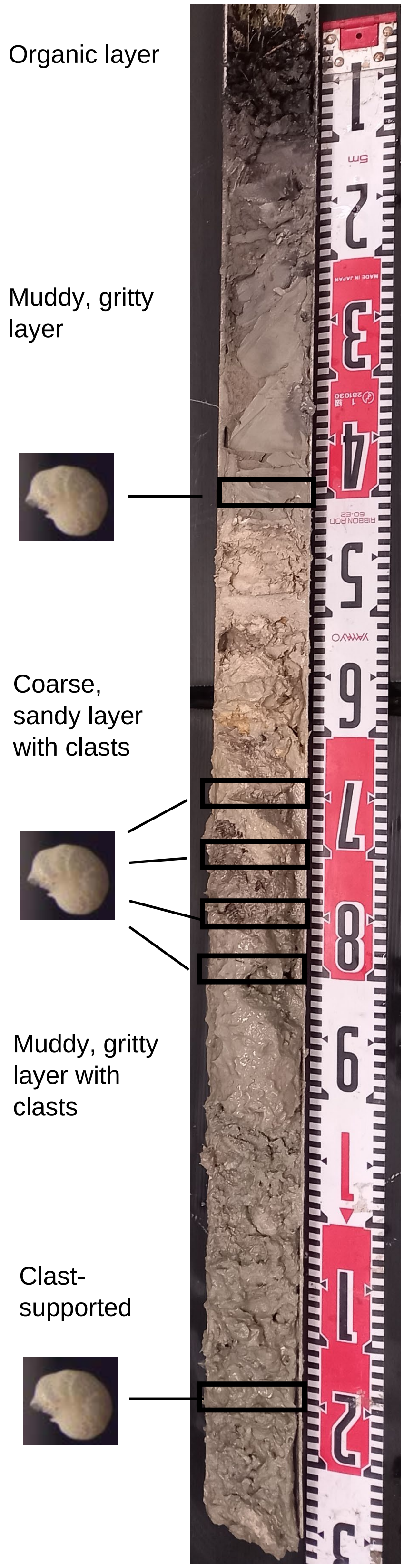

Note. PC4.1A.

PC3.3 contained coral clasts at ~30 cm downcore, which can be an indication of a washover event. Overwash deposits can be distinguished from terrestrial, in-situ sediments due to their coarser sediment size and the presence of marine sediments such as carbonate material or marine organisms (Wang & Horwitz, 2007). This core also contained foraminifera between 15-40 cm downcore, and these foraminifera were either tentatively identified as *Ammonia* species or remained unidentified. A few coral clasts were present in the 1 mm size fraction, as well as roots and siliciclastic grains, but the majority of the sediments consisted of the <63 µ size fraction. Sediments in this size fraction have either undergone extensive weathering and erosion, which have reduced the sediment grains to their smallest possible size based on their mineral composition, or the sediments consist of particulate organic matter. Based on the position of the sediments near the lake's surface, and the presence of abundant organic material in the sedimentary layers, it is assumed that the sediments in the smallest size fraction are organic in nature. The foraminifera in the genus *Ammonia* are known for the wide range of environmental parameters they can tolerate. *Ammonia* species are found in marginal environments such as estuarine, brackish and saltmarsh environments and can tolerate fluctuations in water salinity, temperature, and nutrient availability (Consorti et al., 2021). Since the environmental parameters in the lake were not recorded at the time of core collection, no conclusions can be drawn about the suitability of the environment for the survival of *Ammonia* species. However, based on the small sediment size, the presence of organic and siliciclastic material and the absence of coarser marine sediments, the sediments in the top 40 cm of core PC3.3 were not deemed to represent overwash deposits. Instead, it is hypothesised that the coral clasts originated from the shingle ridge on the western side of the lake, since PC3.3 was collected adjacent to this ridge. The coral clasts could have been dislodged from the ridge during runoff from rainfall, or by animal or human disturbance.

PC4.1A also contained coral clasts and foraminifera in the upper ~15 cm of the core. The sediment layers surrounding the clasts were composed of organic and siliciclastic sediment grains and contained sediments from all measured size fractions, although 60% of the total sediments consisted of the <63 µ size fraction (Figure 15 and 16). Besides the coral clasts, the larger sediment size fractions consisted of roots and organic aggregates. Some shells and shell fragments were also present in the sediments, but no other carbonate material was identified, apart from the coral clasts. Some agglutinated foraminifera were present in the top 10 cm of the core, which were tentatively identified as agglutinated *Paratrochammina* species. Agglutinated foraminifera species construct their tests from material that is present in the environment, and can therefore contain organic or carbonate grains, or even ferric oxide material. These foraminifera therefore don't require marine habitats with high carbonate availability to construct their tests. (Debenay, 2013). Agglutinated foraminifera are also known to live in marginal environments such as mangroves and brackish, intertidal environments, and even in terrestrial environments (Holzmann & Pawlowski, 2002; Meisterfeld et al., 2001). The presence of agglutinated foraminifera is therefore not always indicative of marine sediment provenance. The same applies to shells and shell fragments since these could belong to either marine or terrestrial gastropods. Based on this information, the lack of carbonate sediment grains, and the large proportion of sediments <63 µ, these sediments were not considered to be evidence of a washover event. The same mechanisms for coral clast deposition in PC3.3 are assumed here.

PC3.3 and PC 4.1A both contained depth-specific foraminifera at ~45-50 cm downcore. Because of slight differences in lake surface elevation and the resulting differences in core depths relative to LAT, these depths are considered to represent the same event across both cores. The sediment size distribution in PC3.3 differed from PC4.1 at this depth, with ~95% of the sediments in PC3.3 belonging to the <63 µ size fraction, compared to ~30% in PC4.1A. This is likely the result of the respective locations of the cores relative to the ridge. PC4.1A is situated directly behind the shingle ridge on the southern side of the lake, while PC3.3 is located further inland near the centre of the lake. Washover events have been shown to leave wedge-shaped overwash deposits that thin with distance inland. Overwash sediments also reduce in coarseness with distance inland, due to loss of wave energy as a result of friction (Palmer et al., 2020; Pilarczyk et al., 2014). It is probable that the waves that washed over the ridge would have deposited most of the coarser sediment directly behind the ridge, and only the finer sediments would have been carried further inland towards the centre of the lake.

PC3.3 samples were analysed to a depth of 90 cm and recorded evidence of a washover event between 70-90 cm. PC4.1A was analysed to a depth of 80 cm and recorded washover deposits at similar depths, between 65-80 cm. The sediments in both cores differed in colour and coarseness compared to the sediment layers above, with both cores showing a significant increase in size fractions ≥ 63 µ. The increased coarseness and change in colour are hypothesised to be the result of different sediment provenance compared to the deposit above. As shown by the habitat analyses, sediments on the reef slopes and sea floor around Middle Island mostly consist of grey and brown muds and silts, with no visible sources of light-coloured, coarser sands. The core sediments must therefore be allochthonous to Middle Island, which indicates transport by waves. The coarseness of the washover sediments could also indicate an event of larger magnitude: more intense cyclones generate larger waves, which transfer higher wave energy and can therefore entrain coarser sediment particles. The foraminiferal assemblages in both cores do not initially seem to support the possibility of a higher magnitude event. Both cores contained depth-specific foraminifera that indicate a sediment provenance depth of 5-10 m below LAT, which is the same depth as the deposit above. However, foraminiferal assemblages were analysed for species-specific depth preferences between 0-10 m below LAT, with 10 m being the bottom of the reef slopes and the start of the sea floor. Foraminiferal assemblages from greater depths were not analysed, and as such no conclusions can be drawn about any species-specific preferences at these depths or about their presence in the overwash deposits recorded in the core. As stated by Ryan et al. (2016), water depths in Edgecumbe Bay between Middle Island and Bowen reach a maximum of 14 m below LAT and could be a source of coarser sediments and deeper foraminiferal assemblages. However, this cannot be confirmed until sediment samples are collected, and foraminiferal assemblages are analysed. The same applies to other locations in the vicinity of Middle Island, e.g., Bowen, Abbott point, Cape Gloucester, and Gloucester Island: further research is needed to determine sediment provenance and foraminiferal assemblage characteristics from a greater depth range at these locations.

Due to the sampling resolution of 5 cm intervals, it is uncertain whether the sediments between 65-90 cm are the result of a single washover event, or an accumulation of multiple events with similar magnitudes and sediment provenances. Based on visual inspection of the cores, the sediments appear to be similar in composition and coarseness, which indicates a single event. This is supported by Nott & Jagger (2013), who determined that a washover deposit generated by cyclone Yasi in 2011 was approximately 30-40 cm thick. This is similar to the thickness of the sediment deposits in the Middle Island cores. Cyclone Yasi was a Category 5 cyclone that deposited sediments on top of an existing ridge with a height of ~6.9 m above LAT, slightly higher than the ridge at Middle Island (Nott & Jagger, 2013). Based on this information, the sediments between 65-90 cm downcore in PC3.3 and PC4.1 A are assumed to indicate a single, high-magnitude washover event. Smaller sampling intervals of 1-2 cm would result in higher-resolution reconstructions and could identify more overwash deposits in future studies. Due to the time-consuming nature of sediment analyses and foraminifera identification, some sediment samples from the Middle Island cores still need to be analysed, which could result in the discovery of more overwash deposits for this location.

The sediments from the bottom 15 cm of core PC4.1A were analysed for foraminifera presence and contained two depth-specific foraminifera tests belonging to 0-10 m and 5-10 m below LAT. Due to the colour of the sediments and the reduction in size fractions between 63-500 µ, these deposits were determined to have a different provenance compared to the washover event above it. The sediments in this part of the core also contained organic material in the form of peat, which was absent from the deposits above. Since the bottom of core PC4.1A was clast-supported, this part of the core is assumed to represent the reef flat that existed before the southern shingle ridge was emplaced. When the shingle ridge was deposited, it severed the connection between the embayment and the ocean, transforming the embayment into a marsh environment that dried up over time and turned into an ephemeral lake. The presence of peat indicates that the environment was suitable for the production of organic matter, which was later buried and preserved under the increasing weight of sediment layers deposited on top.

3.4.2 Ages of overwash deposits

The results of the radiocarbon dating analyses had not been returned yet on submission of this thesis. Despite the lack of absolute ages to date the lacustrine sediments at Middle Island, the following information can be inferred based on previous research. Ryan et al. (2016) determined that the southern shingle ridge was emplaced at 4,555 ± 140 yBP. This means that the accumulation of sediments in the lake must have occurred after this time. The overwash deposits are therefore younger than the ridge, and the age of the deposits decreases with decreasing depth downcore. PC3.3 and PC4.1A both measured ~130 cm in length and recorded the presence of overwash deposits at similar depths. This indicates that sediment accumulation occurred at similar rates across the entire lake, which is supported by the lack of relief in the lake’s surface. If 130 cm of sediments were accumulated in ~4,500 years, and if sediment accumulation is assumed to be constant, it can be concluded that accumulation rates were ~0.29 mm a year or ~2.9 cm every 100 years. It is acknowledged that the assumption of constant sediment accumulation is unlikely since the conditions would have been marginal for plant growth in the early stages of lake development. However, without further information about sediment accumulation for this particular location, a constant accumulation rate has to be assumed. The overwash deposits were found at the following heights above the bottom of the core: ~ 15 cm, ~55 cm and ~80 cm. The deepest overwash deposit must therefore have occurred at 4,500 – ((15/2.9) * 100) = ~3,980 years ago. The second overwash deposit is estimated to have occurred at 4,500 – ((55/2.9) * 100) = ~ 2,600 years ago, and the most recent overwash deposit at 4,500 – ((80/2.9) * 100) = ~ 1,740 years ago.

3.4.3 Paleocyclone reconstructions

It was beyond the scope of this research project to model the cyclone characteristics that would have been responsible for the deposition of these overwash deposits. Based on established relationships between wavelength, wave height and water depth however, the following inferences can be made. Waves start interacting with the ocean floor at depths of 1/2 their wavelength, which results in sediment entrainment. Foraminifera from 5-10 m below LAT were found in overwash deposits, which indicates wavelengths of at least 10-20 m. This information, combined with local bathymetric data, can be used in future studies to determine cyclones characteristics that were responsible for the generation of waves with this particular wavelength. However, even without cyclone modelling, a few conclusions can be drawn about the overwash deposits at Middle Island. It is known that waves start breaking, which results in wave energy dissipation and deposition of sediments, at depths that are 1.2-1.4 times the wave height. Two additional factors that influence the potential deposition of overwash deposits at Middle Island are the reef flat on the southern side of the island, as well as the height of the southern shingle ridge. The reef flat elevation was measured to be between 0-1 m above LAT and the tidal range at Middle Island is 3.6 m (Ryan et al., 2016). During LAT, water depth at the reef crest is 0 m, which results in a wave height of 0 m and therefore prohibits the propagation of waves across the reef flat. When only considering a change in tide, highest astronomical tide (HAT) results in water depths of 3.6 m at the reef crest and 2.6 m near the beach. Waves can therefore reach a maximum height of 2.6/1.2=2.2 m near shore, which results in a total inundation depth of 4.8 m. Since the ridge is situated at 5.2 m above the nearshore reef flat, waves at HAT are still unable to overtop the shingle ridge. However, as previously discussed, cyclones cause wave and wind set up and temporarily increase the water depths near shore. Therefore, for a wave to be able to overtop the ridge and deposit sediments in the lake behind it, total inundation levels need to be at least 6.2 m above LAT or 5.2 m above the nearshore reef flat (Figure 3.10).

Figure 3.10a

Waves during LAT

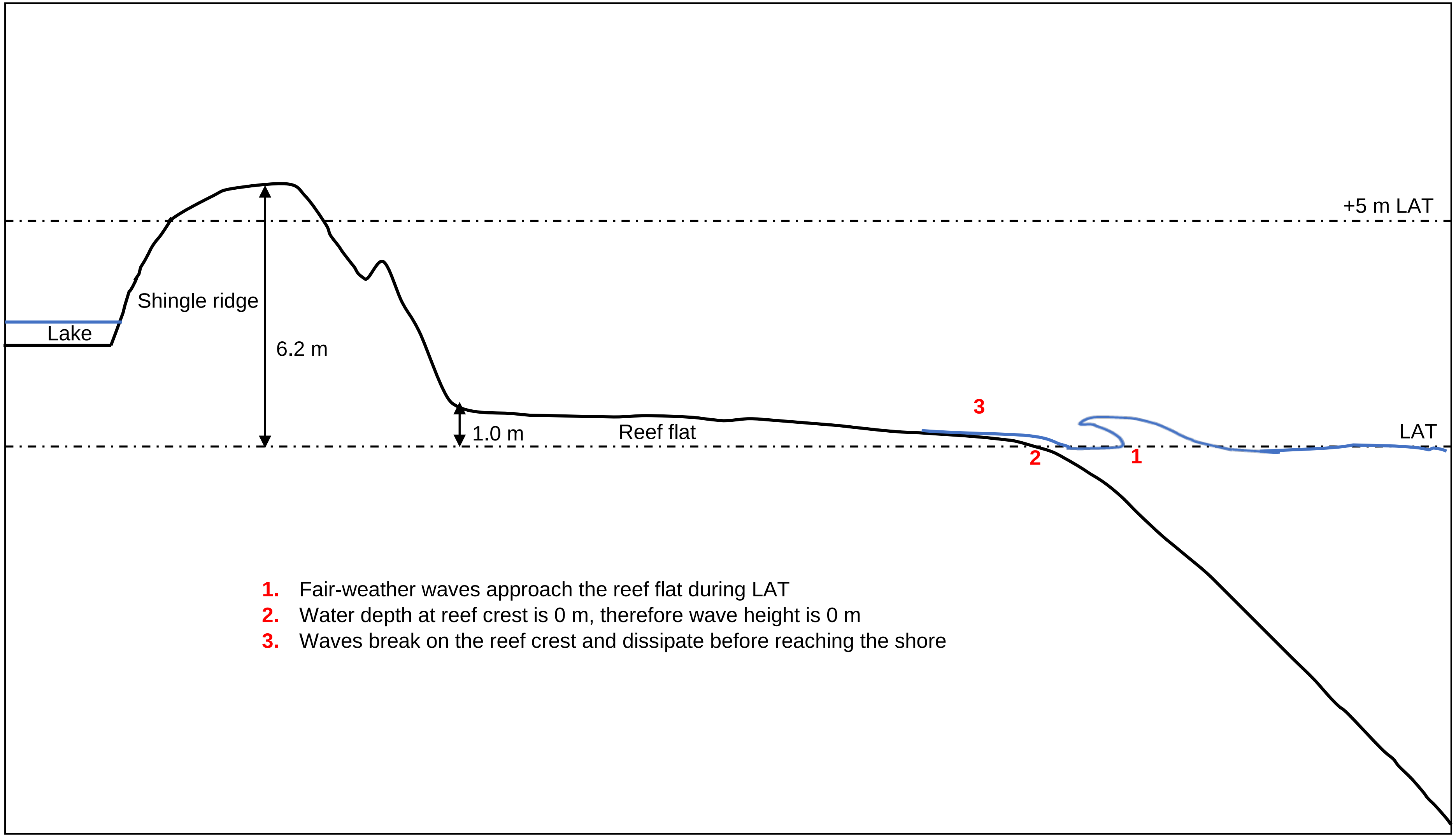

1. Fair-weather waves approach the reef flat during LAT
2. Water depth at reef crest is 0 m, therefore wave height is 0 m
3. Waves break on the reef crest and dissipate before reaching the shore

b

Cyclone-generated waves during HAT

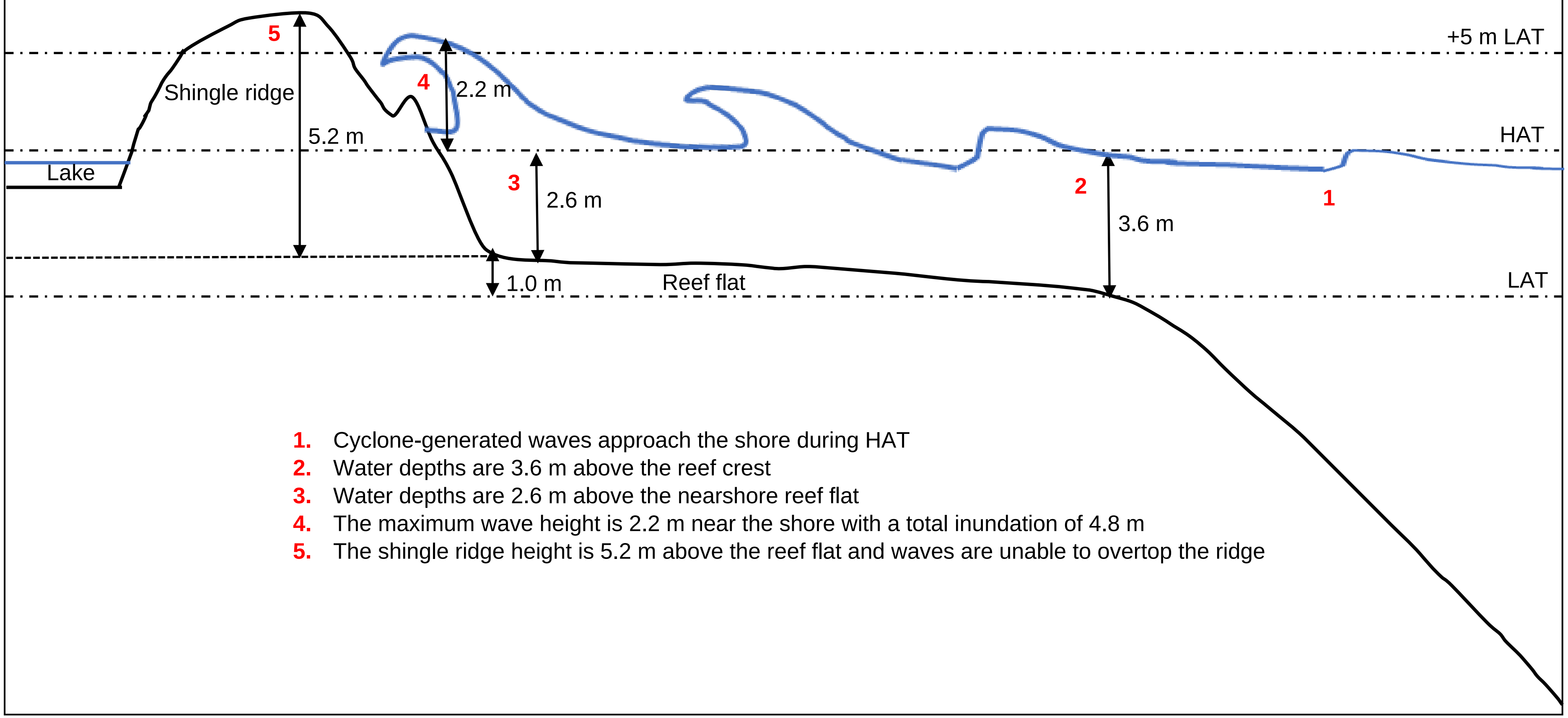

1. Cyclone-generated waves approach the shore during HAT
2. Water depths are 3.6 m above the reef crest
3. Water depths are 2.6 m above the nearshore reef flat
4. The maximum wave height is 2.2 m near the shore with a total inundation of 4.8 m
5. The shingle ridge height is 5.2 m above the reef flat and waves are unable to overtop the ridge

c

Total inundation required for washover into the lake behind the shingle ridge

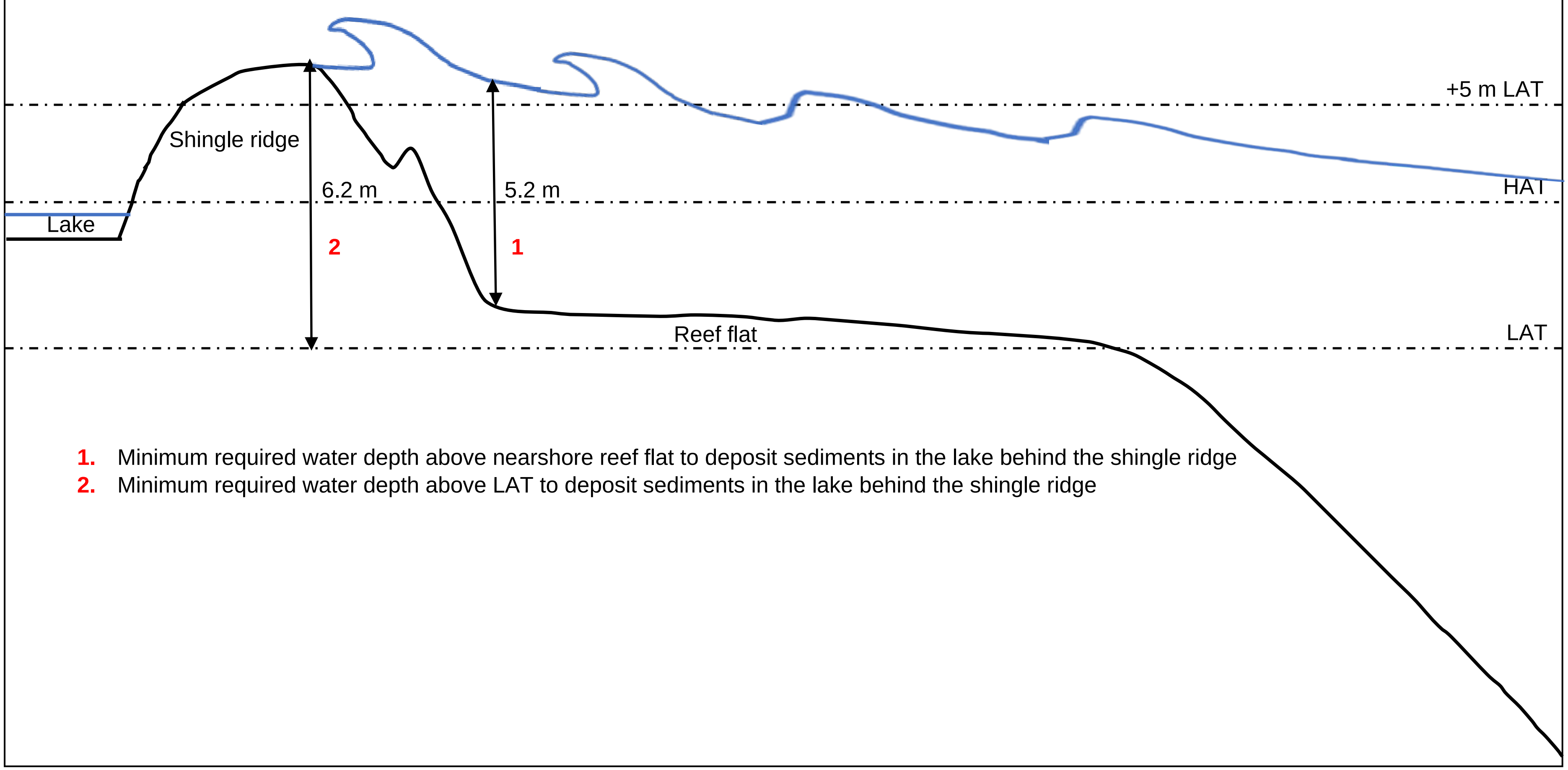

1. Minimum required water depth above nearshore reef flat to deposit sediments in the lake behind the shingle ridge
2. Minimum required water depth above LAT to deposit sediments in the lake behind the shingle ridge

Nott & Jagger (2013) calculated return periods of inundation levels at Rockingham Bay relative to AHD, which is 1.8 m above LAT. If converted to AHD, the ridge at Middle Island has an elevation of 4.4 m above AHD and return periods of 500 years were estimated for this particular inundation height. Forsyth and colleagues (2010) determined that inundations levels of 4.5 m above AHD are associated with cyclones with a central pressure of 880-890 hPa, which are severe Category 5 cyclones. Based on this information, it can therefore be concluded that at least three Category 5 cyclones generated overwash deposits at Middle Island between 4,000-1,740 years ago, which provides an average return period of ~750 years. However, the two most recent cyclones occurred 2,600 and 1,740 years ago, which results in a return period of 430 years. Interestingly, Forsyth and colleagues. (2010) determined that the beach ridge plains at Rockingham Bay recorded a period of lower magnitude events between 1,500-3,400 years ago, which is contradicted by the events recorded at Middle Island. This indicates that future research is needed, both at Middle Island and at other location along the central Great Barrier Reef.

3.5 Conclusion

This study confirmed the validity of a novel research method that used species-specific depth preferences of foraminifera to reconstruct the provenance depth of overwash deposits at Middle Island. Three washover events were recognised in the stratigraphy of collected percussion cores, and the deposits contained foraminifera that originated from 5-10 m below LAT. This information can be used in future cyclone modelling, to reconstruct the cyclone characteristics that generate waves capable of interacting with the sea floor at these depths. Even without cyclone modelling, this study estimated the overwash deposits to be the result of severe Category 5 cyclones that occurred ~3,980, ~2,600 and ~1,740 years ago, based on assumed sedimentation rates in the lake and known relationships between wave height, water depth and inundation levels. These overwash deposits contradict the period of reduced cyclone intensity recorded elsewhere on the Queensland coast and highlight the need for more high-resolution paleotempestological research to resolve these differences.

4. Conclusion

This chapter brings together the major conclusions from the previous chapters to determine if a novel research method, using species-specific depth preferences of foraminifera, can be used to reconstruct paleocyclone occurrences at Middle Island on the central Great Barrier Reef, Queensland, Australia. It also provides some recommendations to further increase the resolution of future paleotempestological studies and the resulting paleocyclone reconstructions.

Plate 4

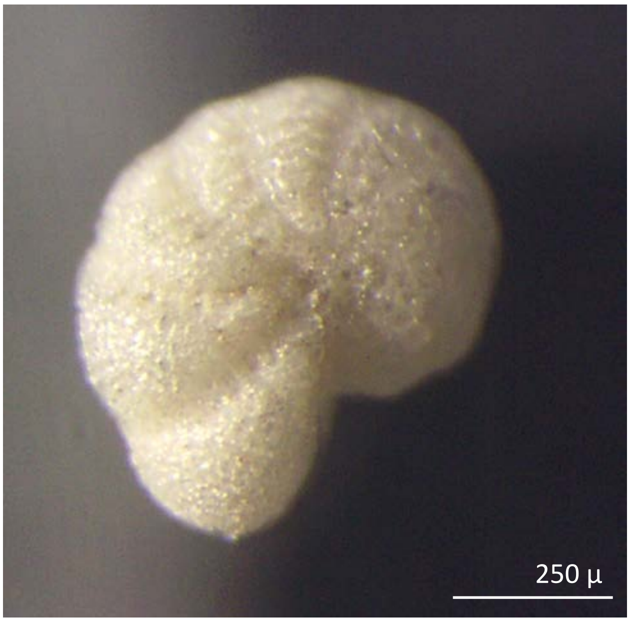

Note. Depth-specific foraminifera species Elphidium hispidulum *from 5-10 m below LAT.*

4.1 Summary

This study aimed to test the following hypothesis: *<u>Foraminifera exhibit species-specific preferences and can be used to reconstruct Holocene paleocyclone occurrences at Middle Island on the central Great Barrier Reef, Queensland, Australia</u>.* This hypothesis was formulated as a result of several identified knowledge gaps: 1) The instrumental cyclone records for Australia are too short to adequately capture long-term variation in cyclone frequency and intensity; 2) Paleotempestological research can extend the instrumental records, but Australia is underrepresented as a research location; 3) Foraminifera are a paleotempestological proxy with the potential to generate high-resolution paleocyclone reconstructions, but foraminifera are rarely used as a proxy in Australia and in Queensland in particular; 4) Species-specific depth preferences of foraminifera have never been used for paleocyclone reconstructions in Queensland.

To test the hypothesis and to reduce the identified knowledge gaps, several objectives were formulated:

1) To describe and quantify the distribution, habitat and depth preferences of contemporary foraminifera from Middle Island on the central GBR;

2) To analyse sediment cores from the ephemeral lake on Middle Island for overwash deposits and foraminiferal presence;

3) To reconstruct Holocene cyclone occurrences at Middle Island based on the collected data;

4) To assess the strengths and limitations of a novel research method that uses species-specific depth preferences of foraminifera to reconstruct paleocyclone occurrences.

By addressing these objectives, this study provides the first description of foraminiferal assemblages and habitat types from the reef flat and reef slopes around Middle Island. It also extends the instrumental cyclone record for the central GBR through the reconstruction of paleocyclone occurrences at Middle Island. Most importantly however, this study successfully employs a novel research method for use in paleocyclone reconstructions, which can greatly improve the resolution of these reconstructions in future studies. In the paragraphs below, the research objectives and associated conclusions are summarised, as well as recommendations for future studies.

Objective 1: To describe and quantify the distribution, habitat, and depth preferences of contemporary foraminifera from Middle Island on the central GBR (Chapter 2)

Foraminiferal assemblages, contained in surficial sediment samples collected from the reef flat and reef slopes around Middle Island, were composed of 61 genera, 146 species and 3,706 identified tests. Since taphonomic degradation of foraminiferal tests indicates long residence times and potential transport from the original habitat to the depositional area, only 2,724 tests with little to no taphonomic degradation were retained for further analyses. Taking spatial autocorrelation into account, dissimilarity analyses revealed a positive and significant relationship between the degree of assemblage dissimilarity and depth below LAT. Indicator species analyses for 5 m depth intervals revealed 17 foraminifera species with species-specific depth preferences: *Amphistegina lobifera* for 5-0 m above LAT, *Ammonia aoteana, Clavulina pacifica, Elphidium advenum, Elphidium excavatum, Elphidium hispidulum, Operculina ammonoides, Parasorites orbiculus, Quinqueloculina crassicarinata, Quinqueloculina parvaggluta, Quinqueloculina polygona, Sahulia conica, Sigmoihauerina involute, Siphonaperta arenata, Spiroloculina communis* and *Textularia dupla* for 5-10 m below LAT and *Elphidium crispum* for 0-10 m below LAT. Specific measurements of environmental parameter values were not obtained, and depth was used as a proxy for the combined effect of the changes in these parameters. If future studies measure specific environmental parameters such as salinity and water temperature, the changes in these parameters can be used to infer species-specific preferences with greater precision.

Drop camera footage, recorded on the reef slopes around Middle Island, revealed a range of reef cover types and suitable habitats for foraminifera such as algae, coral rubble, and bare substrate. Foraminifera assemblage composition conformed to the general knowledge about habitat type preferences of foraminifera species. Poor footage quality due to turbidity and limited visibility prohibited in-depth analyses of the habitat preferences of specific foraminifera species. The recommendation for future studies is to record underwater footage using a hand-held camera and SCUBA equipment, which enables close-up recordings of reef-slope habitats while negating the effects of turbidity and limited visibility on footage quality. Using SCUBA will also facilitate the collection of sediment samples from the reef slopes and a more accurate recording of the collection depths, which will result in smaller depth ranges that foraminifera can be assigned to.

Objective 2: To analyse sediment cores from the ephemeral lake on Middle Island for overwash deposits and foraminiferal presence (Chapter 3)

Nine percussion cores were collected from the ephemeral lake behind the shingle ridge on Middle Island. Two cores were selected for further analysis and visible stratigraphic layers were described in terms of colour and indicators of marine provenance such as coral clasts. Sediments samples from the cores were taken at 5 cm intervals and processed to determine sediment size distribution and foraminifera presence. Based on sediment size distributions, colour changes and the presence of coral clasts and marine foraminifera, three overwash deposits were identified in the cores at ~45-50 cm downcore, 65-90 cm downcore and ~115 cm downcore. Foraminifera were present throughout the majority of the sediment samples from the cores and most species indicated marine provenance, although some identified species are known to survive in marginal environments such as marshes and hypersaline lagoons. Due to the sampling interval, the three identified overwash deposits are a conservative estimate of the total number of washover event that have impacted Middle Island since the emplacement of the ridge around ~4,500 yBP. Adjacent samples were assumed to belong to the same washover event, but smaller sampling intervals of 1-2 cm are recommended for future studies to improve the resolution of paleocyclone reconstructions.

Objective 3: To reconstruct Holocene cyclone occurrences at Middle Island based on the collected data (Chapter 3)

Even though radiocarbon dates from coral clasts submitted for dating are yet to be received, the washover events were estimated to have occurred around ~3,980, ~2,600 and ~1,740 years ago. This estimate was based on the known age of the shingle ridge (~4,500 years old), the assumption that sedimentation rates in the lake have been constant and linear since its formation, and the respective depths of the overwash deposits downcore. The identified overwash deposits contained depth-specific foraminifera species that originated from at least 5-10 m below LAT: *Clavulina pacifica, Elphidium excavatum, Elphidium hispidulum, Quinqueloculina crassicarinata, Sahulia conica, Spiroloculina communis* and *Textularia dupla.* These provenance depths indicate wavelengths of at least 10-20 m based on established wave theory. Cyclone modelling went beyond the scope of this study, and the characteristics of the cyclones responsible for these wavelengths could not be determined. Regardless of modelling limitations, the washover events were attributed to severe Category 5 cyclones based on the height of the shingle ridge, local bathymetric data from Middle Island, and inundation levels calculated for other locations along the Queensland coast. The provenance depth of the overwash deposits is a conservative estimate because foraminiferal assemblages from depths greater than 10 m below LAT were not described. For future studies, it is therefore recommended to identify assemblages from a greater depth range to improve the provenance depth resolution of overwash deposits. It is also recommended to use cyclone modelling to accurately determine the cyclone characteristics that are responsible for generating the wavelengths that are inferred from foraminiferal depth-preferences.

Objective 4: To assess the strengths and limitations of a novel research method that uses species-specific depth preferences of foraminifera to reconstruct paleocyclone occurrences (Chapter 3)

As shown by this study, foraminifera exhibit species-specific depth preferences at Middle Island. Species-specific depth preferences were determined for 5 m intervals due to sampling resolution and sample collection methods, but improved collection methods are hypothesised to increase the resolution of species-specific preferences. Foraminiferal assemblages were identified to a depth of 10 m below LAT, but future studies can identify assemblages from greater depth ranges, especially when the improved collection methods are used. Due to the location-specific gradient of environmental parameters relative to depth, the depth preferences of foraminifera around Middle Island are only applicable to this location. Because environmental parameter values were not recorded, depth at Middle Island was used as a proxy for changes in these parameters. However, foraminifera species at other locations are expected to show similar stratification, based on the location's environmental parameters and their changes with varying depths. By increasing the number of research locations for foraminiferal depth-preferences and by measuring environmental parameter values, a database can be compiled which can inform about species-specific preferences for a range of environmental parameters. The larger the database, the more detailed inferences can be made about species-specific preferences for their optimal habitat.

4.2 Conclusion

Foraminifera have been shown to exhibit species-specific depth preferences at Middle Island. Now that this novel research method has been tested and validated, foraminifera can be used to greatly improve the resolution of paleocyclone reconstructions. Previous studies from Queensland have provided a conservative estimate of total inundation levels and cyclone intensities, using beach ridge heights and cyclone modelling based on short instrumental records. These studies demonstrated location-specific differences in inundation components such as wave run up and wave set up, which complicate paleocyclone reconstructions. Using species-specific preferences of foraminifera at a study site, sediment provenance depth can be determined with great accuracy. Based on established wave theory, these provenance depths can be linked to wavelengths, which can be entered into computer-generated cyclone models to determine the characteristics of the cyclones that were responsible for generating them. By improving the resolution of paleocyclone reconstructions, our instrumental records can be extended, and inferences can be made about long-term variations in cyclone frequency and intensity. These extended cyclone records can be used by governments and disaster management groups to better prepare coastal communities for cyclone impacts, thereby minimising the loss of lives and livelihoods in the future.

References

Ahyong, S., Boyko, C. B., Bailly, N., Bernot, J., Bieler, R., Brandão, S. N., Daly, M., De Grave, S., Gofas, S., Hernandez, F., Hughes, L., Neubauer, T. A., Paulay, G., Boydens, B., Decock, W., Dekeyzer, S., Goharimanesh, M., Vandepitte, L., Vanhoorne, B., . . . Zullini, A. (2024). *World Register of Marine Species (WoRMS)* https://www.marinespecies.org

Armstrong, H., & Brasier, M. (2009). *Microfossils*. Blackwell Publishing. https://doi.org/10.1002/9781118685440

Australian Bureau of Statistics. (2022). *Census data 2021*. Australian Bureau of Statistics. https://abs.gov.au/census/find-census-data/search-by-area

Bakkensen, L. A., & Mendelsohn, R. O. (2019). Global Tropical Cyclone Damages and Fatalities Under Climate Change: An Updated Assessment. In (pp. 179-197). Springer International Publishing. https://doi.org/10.1007/978-3-030-02402-4_9

Beavington-Penney, S. J., & Racey, A. (2004). Ecology of extant nummulitids and other larger benthic Foraminifera; applications in palaeoenvironmental analysis. *Earth-science reviews*, *67*(3-4), 219-265. https://doi.org/10.1016/j.earscirev.2004.02.005

Beck Eichler, P. P., & Barker, C. P. (2020a). *Benthic foraminiferal ecology : indicators of environmental impacts* (1st 2020. ed.). Springer. https://doi.org/10.1007/978-3-030-61463-8

Beck Eichler, P. P., & Barker, C. P. (2020b). Deep in Mud: Benthic Foraminifera Interface Marine Sediment-Water—Sampling, Handling, and Analyzing. In (pp. 29-48). Springer International Publishing AG. https://doi.org/10.1007/978-3-030-61463-8_2

Berkeley, A., Perry, C. T., & Smithers, S. G. (2009). Taphonomic signatures and patterns of test degradation on tropical, intertidal benthic Foraminifera. *Marine micropaleontology*, *73*(3-4), 148-163. https://doi.org/10.1016/j.marmicro.2009.08.002

Berkeley, A., Perry, C. T., Smithers, S. G., & Horton, B. P. (2008). The spatial and vertical distribution of living (stained) benthic foraminifera from a tropical, intertidal environment, north Queensland, Australia. *Marine micropaleontology*, *69*(2), 240-261. https://doi.org/10.1016/j.marmicro.2008.08.002

Berkeley, A., Perry, C. T., Smithers, S. G., Horton, B. P., & Taylor, K. G. (2007). A review of the ecological and taphonomic controls on foraminiferal assemblage development in intertidal environments. *Earth-science reviews*, *83*(3), 205-230. https://doi.org/10.1016/j.earscirev.2007.04.003

Bradley, R. S. (2015). *Paleoclimatology : reconstructing climates of the quaternary*. Elsevier.

Braun, E., Meyer, B., Deocampo, D., & Kiage, L. M. (2017). A 3000 yr paleostorm record from St. Catherines Island, Georgia. *Estuarine, coastal and shelf science*, *196*, 360-372. https://doi.org/10.1016/j.ecss.2017.05.021

Brill, D., Jankaew, K., Neubauer, N.-P., Kelletat, D., Scheffers, A., Voett, A., & Broeckner, H. (2014). Holocene coastal evolution of southwest Thailand - implications for the site-specific preservation of paleotsunami deposits. *Zeitschrift fuer Geomorphologie*, *58*(3), 273-303.

Brill, D., May, S. M., Engel, M., Reyes, M., Pint, A., Opitz, S., Dierick, M., Gonzalo, L. A., Esser, S., & Brueckner, H. (2016). Typhoon Haiyan's sedimentary record in coastal environments of the

Philippines and its palaeotempestological implications. *Natural hazards and earth system sciences*, *16*(12), 2799-2822. https://doi.org/10.5194/nhess-16-2799-2016

Brill, D., Seeger, K., Pint, A., Reize, F., Hlaing, K. T., Seeliger, M., Opitz, S., Win, K. M. M., Nyunt, W. T., Aye, N., Aung, A., Kyaw, K., Kraas, F., & Brueckner, H. (2020). Modern and historical tropical cyclone and tsunami deposits at the coast of Myanmar; implications for their identification and preservation in the geological record. *Sedimentology*, *67*(3), 1431-1459. https://doi.org/10.1111/sed.12586

Brönnimann, S. (2015). *Climatic Changes Since 1700*. Springer International Publishing. https://doi.org/10.1007/978-3-319-19042-6

Bureau of Meteorology. (2021). *South Pacific Tropical Cyclone Outlook for 2021 to 2022*. Bureau of Meteorology. http://www.bom.gov.au/climate/cyclones/south-pacific/archive/20211012.archive.shtml

Bureau of Meteorology. (2024a). *Australian tropical cyclone season long-range forecast 2023-2024*. Commonwealth of Australia, Bureau of Meteorology. http://www.bom.gov.au/climate/cyclones/australia/

Bureau of Meteorology. (2024b). *Climate statistics for Australian locations*. Bureau of Meteorology. http://www.bom.gov.au/climate/data/index.shtml

Chand, S. S., Dowdy, A. J., Ramsay, H. A., Walsh, K. J. E., Tory, K. J., Power, S. B., Bell, S. S., Lavender, S. L., Ye, H., & Kuleshov, Y. (2019). Review of tropical cyclones in the Australian region: Climatology, variability, predictability, and trends. *Wiley interdisciplinary reviews. Climate change*, *10*(5), n/a. https://doi.org/10.1002/wcc.602

Chang, E. K. M., & Guo, Y. (2007). Is the number of North Atlantic tropical cyclones significantly underestimated prior to the availability of satellite observations? *Geophysical research letters*, *34*(14), L14801-n/a. https://doi.org/10.1029/2007GL030169

Cheal, A. J., MacNeil, M. A., Emslie, M. J., & Sweatman, H. (2017). The threat to coral reefs from more intense cyclones under climate change. *Global change biology*, *23*(4), 1511-1524. https://doi.org/10.1111/gcb.13593

Chen, T., Roff, G., Feng, Y., & Zhao, J. (2019). Tropical sand cays as natural paleocyclone archives. *Geophysical research letters*, *46*(16), 9796-9803. https://doi.org/10.1029/2019GL084274

Chu, P.-S., & Murakami, H. (2022). *Climate Variability and Tropical Cyclone Activity* (1 ed.). Cambridge University Press.

Coates, L., Haynes, K., Radford, D., D'Arcy, R, Smith, C., van den Honert R & Gissing, A. . (2017). *An analysis of human fatalities from cyclones, earthquakes and severe storms in Australia.* . B. a. N. H. C. R. Centre.

Croux, C., & Dehon, C. (2010). Influence functions of the Spearman and Kendall correlation measures. *Statistical methods & applications*, *19*(4), 497-515. https://doi.org/10.1007/s10260-010-0142-z

Debenay, J.-P. (2013). A Guide to 1,000 Foraminifera from Southwestern Pacific, New Caledonia. *Journal of foraminiferal research*, *43*(3), 314-315. https://doi.org/10.2113/gsjfr.43.3.314

Delaine, M., Armynot du Chatelet, E., Bout-Roumazeilles, V., Goubert, E., Le Cadre, V., Recourt, P., Trentesaux, A., & Arthuis, R. (2015). Multiproxy approach for Holocene paleoenvironmental reconstructions from microorganisms (testate amoebae and Foraminifera) and sediment analyses; the infilling of the Loire Valley in Nantes (France). *Holocene (Sevenoaks)*, *25*(3), 407-420. https://doi.org/10.1177/0959683614561883

Donnelly, C., Kraus, N., & Larson, M. (2006). State of Knowledge on Measurement and Modeling of Coastal Overwash. *Journal of coastal research*, *22*(4), 965-991. https://doi.org/10.2112/04-0431.1

Du, S., Li, B., Chen, M., Xiang, R., Niu, D., & Si, Y. (2016). Paleotempestology evidence recorded by eolian deposition in the Bohai Sea coastal zone during the last interglacial period. *Marine geology*, *379*, 78-83. https://doi.org/10.1016/j.margeo.2016.05.013

Edgar, K. M., Anagnostou, E., Pearson, P. N., & Foster, G. L. (2015). Assessing the impact of diagenesis on delta (super 11) B, delta (super 13) C, delta (super 18) O, Sr/Ca and B/Ca values in fossil planktic foraminiferal calcite. *Geochimica et cosmochimica acta*, *166*, 189-209. https://doi.org/10.1016/j.gca.2015.06.018

Engel, M., May, S. M., Scheffers, A., Squire, P., Pint, A., Kelletat, D., & Brueckner, H. (2015). Prograded foredunes of Western Australia's macro-tidal coast; implications for Holocene sea-level change and high-energy wave impacts. *Earth surface processes and landforms*, *40*(6), 726-740. https://doi.org/10.1002/esp.3663

Forcino, F. L., Leighton, L. R., Twerdy, P., & Cahill, J. F. (2015). Reexamining Sample Size Requirements for Multivariate, Abundance-Based Community Research: When Resources are Limited, the Research Does Not Have to Be. *PloS one*, *10*(6), e0128379-e0128379. https://doi.org/10.1371/journal.pone.0128379

Förderer, M., Rödder, D., & Langer, M. R. (2018). Patterns of species richness and the center of diversity in modern Indo-Pacific larger foraminifera. *Scientific reports*, *8*(1), 8189-8189. https://doi.org/10.1038/s41598-018-26598-9

Forsyth, A. J. (2013). *Beach ridge records of late-Holocene tropical cyclone behaviour* [James Cook University]. JCU eTheses.

Forsyth, A. J., Nott, J., & Bateman, M. D. (2010). Beach ridge plain evidence of a variable late-Holocene tropical cyclone climate, north Queensland, Australia. *Palaeogeography, palaeoclimatology, palaeoecology*, *297*(3-4), 707-716. https://doi.org/10.1016/j.palaeo.2010.09.024

Frappier, A., Knutson, T., Liu, K.-B., & Emanuel, K. (2007). Perspective: coordinating paleoclimate research on tropical cyclones with hurricane-climate theory and modelling. *Tellus. Series A, Dynamic meteorology and oceanography*, *59*(4), 529-537. https://doi.org/10.1111/j.1600-0870.2007.00250.x

Geonadir. (2024). *Geonadir. Environmental Drone Mapping Software*. Retrieved 03/05/2024 from https://geonadir.com/

Google Earth. (2024). *Middle Island, Queensland, Australia*. Google Earth.

Haig, J., Nott, J., & Reichart, G.-J. (2014). Australian tropical cyclone activity lower than at any time over the past 550-1,500 years. *Nature (London)*, *505*(7485), 667-671. https://doi.org/10.1038/nature12882

Haslett, S. K. (2001). The palaeoenvironmental implications of the distribution of intertidal Foraminifera in a tropical Australian estuary; a reconnaissance study. *Australian geographical studies*, *39*(1), 67-74. https://doi.org/10.1111/1467-8470.00130

Henderson, D., & Harper, B. (2003). *Queensland Climate Change and Community Vulnerability to Tropical Cyclones: Cyclone Hazards Assessment - Stage 4*.

Hippensteel, S. P., & Garcia, W. J. (2014). Micropaleontological evidence of prehistoric hurricane strikes from southeastern North Carolina. *Journal of coastal research*, *30*(6), 1157-1172. https://doi.org/10.2112/JCOASTRES-D-12-00180.1

Hohenegger, J. (1994). Distribution of Living Larger Foraminifera NW of Sesoko-Jima, Okinawa, Japan. *Marine ecology (Berlin, West)*, *15*(3-4), 291-334. https://doi.org/10.1111/j.1439-0485.1994.tb00059.x

Hohenegger, J. (1996). Remarks on the distribution of larger foraminifera (Protozoa) from Belau (Western Carolines).

Hohenegger, J. (2004). Depth coenoclines and environmental considerations of western Pacific larger Foraminifera. *Journal of foraminiferal research*, *34*(1), 9-33. https://doi.org/10.2113/0340009

Hohenegger, J., Yordanova, E., Nakano, Y., & Tatzreiter, F. (1999). Habitats of larger Foraminifera on the upper reef slope of Sesoko Island, Okinawa, Japan. *Marine micropaleontology*, *36*(2-3), 109-168. https://doi.org/10.1016/S0377-8398(98)00030-9

Holzmann, M., & Pawlowski, J. (2002). Freshwater foraminiferans from Lake Geneva; past and present. *Journal of foraminiferal research*, *32*(4), 344-350. https://doi.org/10.2113/0320344

Horton, B. P., Culver, S. J., Hardbattle, M. I. J., Larcombe, P., Milne, G. A., Morigi, C., Whittaker, J. E., & Woodroffe, S. A. (2007). Reconstructing Holocene sea-level change for the central Great Barrier Reef (Australia) using subtidal Foraminifera. *Journal of foraminiferal research*, *37*(4), 327-343. https://doi.org/10.2113/gsjfr.37.4.327

Horton, B. P., Larcombe, P., Woodroffe, S. A., Whittaker, J. E., Wright, M. R., & Wynn, C. (2003). Contemporary foraminiferal distributions of a mangrove environment, Great Barrier Reef coastline, Australia; implications for sea-level reconstructions. *Marine geology*, *198*(3-4), 225-243. https://doi.org/10.1016/S0025-3227(03)00117-8

Hussain, S. M., Elakkiya, P., Elumalai, K., Jonathan, M. P., & Nagarajan, R. (2013). Evidences for extreme wave events in Velanganni coast, southeast of India. *Boletín de la Sociedad Geológica Mexicana*, *65*(1), 201-205. https://doi.org/10.18268/BSGM2013v65n1a15

Isaack, A., Gischler, E., Hudson, J. H., Anselmetti, F. S., Lohner, A., Vogel, H., Garbode, E., & Camoin, G. F. (2016). A new model evaluating Holocene sediment dynamics; insights from a mixed carbonate-siliciclastic lagoon (Bora Bora, Society Islands, French Polynesia, South Pacific). *Sedimentary geology*, *343*, 99-118. https://doi.org/10.1016/j.sedgeo.2016.08.002

Jain, S. (2020). *Fundamentals of Invertebrate Palaeontology: Microfossils*. Springer (India) Private Limited.

Javaux, E. J., & Scott, D. B. (2003). Illustration of modern benthic Foraminifera from Bermuda and remarks on distribution in other subtropical/tropical areas. *Palaeontologia electronica*, *6*(1).

Jeong, J. O., Jeon, Y., & Sohn, Y. K. (2022). Geological record of a Cretaceous seismic event paired with multiple volcanic eruptions. *Terra nova (Oxford, England)*, *34*(1), 83-90. https://doi.org/10.1111/ter.12565

Johnson, J. (2017). *Depositional and Palaeoecological Characteristics of Incipient and Submerged Coral Reefs on the Inner-shelf of Australia's Great Barrier Reef* (Publication Number 30398154) [Ph.D., University of Exeter (United Kingdom)]. ProQuest Central. England. http://hdl.handle.net/10871/32954

Jones, P. D., Briffa, K. R., Osborn, T. J., Lough, J. M., van Ommen, T. D., Vinther, B. M., Luterbacher, J., Wahl, E. R., Zwiers, F. W., Mann, M. E., Schmidt, G. A., Ammann, C. M., Buckley, B. M., Cobb, K. M., Esper, J., Goosse, H., Jansen, E., Kiefer, T., Kull, C., . . . Xoplaki, E. (2009). High-resolution palaeoclimatology of the last millennium: a review of current status and future prospects. *The Holocene*, *19*(1), 3-49.

Kimoto, K. (2015). Planktic Foraminifera. In (pp. 129-178). Springer Japan. https://doi.org/10.1007/978-4-431-55130-0_7

Kitazato, H., & M. Bernhard, J. (2014). *Approaches to Study Living Foraminifera Collection, Maintenance and Experimentation* (1st 2014. ed.). Springer Japan. https://doi.org/10.1007/978-4-431-54388-6

Knutson, T., Camargo, S. J., Chan, J. C. L., Emanuel, K., Ho, C.-H., Kossin, J., Mohapatra, M., Satoh, M., Sugi, M., Walsh, K., & Wu, L. (2020). Tropical Cyclones and Climate Change Assessment: Part II: Projected Response to Anthropogenic Warming. *Bulletin of the American Meteorological Society*, *101*(3), E303-E322. https://doi.org/10.1175/BAMS-D-18-0194.1

Knutson, T. R., McBride, J. L., Chan, J., Emanuel, K., Holland, G., Landsea, C., Held, I., Kossin, J. P., Srivastava, A. K., & Sugi, M. (2010). Tropical cyclones and climate change. *Nature geoscience*, *3*(3), 157-163. https://doi.org/10.1038/ngeo779

Kosciuch, T. J., Pilarczyk, J. E., Hong, I., Fritz, H. M., Horton, B. P., Rarai, A., Harrison, M. J., & Jockley, F. R. (2018). Foraminifera reveal a shallow nearshore origin for overwash sediments deposited by Tropical Cyclone Pam in Vanuatu (South Pacific). *Marine geology*, *396*, 171-185. https://doi.org/10.1016/j.margeo.2017.06.003

Kumar, L. (2020). *Climate Change and Impacts in the Pacific* (1st 2020. ed.). Springer International Publishing. https://doi.org/10.1007/978-3-030-32878-8

Lallemand, S., Lehu, R., Retif, F., Hsu, S.-K., Babonneau, N., Ratzov, G., Bassetti, M.-A., Dezileau, L., Hsieh, M.-L., & Dominguez, S. (2016). A approximately 3000 years-old sequence of extreme events revealed by marine and shore deposits east of Taiwan. *Tectonophysics*, *692*, 325-341. https://doi.org/10.1016/j.tecto.2015.11.001

Landsea, C. W., Glenn, D. A., Bredemeyer, W., Chenoweth, M., Ellis, R., Gamache, J., Hufstetler, L., Mock, C., Perez, R., Prieto, R., Sanchez-Sesma, J., Thomas, D., & Woolcock, L. (2008). A reanalysis of the 1911-20 Atlantic hurricane database. *Journal of climate*, *21*(10), 2138-2168. https://doi.org/10.1175/2007JCLI1119.1

Lane, P., Donnelly, J. P., Woodruff, J. D., & Hawkes, A. D. (2011). A decadally-resolved paleohurricane record archived in the late Holocene sediments of a Florida sinkhole. *Marine geology*, *287*(1-4), 14-30. https://doi.org/10.1016/j.margeo.2011.07.001

Leonard, S., & Nott, J. (2016). A Holocene fluvial archive of the Mulgrave River, northeastern Australia; influence of tropical cyclones and sediment delivery to the Great Barrier Reef. *Palaeogeography, palaeoclimatology, palaeoecology*, *441*, 845-853. https://doi.org/10.1016/j.palaeo.2015.10.033

Lewis, S. E., Sloss, C. R., Murray-Wallace, C. V., Woodroffe, C. D., & Smithers, S. G. (2013). Post-glacial sea-level changes around the Australian margin; a review. *Quaternary science reviews*, *74*, 115-138. https://doi.org/10.1016/j.quascirev.2012.09.006

Liu, K.-b. (2007a). PALEOCLIMATE RECONSTRUCTION | Paleotempestology. In *Encyclopedia of Quaternary Science* (pp. 1974-1985). Elsevier. https://doi.org/10.1016/b0-44-452747-8/00023-5

Liu, K.-b. (2007b). Uncovering Prehistoric Hurricane Activity: Examination of the geological record reveals some surprising long-term trends. *American scientist*, *95*(2), 126-133.

Luo, Q., Hu, K., Liu, W., & Wu, H. (2022). Scientometric Analysis for Spatial Autocorrelation-Related Research from 1991 to 2021. *ISPRS international journal of geo-information*, *11*(5), 309. https://doi.org/10.3390/ijgi11050309

Mamo, B. L. (2016). Benthic Foraminifera from the Capricorn Group, Great Barrier Reef, Australia. *Zootaxa*, *4215*(1), zootaxa.4215.4211.4211-zootaxa.4215.4211.4211. https://doi.org/10.11646/zootaxa.4215.1.1

May, S. M., Brill, D., Engel, M., Scheffers, A., Pint, A., Opitz, S., Wennrich, V., Squire, P., Kelletat, D., & Brueckner, H. (2015). Traces of historical tropical cyclones and tsunamis in the Ashburton Delta (north-west Australia). *Sedimentology*, *62*(6), 1546-1572. https://doi.org/10.1111/sed.12192

McAneney, J., Sandercock, B., Crompton, R., Mortlock, T., Musulin, R., Pielke, R., & Gissing, A. (2019). Normalised insurance losses from Australian natural disasters: 1966-2017. *Environmental hazards*, *18*(5), 414-433. https://doi.org/10.1080/17477891.2019.1609406

Meisterfeld, R., Holzmann, M., & Pawlowski, J. a. n. (2001). Morphological and Molecular Characterization of a New Terrestrial Allogromiid Species: Edaphoallogromia australica gen. et spec. nov. (Foraminifera) from Northern Queensland (Australia). *Protist*, *152*(3), 185-192. https://doi.org/10.1078/1434-4610-00058

Milker, Y., Dura, T., & Horton, B. P. (2022). The response of Foraminifera to rapid sea-level rise from tidal restoration of Ni-les'tun Marsh, Oregon, U.S.A. *Marine geology*, *445*, 106757. https://doi.org/10.1016/j.margeo.2022.106757

Miller, C. S., Leroy, S. A. G., Izon, G., Lahijani, H. A. K., Marret, F., Cundy, A. B., & Teasdale, P. A. (2013). Palynology; a tool to identify abrupt events; an example from Chabahar Bay, southern Iran. *Marine geology*, *337*, 195-201. https://doi.org/10.1016/j.margeo.2013.03.004

Mortlock, T. R., Nott, J., Crompton, R., & Koschatzky, V. (2023). A long-term view of tropical cyclone risk in Australia. *Natural hazards (Dordrecht)*, *118*(1), 571-588. https://doi.org/10.1007/s11069-023-06019-5

Muller, J., Collins, J. M., Gibson, S., & Paxton, L. (2017). Recent Advances in the Emerging Field of Paleotempestology. In (Vol. 3, pp. 1-33). Springer International Publishing. https://doi.org/10.1007/978-3-319-47594-3_1

Munksgaard, N. C., Zwart, C., Kurita, N., Bass, A., Nott, J., & Bird, M. I. (2015). Stable isotope anatomy of tropical cyclone ita, North-Eastern Australia, April 2014. *PloS one*, *10*(3), e0119728-e0119728. https://doi.org/10.1371/journal.pone.0119728

Murnane, R. J., & Liu, K.-b. (2004). *Hurricanes and typhoons : past, present, and future*. Columbia University Press.

Murray, J. W. (2006). *Ecology and applications of benthic foraminifera*. Cambridge University Press.

Murray, J. W. (2013). Living benthic Foraminifera; biogeographical distributions and the significance of rare morphospecies. *Journal of micropalaeontology*, *32*(1), 1-58. https://doi.org/10.1144/jmpaleo2012-010

Nobes, K., & Uthicke, S. (2008). *Benthic foraminifera of the Great Barrier Reef: a guide to species potentially useful as water quality indicators*. R. a. R. R. Centre.

Nott, J. (2003). Tsunami or Storm Waves?:Determining the Origin of a Spectacular Field of Wave Emplaced Boulders Using Numerical Storm Surge and Wave Models and Hydrodynamic Transport Equations. *Journal of coastal research*, *19*(2), 348-356.

Nott, J. (2009). Long-term natural variability of tropical cyclones in Australia. In (pp. 35-59). Springer. https://doi.org/10.1007/978-0-387-09410-6_3

Nott, J. (2014). Grain size and the origin of wave constructed beach ridges; a discussion of 'Beach ridges and prograded beach deposits as palaeoenvironment records'. *Earth-science reviews*, *132*, 82-84. https://doi.org/10.1016/j.earscirev.2013.07.011

Nott, J., Chague-Goff, C., Goff, J., Sloss, C., & Riggs, N. (2013). Anatomy of sand beach ridges: Evidence from severe Tropical Cyclone Yasi and its predecessors, northeast Queensland, Australia. *Journal of geophysical research. Earth surface*, *118*(3), 1710-1719. https://doi.org/10.1002/jgrf.20122

Nott, J., Haig, J., Neil, H., & Gillieson, D. (2007). Greater frequency variability of landfalling tropical cyclones at centennial compared to seasonal and decadal scales. *Earth and planetary science letters*, *255*(3-4), 367-372. https://doi.org/10.1016/j.epsl.2006.12.023

Nott, J., & Hayne, M. (2001). High frequency of "super-cyclones" along the Great Barrier Reef over the past 5,000 years. *Nature (London)*, *413*(6855), 508-512. https://doi.org/10.1038/35097055

Nott, J., Smithers, S., Walsh, K., & Rhodes, E. (2009). Sand beach ridges record 6000 year history of extreme tropical cyclone activity in northeastern Australia. *Quaternary science reviews*, *28*(15-16), 1511-1520. https://doi.org/10.1016/j.quascirev.2009.02.014

Nott, J. F. (2003). Intensity of prehistoric tropical cyclones. *Journal of Geophysical Research*, *108*(D7), 4212-n/a. https://doi.org/10.1029/2002JD002726

Nott, J. F., & Jagger, T. H. (2013). Deriving robust return periods for tropical cyclone inundations from sediments. *Geophysical research letters*, *40*(2), 370-373. https://doi.org/10.1029/2012GL054455

Oliva, F., Viau, A. E., Peros, M. C., & Bouchard, M. (2018). Paleotempestology database for the western North Atlantic basin. *Holocene (Sevenoaks)*, *28*(10), 1664-1671. https://doi.org/10.1177/0959683618782598

Orpin, A. R., Haig, D. W., & Woolfe, K. J. (1999). Sedimentary foraminiferal facies in Exmouth Gulf, in arid tropical northwestern Australia. *Australian journal of earth sciences*, *46*(4), 607-621. https://doi.org/10.1046/j.1440-0952.1999.00728.x

Palmer, S. E., Burn, M. J., & Holmes, J. (2020). A multiproxy analysis of extreme wave deposits in a tropical coastal lagoon in Jamaica, West Indies. *Natural hazards (Dordrecht)*, *104*(3), 2531-2560. https://doi.org/10.1007/s11069-020-04284-2

Perry, C. (2011). Holocene High Energy Window. In (pp. 558-561). Springer Netherlands. https://doi.org/10.1007/978-90-481-2639-2_95

Perry, C. T., Smithers, S. G., Kench, P. S., & Pears, B. (2014). Impacts of Cyclone Yasi on nearshore, terrigenous sediment-dominated reefs of the central Great Barrier Reef, Australia. *Geomorphology (Amsterdam, Netherlands)*, *222*, 92-105. https://doi.org/10.1016/j.geomorph.2014.03.012

Peters, J. L., Benetti, S., Dunlop, P., & Wheeler, A. J. (2020). Sedimentary and foraminiferal records of late Quaternary environmental change west of Ireland and implications for the last British-Irish ice sheet. *Journal of quaternary science*, *35*(5), 609-624. https://doi.org/10.1002/jqs.3208

Pilarczyk, J. E., Dura, T., Horton, B. P., Engelhart, S. E., Kemp, A. C., & Sawai, Y. (2014). Microfossils from coastal environments as indicators of paleo-earthquakes, tsunamis and storms. *Palaeogeography, palaeoclimatology, palaeoecology*, *413*, 144-157. https://doi.org/10.1016/j.palaeo.2014.06.033

Pilarczyk, J. E., Horton, B. P., Soria, J. L. A., Switzer, A. D., Siringan, F. P., Fritz, H. M., Khan, N. S., Ildefonso, S., Doctor, A. A., & Garcia, M. L. (2016). Micropaleontology of the 2013 Typhoon Haiyan overwash sediments from the Leyte Gulf, Philippines. *Sedimentary geology*, *339*, 104-114. https://doi.org/10.1016/j.sedgeo.2016.04.001

Poirier, R. K., Gaetano, M. Q., Acevedo, K., Schaller, M. F., Raymo, M. E., & Kozdon, R. (2021). Quantifying diagenesis, contributing factors, and resulting isotopic bias in benthic Foraminifera using the Foraminiferal Preservation Index; implications for geochemical proxy records. *Paleoceanography and paleoclimatology*, *36*(5), n/a. https://doi.org/10.1029/2020PA004110

Prazeres, M., Roberts, T. E., & Pandolfi, J. M. (2016). Shifts in species abundance of large benthic foraminifera Amphistegina: the possible effects of Tropical Cyclone Ita. *Coral reefs*, *36*(1), 305-309. https://doi.org/10.1007/s00338-016-1497-x

Puotinen, M. L. (2004). *Tropical cyclone impacts on coral reef communities : modelling the disturbance regime in the Great Barrier Reef region, 1969-2003* James Cook University]. Townsville, Qld.

Ricotta, C., & Podani, J. (2017). On some properties of the Bray-Curtis dissimilarity and their ecological meaning. *Ecological complexity*, *31*, 201-205. https://doi.org/10.1016/j.ecocom.2017.07.003

Roberts, A., Austin, W., Evans, K., Bird, C., Schweizer, M., & Darling, K. (2016). A new integrated approach to taxonomy: The fusion of molecular and morphological systematics with type material in benthic foraminifera. *PloS one*, *11*(7), e0158754-e0158754. https://doi.org/10.1371/journal.pone.0158754

Ryan, E. J. (2016). *Fringing reef growth on the central Great Barrier Reef : signatures of sea-level change, storms and sedimentation* James Cook University].

Ryan, E. J., Smithers, S. G., Lewis, S. E., Clark, T. R., & Zhao, J. X. (2016). The influence of sea level and cyclones on Holocene reef flat development; Middle Island, central Great Barrier Reef. *Coral reefs*, *35*(3), 805-818. https://doi.org/10.1007/s00338-016-1453-9

Saraswati, P. K. (2021). *Foraminiferal Micropaleontology for Understanding Earth's History*. Elsevier.

Schiebel, R., & Hemleben, C. (2005). Modern planktic Foraminifera. *Paläontologische Zeitschrift*, *79*(1), 135-148. https://doi.org/10.1007/BF03021758

Seears, H. A., Darling, K. F., & Wade, C. M. (2012). Ecological partitioning and diversity in tropical planktonic foraminifera. *BMC evolutionary biology*, *12*(1), 54-54. https://doi.org/10.1186/1471-2148-12-54

Sen, A., & Bhadury, P. (2015). Molecular diversity of benthic foraminifera from tropical and subtropical coastal settings- a concise review. *Indian journal of marine sciences*, *44*(7), 951-960.

Sengupta, D., Choi, Y. R., Tian, B., Brown, S., Meadows, M., Hackney, C. R., Banerjee, A., Li, Y., Chen, R., & Zhou, Y. (2023). Mapping 21st Century Global Coastal Land Reclamation. *Earth's future*, *11*(2), n/a. https://doi.org/10.1029/2022EF002927

Sharkov, E. A. (2012). *GLOBAL TROPICAL CYCLOGENESIS* (2nd 2012. ed.). Springer Berlin Heidelberg. https://doi.org/10.1007/978-3-642-13296-4

Shennan, I., Long, A., & Horton, B. P. (2015). *Handbook of sea-level research*. Wiley-Blackwell.

Siahsarani, A., Karami Khaniki, A., Aliakbari Bidokhti, A.-A., & Azadi, M. (2021). Numerical Modeling of Tropical Cyclone-Induced Storm Surge in the Gulf of Oman Using a Storm Surge–Wave–Tide Coupled Model. *Ocean science journal*, *56*(3), 225-240. https://doi.org/10.1007/s12601-021-00027-x

Smithers, S. G., & Hoeke, R. K. (2014). Geomorphological impacts of high latitude storm waves on low latitude reef islands; observations of the December 2008 event on Nukutoa, Takuu, Papua New Guinea. *Geomorphology (Amsterdam, Netherlands)*, *222*, 106-121. https://doi.org/10.1016/j.geomorph.2014.03.042

Soria, J. L. A., Switzer, A. D., Pilarczyk, J. E., Tang, H., Weiss, R., Siringan, F., Manglicmot, M., Gallentes, A., Lau, A. Y. A., Cheong, A. Y. L., & Koh, T. W. L. (2018). Surf beat-induced overwash during Typhoon Haiyan deposited two distinct sediment assemblages on the carbonate coast of Hernani, Samar, central Philippines. *Marine geology*, *396*, 215-230. https://doi.org/10.1016/j.margeo.2017.08.016

Strotz, L. C., Mamo, B. L., & Dominey-Howes, D. (2016). Effects of cyclone-generated disturbance on a tropical reef foraminifera assemblage. *Scientific reports*, *6*(1), 24846-24846. https://doi.org/10.1038/srep24846

Tamura, T. (2012). Beach ridges and prograded beach deposits as palaeoenvironment records. *Earth-science reviews*, *114*(3-4), 279-297. https://doi.org/10.1016/j.earscirev.2012.06.004

Tamura, T. (2014). Aeolian transport of coarse sand over beach ridges in NE Australia; a reply to a discussion of 'Beach ridges and prograded beach deposits as palaeoenvironment records'. *Earth-science reviews*, *132*, 85-87. https://doi.org/10.1016/j.earscirev.2013.11.008

Tichy, L., & Chytry, M. (2006). Statistical determination of diagnostic species for site groups of unequal size. *Journal of vegetation science*, *17*(6), 809-818. https://doi.org/10.1658/1100-9233(2006)17[809:sdodsf]2.0.co;2

Unnikrishnan, A. S., Tangang, F., & Durrheim, R. J. (2022). Mapping of Coastal Inundation Due to Tropical Cyclones: A Numerical Study for the Indian Coasts. In (pp. 305-340). Springer. https://doi.org/10.1007/978-981-19-2511-5_11

Wahiduzzaman, M., Cheung, K. K., Luo, J.-J., & Bhaskaran, P. K. (2022). A spatial model for predicting North Indian Ocean tropical cyclone intensity: Role of sea surface temperature and tropical cyclone heat potential. *Weather and climate extremes*, *36*, 100431. https://doi.org/10.1016/j.wace.2022.100431

Walsh, K. J. E., McBride, J. L., Klotzbach, P. J., Balachandran, S., Camargo, S. J., Holland, G., Knutson, T. R., Kossin, J. P., Lee, T.-c., Sobel, A., & Sugi, M. (2016). Tropical cyclones and climate change. *Wiley interdisciplinary reviews. Climate change*, *7*(1), 65-89. https://doi.org/10.1002/wcc.371

Wang, P., & Horwitz, M. H. (2007). Erosional and depositional characteristics of regional overwash deposits caused by multiple hurricanes. *Sedimentology*, *54*(3), 545-564. https://doi.org/10.1111/j.1365-3091.2006.00848.x

Weatherzone. (2024). *Satellite image of cyclone Jasper*. Weatherzone. https://www.weatherzone.com.au/

Williams, H., Choowong, M., Phantuwongraj, S., Surakietchai, P., Thongkhao, T., Kongsen, S., & Simon, E. (2016). Geologic records of Holocene typhoon strikes on the Gulf of Thailand coast. *Marine geology*, *372*, 66-78. https://doi.org/10.1016/j.margeo.2015.12.014

Woodroffe, S. A., Horton, B. P., Larcombe, P., & Whittaker, J. E. (2005). Intertidal mangrove Foraminifera from the central Great Barrier Reef shelf, Australia; implications for sea-level reconstruction. *Journal of foraminiferal research*, *35*(3), 259-270. https://doi.org/10.2113/35.3.259

Woodruff, J. D., Irish, J. L., & Camargo, S. J. (2013). Coastal flooding by tropical cyclones and sea-level rise. *Nature (London)*, *504*(7478), 44-52. https://doi.org/10.1038/nature12855

Xiong, H., Huang, G., Fu, S., & Qian, P. (2018). Progress in the Study of Coastal Storm Deposits. *Ocean science journal*, *53*(2), 149-164. https://doi.org/10.1007/s12601-018-0019-x

Yao, Q., Liu, K.-b., Wu, Y., Aragón-Moreno, A. A., Rodrigues, E., Cohen, M., de Souza, A. V., Farfán, L. M., & Antinao, J. L. (2021). A multi-proxy record of hurricanes, tsunami, and postdisturbance ecosystem changes from coastal southern Baja California. *The Science of the total environment*, *796*, 149011-149011. https://doi.org/10.1016/j.scitotenv.2021.149011

Yin, K., Xu, S., Zhao, Q., Zhang, N., & Li, M. (2021). Effects of sea surface warming and sea-level rise on tropical cyclone and inundation modeling at Shanghai coast. *Natural hazards (Dordrecht)*, *109*(1), 755-784. https://doi.org/10.1007/s11069-021-04856-w

Yoshida, K., Sugi, M., Mizuta, R., Murakami, H., & Ishii, M. (2017). Future Changes in Tropical Cyclone Activity in High-Resolution Large-Ensemble Simulations. *Geophysical research letters*, *44*(19), 9910-9917. https://doi.org/10.1002/2017GL075058

Appendices

Appendix 1

Contemporary foraminifera from the reef flat and reef slopes around Middle Island

	Depth relative LAT	Adelosina bicornis	Affinetrina bassensis	Alveolinella quoyi	Ammomassilina alveoliniformis	Ammonia aoteana	Ammonia convexa	Ammonia ketienziensis	Ammonia tepida	Amphisorus hemprichii	Amphistegina bicirculata	Amphistegina lessonii	Amphistegina lobifera	Amphistegina papillosa	Anomalinoides colligera	Anomalinoides globulosus	Borelis schlumbergeri	Calcarina gaudichaudii	Calcarina hispida	Calcarina mayori	Calcarina spengleri	Caronia exilis	Chrysalidinella dimorpha	Clavulina angularis	Clavulina multicamerata	Clavulina pacifica	Cycloforina rugosa	Cymbaloporella tabellaeformis	Cymbaloporetta bradyi	Cymbaloporetta sp.	Dendritina sp.	Elphidium advena	Elphidium botaniense	Elphidium craticulatum	Elphidium crispum	Elphidium excavatum	Elphidium fichtelianum	Elphidium fijiense	Elphidium hispidulum	Elphidium lene	Elphidium macellum
RF1	***0.0***	0	0	0	0	0	0	0	0	0	0	5	32	0	0	0	0	0	3	3	0	0	0	0	0	0	0	0	0	0	0	0	0	13	3	0	0	0	0	0	0
RF2	***0.0***	0	0	0	0	0	0	0	0	1	0	4	35	0	0	0	0	0	2	0	0	0	0	0	0	0	0	0	0	0	0	0	0	17	0	0	0	0	0	0	0
RF3	***0.0***	0	0	0	0	0	0	0	0	0	0	4	38	0	0	0	0	0	1	1	0	0	0	0	0	0	0	0	0	0	0	0	0	19	0	0	0	0	0	0	0
RF4	***1.0***	0	0	1	0	0	0	0	0	0	0	2	17	0	0	0	0	0	0	0	0	0	0	0	0	0	0	0	0	0	0	0	2	7	0	0	0	0	1	0	0
RF5	***1.0***	0	0	0	0	0	0	0	0	0	0	1	9	0	0	0	0	0	3	0	0	0	0	0	0	0	0	0	0	1	0	0	0	11	2	0	1	0	0	0	0
RF6	***1.0***	0	0	0	0	0	0	0	0	0	0	2	6	0	0	0	0	0	0	0	0	0	0	0	0	0	0	0	2	0	0	0	2	4	1	0	0	0	0	0	0
2.5m	***-0.5***	0	0	0	0	0	0	0	0	2	1	4	3	1	0	0	0	0	10	7	0	0	0	0	0	0	0	0	1	0	5	0	0	6	19	0	0	0	1	0	2
4.0m	***-2.0***	0	1	0	0	0	0	0	0	0	4	21	1	1	0	0	0	0	2	3	1	0	0	0	0	0	0	1	1	0	0	0	4	4	17	0	0	0	2	0	0
6.0m	***-4.0***	0	0	0	0	0	0	0	0	3	0	39	26	4	0	0	0	1	62	41	0	0	0	0	0	0	0	0	0	0	1	0	5	52	19	0	0	1	0	0	0
301	***-5.5***	0	1	14	1	1	1	0	0	2	6	7	3	4	0	0	2	0	14	3	0	0	0	1	2	2	2	0	2	0	4	1	2	44	17	1	1	1	21	1	1
8.0m	***-6.0***	0	0	1	0	1	0	0	0	1	0	10	1	1	0	1	0	0	22	21	1	0	0	0	0	0	0	0	0	0	0	0	1	7	12	0	0	0	2	0	0
302	***-9.0***	1	0	28	0	0	0	0	1	1	5	12	2	3	1	0	4	0	13	6	0	1	2	1	2	5	3	0	3	0	3	2	1	38	18	1	1	0	31	1	1
12.0m	***-10.0***	0	0	0	0	3	0	1	0	2	0	12	12	25	0	0	0	0	26	11	0	0	0	0	0	4	0	0	0	0	2	1	0	109	44	1	0	0	10	0	0
0	0.0	0	0	0	0	0	0	0	0	0	0	0	0	0	0	0	0	0	0	0	0	0	0	0	0	0	0	0	0	0	0	0	0	0	0	0	0	0	0	0	0
Species	***0.0***	1	2	44	1	5	1	1	1	12	16	123	185	39	1	1	6	1	158	96	2	1	2	2	4	11	5	1	9	1	15	4	17	331	152	3	3	2	68	2	4
0	*0.0*	0	0	0	0	0	0	0	0	0	0	0	0	0	0	0	0	0	0	0	0	0	0	0	0	0	0	0	0	0	0	0	0	0	0	0	0	0	0	0	0
Genus	***0.0***	1	2	44	1	0	0	8	0	12	0	0	363	0	0	2	6	0	0	257	0	1	2	0	17	0	5	1	0	10	15	0	0	0	0	0	586	0	0	0	0

	Depth relative LAT	Elphidium mortonbayense	Epistomaroides polystomelloides	Eponides (cribro)repandus	Fijiella simplex	Flintina bradyana	Flintinoides labiosa	Globorotalia fijiana	Hauerina diversa	Hauerina pacifica	Heterostegina depressa	Lachlanella barnardi	Lamellodiscorbis dimidiatus	Marginopora vertebralis	Massilina secans	Miliolinella fichteliana	Miliolinella pilasensis	Miliolinella semicostata	Miliolinella sp.	Miliolinella subrotunda	Naxotia attenuata	Neorotalia calcar	Operculina ammonoides	Operculina gaimardi	Parasorites orbitoloitoides	Paratrochammina simplissima	Peneroplis pertusus	Peneroplis planatus	Planispirinella exigua	Planogypsina acervalis	Planorbulinella larvata	Polysegmentina circinata	Pseudohauerina fragilissima	Pseudohauerina orientalis	Pseudolachlanella eburnea	Pseudomassilina australis	Pseudomassilina macilenta	Pseudomassilina sp.	Pyrgo denticulata	Pyrgo phlegeri	Pyrgo striolata
RF1	***0.0***	0	2	0	0	0	0	0	0	0	2	0	0	0	0	0	0	0	0	0	0	2	0	0	0	0	3	0	0	0	0	0	0	0	0	0	0	0	0	0	0
RF2	***0.0***	0	1	1	0	0	0	0	1	0	2	0	0	0	0	0	0	0	0	0	0	0	1	0	0	0	4	1	0	0	0	0	0	0	0	0	0	0	0	0	0
RF3	***0.0***	0	0	1	0	0	0	0	0	0	0	0	0	0	0	0	0	0	0	0	0	0	0	0	0	0	0	1	0	0	0	0	0	0	0	0	0	0	0	0	0
RF4	***1.0***	0	3	3	0	0	0	1	0	0	1	0	3	1	0	0	0	0	0	0	0	2	0	0	0	0	5	5	0	0	1	1	0	0	0	0	0	0	0	1	0
RF5	***1.0***	2	2	0	0	0	0	0	0	0	3	0	3	0	0	0	0	0	0	0	0	3	0	0	0	0	11	4	0	0	0	0	0	0	0	0	0	0	0	0	0
RF6	***1.0***	0	0	0	1	0	0	0	0	0	0	1	1	0	0	0	1	1	0	0	0	2	0	0	0	0	3	1	0	0	1	0	0	0	0	0	0	0	0	0	0
2.5m	***-0.5***	0	10	6	0	0	0	0	0	2	1	0	2	1	0	0	0	0	0	0	0	44	1	1	0	0	29	17	0	1	2	3	0	0	0	0	0	0	0	0	0
4.0m	***-2.0***	1	0	1	0	0	0	0	17	6	5	1	6	0	1	0	2	0	0	0	0	13	4	0	0	0	6	3	0	1	1	16	0	3	1	0	0	0	3	0	1
6.0m	***-4.0***	4	6	12	0	0	0	0	1	0	9	0	0	3	0	0	0	0	0	0	0	26	0	1	0	0	23	3	0	0	0	1	0	2	0	0	0	0	0	0	0
301	***-5.5***	7	4	6	0	0	0	0	1	2	1	1	1	0	0	1	1	0	1	0	1	15	7	1	1	1	37	11	0	1	0	1	1	1	0	1	1	0	0	0	0
8.0m	***-6.0***	0	2	13	0	0	0	0	1	0	1	0	3	1	0	0	0	0	0	1	0	21	3	3	0	0	8	9	0	1	0	3	0	0	0	0	0	0	1	1	1
302	***-9.0***	11	2	5	0	1	1	0	3	6	1	1	3	2	0	1	0	1	1	0	1	11	15	1	2	0	37	15	2	1	0	1	0	3	0	0	0	0	0	0	0
12.0m	***-10.0***	12	1	21	0	0	0	0	1	6	18	3	0	1	0	0	0	0	0	0	0	7	56	6	1	0	26	7	0	0	0	1	0	1	0	0	0	1	0	0	0
0	0.0	0	0	0	0	0	0	0	0	0	0	0	0	0	0	0	0	0	0	0	0	0	0	0	0	0	0	0	0	0	0	0	0	0	0	0	0	0	0	0	0
Species	***0.0***	37	33	69	1	1	1	1	25	22	44	7	22	9	1	2	4	2	2	1	2	146	87	13	4	1	##	77	2	5	5	27	1	10	1	1	1	1	4	2	2
0	*0.0*	0	0	0	0	0	0	0	0	0	0	0	0	0	0	0	0	0	0	0	0	0	0	0	0	0	0	0	0	0	0	0	0	0	0	0	0	0	0	0	0
Genus	***0.0***	0	33	69	1	1	1	1	0	47	44	7	22	9	1	0	0	0	11	0	2	146	0	##	4	1	0	##	2	5	5	27	0	11	1	0	3	0	0	8	0

	Depth relative LAT	Quinqueloculina agglutinans	Quinqueloculina auberiana	Quinqueloculina bicarinata	Quinqueloculina bradyana	Quinqueloculina carinatastriata	Quinqueloculina corrugata	Quinqueloculina crassicarinata	Quinqueloculina cuvieriana	Quinqueloculina debenayi	Quinqueloculina delicatula	Quinqueloculina disparilis	Quinqueloculina latidentella	Quinqueloculina neocylindrica	Quinqueloculina parkeri	Quinqueloculina parvaggluta	Quinqueloculina philippinensis	Quinqueloculina polygona	Quinqueloculina sp.	Quinqueloculina subcuneata	Quinqueloculina subparkeri	Quinqueloculina sulcata	Rosalina bradyi	Rosalina globularis	Rosalina orientalis	Rosalina sp.	Rotorbis auberii	Sahulia barkeri	Sahulia conica	Sigmoihauerina involuta	Siphonaperta arenata	Siphonaperta distorqueata	Siphonina tubulosa	Sorites orbiculus	Spirillina sp.	Spiroloculina acescata	Spiroloculina angulata	Spiroloculina antillarum	Spiroloculina clara	Spiroloculina communis	Spiroloculina convexa
RF1	***0.0***	0	0	0	0	0	0	0	0	0	0	0	0	0	0	0	0	0	0	0	0	0	0	0	0	0	0	0	0	0	0	0	0	0	0	0	0	0	0	0	0
RF2	***0.0***	0	0	0	0	0	0	0	0	0	0	0	0	0	0	0	1	0	0	0	0	0	0	0	0	0	0	0	0	0	0	0	0	0	0	0	0	0	0	0	0
RF3	***0.0***	0	1	0	0	0	0	0	0	0	0	0	0	0	0	0	0	0	0	0	0	0	0	0	0	0	0	0	0	0	0	0	0	0	0	0	0	0	0	0	0
RF4	***1.0***	0	10	2	1	0	0	0	1	3	0	0	0	0	0	0	0	0	0	1	0	0	0	0	0	0	0	0	0	0	0	0	0	0	0	0	0	1	0	0	0
RF5	***1.0***	0	12	1	0	0	2	0	0	0	0	1	0	0	0	2	0	0	0	0	0	0	0	0	0	0	0	0	0	0	0	1	0	0	0	0	0	0	0	0	0
RF6	***1.0***	0	8	1	0	1	0	0	4	1	0	0	0	0	1	0	0	0	0	0	0	0	0	0	0	0	0	0	0	0	0	0	0	1	0	0	0	2	0	0	0
2.5m	***-0.5***	0	14	0	0	0	4	0	1	0	0	1	0	0	1	1	0	1	0	2	1	0	0	0	0	1	0	1	0	0	0	2	0	3	0	1	0	2	0	0	0
4.0m	***-2.0***	0	9	1	1	0	3	0	2	0	0	0	0	0	2	1	0	2	0	1	0	0	0	0	0	0	1	0	0	0	0	0	0	1	0	0	0	0	1	0	0
6.0m	***-4.0***	1	2	0	0	0	0	0	0	0	0	0	0	0	2	0	2	0	1	0	0	0	0	0	0	0	0	0	1	0	0	1	0	2	1	0	0	0	0	0	0
301	***-5.5***	3	10	1	0	0	7	1	3	0	1	1	1	0	1	15	2	3	1	0	1	0	1	0	1	1	1	5	2	1	2	2	1	1	0	1	1	1	1	1	1
8.0m	***-6.0***	0	5	0	0	0	2	0	0	0	0	0	0	0	4	1	0	3	0	0	0	0	0	1	0	0	0	0	1	0	0	2	0	1	0	0	0	0	0	0	0
302	***-9.0***	2	4	2	1	0	8	2	0	0	0	0	1	1	1	20	5	3	1	1	2	0	0	0	0	1	0	11	2	2	1	1	0	0	0	0	0	1	0	4	1
12.0m	***-10.0***	1	1	1	0	3	1	3	0	0	0	0	0	0	0	21	13	4	0	1	2	1	0	0	0	0	1	0	3	2	2	3	0	2	0	0	0	0	1	2	0
0	0.0	0	0	0	0	0	0	0	0	0	0	0	0	0	0	0	0	0	0	0	0	0	0	0	0	0	0	0	0	0	0	0	0	0	0	0	0	0	0	0	0
Species	**0.0**	7	76	9	3	4	27	6	11	4	1	3	2	1	12	61	23	16	3	6	6	1	1	1	1	3	3	17	9	5	5	12	1	11	1	2	1	7	3	7	2
0	*0.0*	0	0	0	0	0	0	0	0	0	0	0	0	0	0	0	0	0	0	0	0	0	0	0	0	0	0	0	0	0	0	0	0	0	0	0	0	0	0	0	0
Genus	***0.0***	0	0	0	0	0	0	0	0	0	153	0	0	0	0	0	0	0	0	0	0	0	0	0	6	0	3	0	26	5	0	17	1	11	1	0	0	0	0	0	0

	Depth relative LAT	Spiroloculina corrugata	Spiroloculina depressa	Spiroloculina elegans	Spiroloculina elegantissima	Spiroloculina eximia	Spiroloculina sp.	Spiroloculina subimpressa	Spirotextularia fistulosa	Textularia agglutinans	Textularia candeiana	Textularia dupla	Textularia foliacea	Textularia occidentalis	Textularia oceanica	Textularia sp.	Tretomphalus bulloides	Triloculina barnardi	Triloculina latiformis	Triloculina marshallana	Triloculina oblonga	Triloculina striatotrigonula	Triloculina terquemiana	Triloculina tricarinata	Triloculina trigonula	Valvulineria rugosa	Varidentella neostriatula
RF1	***0.0***	0	0	0	0	0	0	0	0	0	0	0	0	0	0	0	0	0	0	0	0	0	0	0	0	0	0
RF2	***0.0***	0	0	0	0	0	0	0	0	0	0	0	0	0	0	0	0	0	0	0	0	0	0	0	0	0	0
RF3	***0.0***	0	0	0	0	0	0	0	0	0	0	0	0	0	0	0	0	0	0	0	0	0	0	0	0	0	0
RF4	***1.0***	0	0	0	0	0	0	0	0	0	0	0	0	0	0	0	0	4	0	0	2	0	0	0	0	0	0
RF5	***1.0***	0	0	0	0	0	0	0	0	0	0	0	0	0	0	0	0	8	0	0	0	0	0	0	1	0	0
RF6	***1.0***	0	0	0	0	0	0	0	0	0	0	0	0	0	0	0	0	14	0	0	0	0	0	0	0	0	0
2.5m	***-0.5***	0	0	0	0	0	0	0	0	1	0	0	0	0	0	0	0	5	0	0	0	0	0	0	1	0	0
4.0m	***-2.0***	0	0	2	0	0	0	0	0	2	0	0	0	0	0	0	1	3	0	0	0	0	0	0	4	3	0
6.0m	***-4.0***	0	0	0	0	0	0	0	0	3	0	0	0	0	0	0	0	4	1	0	0	0	0	0	2	0	0
301	***-5.5***	0	0	0	0	2	0	3	0	9	0	2	1	0	0	0	0	5	1	1	0	1	0	0	1	1	1
8.0m	***-6.0***	0	0	4	0	0	0	0	0	0	0	0	0	0	0	0	0	1	0	0	0	0	0	0	1	0	0
302	***-9.0***	2	1	0	0	4	1	1	1	7	1	4	3	2	2	0	0	2	0	0	0	1	1	1	2	0	0
12.0m	***-10.0***	0	0	0	1	1	0	0	0	3	0	2	0	1	1	1	0	4	1	0	0	0	1	0	2	0	0
0	0.0	0	0	0	0	0	0	0	0	0	0	0	0	0	0	0	0	0	0	0	0	0	0	0	0	0	0
Species	***0.0***	2	1	6	1	7	1	4	1	25	1	8	4	3	3	1	1	50	3	1	2	2	2	1	14	4	1
0	*0.0*	0	0	0	0	0	0	0	0	0	0	0	0	0	0	0	0	0	0	0	0	0	0	0	0	0	0
Genus	***0.0***	22	0	0	0	0	0	0	1	0	0	0	45	0	0	0	1	0	0	0	0	75	0	0	0	4	1

…Appendix 1 continued

Appendix 2

Foraminifera identified in percussion cores PC3.3 and PC4.1A. Foraminifera marked in dark green belong to 5-10 m below LAT, foraminifera marked in light green belong to 0-10 m below LAT

	Affinetrina bassensis	Ammonia sp.	Ammonia tepida	Ammospaeroidina sphaeroidiniformis	Amphistegina bicirculata	Clavulina multicamerata	Clavulina pacifica	Cornuspira planorbis	Coscinospira hemprichii	Cyclorina rugosa	Cymbaloporetta bradyi	Cymbaloporetta sp.	Elphidium botaniense	Elphidium clavatum	Elphidium craticulatum	Elphidium crispum	Elphidium excavatum	Elphidium hispidulum	Elphidium macellum	Elphidium milletti	Elphidium sp.	Epistomaroides polystomelloides	Eponides (cribro)repandus
PC3.3 15 cm		1																					
PC3.3 20 cm		13																					
PC3.3 25 cm		21																					
PC3.3 30 cm		3																					
PC3.3 35 cm		2																					
PC3.3 40 cm		1																					
PC3.3 50 cm		1																					
PC3.3 60 cm															10								
PC3.3 65 cm															5						1		
PC3.3 70 cm														1	29			6	1		3		
PC3.3 75 cm															7								
PC3.3 80 cm															7								
PC3.3 85 cm															5								
PC3.3 90 cm	1	1									2	1			9			5			1		1
PC4.1A 5 cm																							
PC4.1A 10 cm																							
PC4.1A 40 cm																							
PC4.1A 45 cm															10			2			3		
PC4.1A 50 cm			5												1								
PC4.1A 55 cm		2	2										1		2					1	3		
PC4.1A 60 cm	1																						
PC4.1A 65 cm		1	1		1		1	1		1	5	3			1			9			2		
PC4.1A 70 cm	2					1				1		4			1	1		4			1	2	
PC4.1A 75 cm	1							3							1			1					
PC4.1A 80 cm	1	1		1		4		2			3						1	1		1		2	
PC4.1A 115 cm	1					1					2					1							
PC4.1A 120 cm	1								1						1							1	
PC4.1A 125 cm																							

	Hanzawaia grossepunctata	Hauerina diversa	Hauerina earlandi	Hauerina pacifica	Lachlanella barnardi	Lachlanella sp.	Lamellodiscorbis dimidiatus	Miliolinae sp.	Miliolinella oceanica	Miliolinella pilasensis	Miliolinella sp.	Miliolinella subrotunda	Neorotalia calcar	Paratrochammina sp.	Peneroplis pertusus	Planispirillina inaequalis	Planogypsina acervalis	Polysegmentina circinata	Pseudolachlanella eburnea	Pyrgo denticulata	Pyrgo oblonga	Pyrgo phlegeri	Pyrgo sp.
PC3.3 15 cm																							
PC3.3 20 cm											1												
PC3.3 25 cm																							
PC3.3 30 cm																							
PC3.3 35 cm																							
PC3.3 40 cm																							
PC3.3 50 cm																							
PC3.3 60 cm																							
PC3.3 65 cm																							
PC3.3 70 cm																							
PC3.3 75 cm																							
PC3.3 80 cm																							
PC3.3 85 cm																							
PC3.3 90 cm							6																
PC4.1A 5 cm														16									
PC4.1A 10 cm														5									
PC4.1A 40 cm														1									
PC4.1A 45 cm																							
PC4.1A 50 cm																							
PC4.1A 55 cm																							
PC4.1A 60 cm							1					1											
PC4.1A 65 cm							49				5	1	1				1		2			1	
PC4.1A 70 cm	1						31				1	1	1		1						1	1	
PC4.1A 75 cm				1			31	2	1	1		3	1		5			1	1				
PC4.1A 80 cm		1				1	20			3		2	6		2	1				1			1
PC4.1A 115 cm						1	6				1		8		3								
PC4.1A 120 cm			1	1	1	1	3	1					1		1								
PC4.1A 125 cm	1						2						4		1								

	Quinqueloculina agglutinans	Quinqueloculina auberiana	Quinqueloculina bicarinata	Quinqueloculina bosciana	Quinqueloculina bradyana	Quinqueloculina carinatastriata	Quinqueloculina collumnosa	Quinqueloculina corrugata	Quinqueloculina crassicarinata	Quinqueloculina cuvieriana	Quinqueloculina debenayi	Quinqueloculina delicatula	Quinqueloculina disparilis	Quinqueloculina distorqueata	Quinqueloculina jugosa	Quinqueloculina laticentella	Quinqueloucina neocylindrica	Quinqueloculina parkeri	Quinqueloculina seminulum	Quinqueloculin sp.	Quinqueloculina subparkeri	Quinqueloculina tropicalis	Reussella spinulosa	Reussella sp.	Rosalina sp.	Rotorbinella lepida	Rotorbis auberii	Sahulia conica	Sigmoilinella sp.	Siphogenerina raphana	Spiroloculina acescata	Spiroloculina antillarum	Spiroloculina caduca	Spiroloculina communis	Spiroloculina depressa	Spiroloculina elegans	Spiroloculina eximia	Spiroloculina sp.	Spiroloculina subimpressa	Textularia dupla	Triloculina barnardi	Triloculina fichteliana	Triloculina marshallana	Triloculina oblonga	Triloculina rotunda	Triloculina sp.	Triloculina striatotrigonula	Triloculina terquemiana	Triloculina trigonula	Unknown	Varidentella neostriatula
PC3.3 15 cm																																																		1	
PC3.3 20 cm																																																		10	
PC3.3 25 cm																																																		1	
PC3.3 30 cm																																																		1	
PC3.3 35 cm																																																		4	
PC3.3 40 cm																																																			
PC3.3 50 cm																																								1											
PC3.3 60 cm																																																			
PC3.3 65 cm																																																			
PC3.3 70 cm																																																			
PC3.3 75 cm																																																			
PC3.3 80 cm																																																			
PC3.3 85 cm																								1																										1	
PC3.3 90 cm	1					2		2										1																			1	1										2	1		2
PC4.1A 5 cm																																																			
PC4.1A 10 cm																																																			
PC4.1A 40 cm																																																			
PC4.1A 45 cm																																																		2	
PC4.1A 50 cm																																																			
PC4.1A 55 cm																																																			
PC4.1A 60 cm		1																																																	
PC4.1A 65 cm		2			1	8		4	1		1		1					2	2	6		1	1		1				2							6		1			18		1			1	3	2	1		3
PC4.1A 70 cm		5				3		1	1										2	2	1													1		7	1	2		1	5		1				1	1			13
PC4.1A 75 cm		5	1		2	9	1	2					1		3	1	1			2		1									1		1	1	1	4	1	2	1		5		1	1				2			2
PC4.1A 80 cm		6	4	1		5						1		1		1				3										1		2				2		2			2				2	1		1		1	8
PC4.1A 115 cm		1									1			1					1	3								1				1				1		1			4	1	1								4
PC4.1A 120 cm		1						1										2																		1					2										
PC4.1A 125 cm		2								1										1						1	1														1										1

…Appendix 2 continued